ISSN: 2153-1196 Volume 12, Number 14, December 2021

Scientific Research Publishing

Journal of Modern Physics

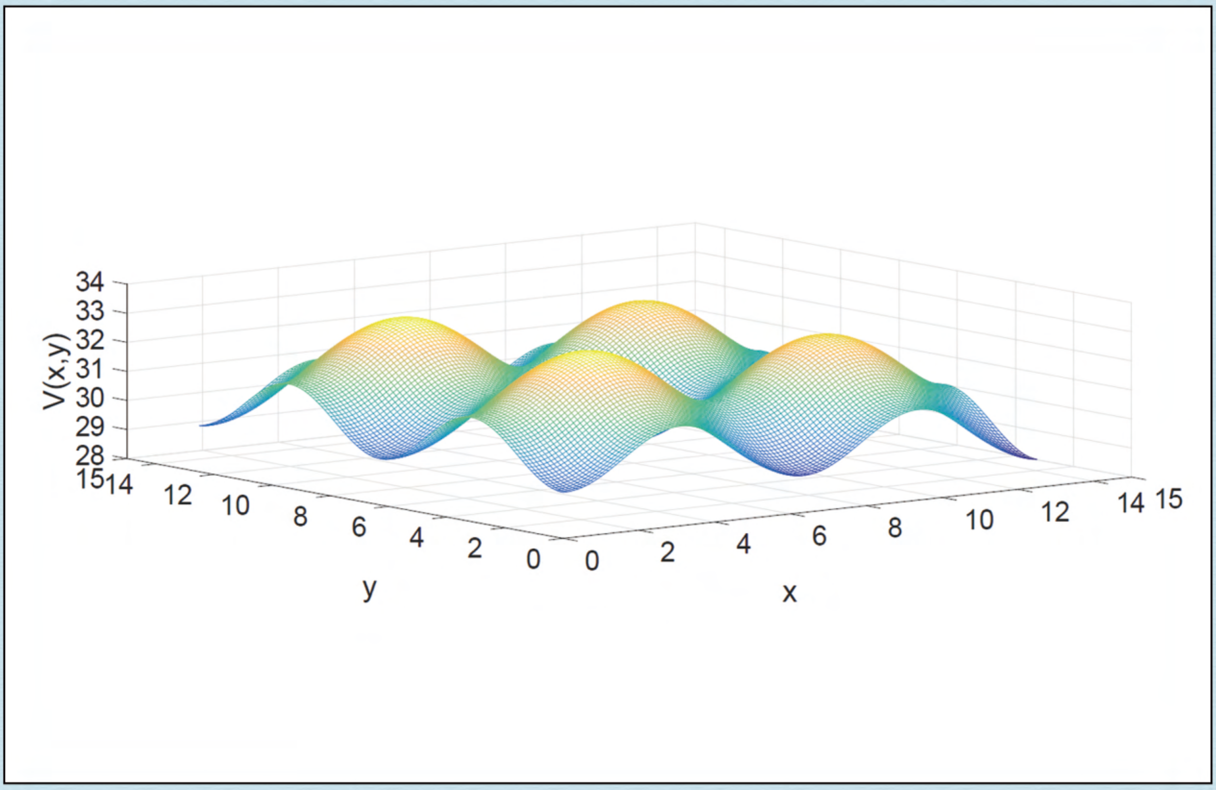

ISSN: 2153-1196

https://www.scirp.org/journal/jmp

Journal Editorial Board

ISSN: 2153-1196 (Print) ISSN: 2153-120X (Online)
https://www.scirp.org/journal/jmp

Journal of Modern Physics, 2021, 12, 1931-2040
https://www.scirp.org/journal/jmp
ISSN Online: 2153-120X
ISSN Print: 2153-1196

Table of Contents

Volume 12 Number 14 December 2021

Motion of Particles at the Fundamental Level: NLHV Theory Predictions for a Spiral Gait Locus

D. J. Pons....................1931

Koide Lepton Relation Explained by Lepton Radius (Compton Wavelength)/4

T. R. Mongan....................1954

Multidimensional Effects on Diffusion of a Particle in Tilted Periodic Potentials

H. H. Luo, Z. W. Bai....................1960

Some Consequences of a Simple Approach for Constructing a Theory of a Relativistic Fermi Gas

R. Lopez-Boada, L. Grave de Peralta....................1966

Evolution of Life Forms in Our Universe

R. M. L. Baker Jr., B. S. Baker, J. H. M. Fontana....................1975

The Quantum Redshift Effect of Photon

Z. L. Xu....................2003

Difference between the Time Intervals in the Special Relativistic Theory Calculated with the Aid of an Invariance Property between the Mechanical Expressions

S. Olszewski....................2031

The figure on the front cover is from the article published in Journal of Modern Physics, 2021, Vol. 12, No. 14, pp. 1960-1965 by Huanhuan Luo and Zhanwu Bai.

Journal of Modern Physics (JMP)
Journal Information

SUBSCRIPTIONS

The *Journal of Modern Physics* (Online at Scientific Research Publishing, https://www.scirp.org/) is published monthly by Scientific Research Publishing, Inc., USA.

Subscription rates:
Print: $89 per issue.
To subscribe, please contact Journals Subscriptions Department, E-mail: sub@scirp.org

SERVICES

Advertisements
Advertisement Sales Department, E-mail: service@scirp.org

Reprints (minimum quantity 100 copies)
Reprints Co-ordinator, Scientific Research Publishing, Inc., USA.
E-mail: sub@scirp.org

COPYRIGHT

PRODUCTION INFORMATION

For manuscripts that have been accepted for publication, please contact:
E-mail: jmp@scirp.org

Journal of Modern Physics, 2021, 12, 1931-1953
https://www.scirp.org/journal/jmp
ISSN Online: 2153-120X
ISSN Print: 2153-1196

Motion of Particles at the Fundamental Level: NLHV Theory Predictions for a Spiral Gait Locus

Dirk J. Pons

Department of Mechanical Engineering, University of Canterbury, Christchurch, New Zealand
Email: dirk.pons@canterbury.ac.nz

How to cite this paper: Pons, D.J. (2021) Motion of Particles at the Fundamental Level: NLHV Theory Predictions for a Spiral Gait Locus. *Journal of Modern Physics*, **12**, 1931-1953.
https://doi.org/10.4236/jmp.2021.1214110

Received: October 12, 2021
Accepted: December 14, 2021
Published: December 17, 2021

Abstract

Context: The existing literature on particle motion at the fundamental level is sparse. Particles, whether classical or quantum, are assumed to move with a continuous (even if uncertain) velocity. **Purpose:** The work prospects for a descriptive theory of particle motion from a non-local hidden-variable (NLHV) perspective. This is worth attempting for the potential to better understand fundamental dynamics and kinematics. **Method:** The new physics provided by the cordus theory was used to infer the mathematical representation of the energisation behaviour of the inner structures, specifically the reactive ends. From this, the motion function of the particle as a whole was determined. **Findings:** In three dimensional space, the motion of each reactive end is an irregular spiral displacement locus. The motion comprises a movement phase and a brief immobile phase. This is called a "gait" as it is reminiscent of biological locomotion. **Originality:** A novel theory of particle motion is offered. The theory predicts that motion comprises a complex spiral locus of the particle. This is unique among theories of physics. Further contributions are the provision of explanations for several physical phenomena: ponderomotive force, the nature of momentum, and bremsstrahlung radiation. Specifically, the theory explains why photon emission would be increasingly concentrated in the forward direction with increased electron energy. The theory provides a means to bridge quantum mechanics and special relativity, because it accommodates both particle uncertainty and field transmissions.

Keywords

Fundamental Physics, Particle Motion, New Physics, NLHV Theory, Wave Equation

1. Introduction

This paper addresses the ontological question of how particles move. The physical laws and mathematical descriptions for velocity and momentum are well-understood in physics and engineering, and not under debate here. However, there is a lack of explanation of motion at the level of the fundamental particle. In classical mechanics, the velocity of a particle corresponds to the rate at which its location moves along a spatial trajectory, and this motion is presumed to be continuous. The question of *how* the particle moves is therefore somewhat irrelevant when assuming a smooth space-time. It is simply taken for granted that motion exists and is smooth. The existing literature on particle motion at the fundamental level is sparse. There appears to have been a general assumption that particles, whether classical or quantum, move with a continuous (even if uncertain) velocity.

However, if space and time are discrete in some way, which is what quantum mechanics (QM) implies, then the question *does* become relevant. In quantum mechanics, the location is intrinsically uncertain, being represented with a probability distribution. How that relates to motion along the locus is ambiguous. An explicit trajectory representation of this is provided by the de Broglie-Bohm pilot wave theory [1] [2], though that theory is not widely accepted and does not generalise to a broader theory of physics. The Dirac equation provides a wave equation with a relativistic component. It therefore includes both special relativity and quantum mechanics. The quantum Langevin equation provides a mathematical representation of the stochastic displacement and velocity behaviour of free Brownian particles in a thermal heat bath [3] [4] [5]. However neither provide an ontological explanation for motion. An additional complexity arises because particles also have a de Broglie frequency, and how this relates to motion is unclear. The fundamental physics literature is almost non-existent on the ontological question of how particles move.

Hence there is an unsolved problem in describing how particles move at a more fundamental level. While it is possible to mathematically represent the observed mechanics of where particles move, there is as yet no satisfactory explanation of how this behaviour arises. Examples of these foundational questions are: How does force cause velocity to change? Why is the product of velocity and mass (momentum) conserved? What are the deeper reasons for the laws concerning motion to have the forms they do?

The purpose of the current work was to prospect for a descriptive theory of particle motion, from a non-local hidden-variable perspective. This is worth attempting for the potential to better understand fundamental dynamics and kinematics. The approach uses the new physics provided by the cordus non-local hidden-variable (NLHV) theory [6]. The results predict that particle motion comprises a movement phase and a brief immobile phase. This is called a “gait” as it is reminiscent of biological locomotion.

2. Method

2.1. Overall Approach

A new approach was taken based on hidden variable theory, rather than using classical continuum mechanics, quantum mechanics, or string theory. Specifically, a theory-building approach was taken, starting with the existing cordus NLHV theory. As a hidden variable theory, this proposes that fundamental particles have physical substructures, and the observable properties of the particle arise from these substructures. The identity of these substructures has been inferred by consideration of known phenomena [7]. The theory-building approach used to construct the cordus theory generally was to apply abductive reasoning. This started with empirical established phenomena (the double-slit device was the original starting point), and then sought explanations that met three main principles: economical in the number of hidden variables proposed (parsimonious); sufficient to qualitatively explain the phenomenon; and consistent with other published parts of the theory. More description of the general method may be found in [8].

2.2. Context

The cordus theory proposes that particles are two-ended string-like structures, with substructures of reactive ends, fibril, and discrete forces. The numbers and types of discrete forces determine particle identity (electron, proton, etc.). The de Broglie frequency for the particle corresponds to the alternate energisation of the two reactive ends, and this is important in what follows.

The structure of the electron is shown in **Figure 1** by way of an example. Further details about the structure and behaviour of particles under this theory are provided in the references below.

These are radical elements, and each of them has been elaborated and tested in other papers. The theory may seem unorthodox compared to QM, but has been shown to have wide applicability, see **Table 1**. It also explains several phenomena that otherwise have no explanation in conventional mechanics or quantum mechanics. The theory is compatible with quantum mechanics (which becomes a stochastic simplification of a deeper and more deterministic mechanics), general relativity (but introduces a new parameter called the fabric density of space), and string theory (both propose open string-like structures, and the number of parameters required to define a cordus particle is the same as some versions of string theory). However the theory does not trace its origin to any of those theories, but is instead an emergent designed solution, where the substructures were determined by logical consideration of what hidden structures a particle would need, for it to behave in the way that is observed (requisite variability).

2.3. Approach to the Motion Problem

In the present work, the theory-building used the same logical considerations to infer a mechanism for how a particle would assuming the general assumptions of the cordus theory were valid. The literature is exceedingly sparse on how a particle might move at the deeper level, so no specific insights were gained from

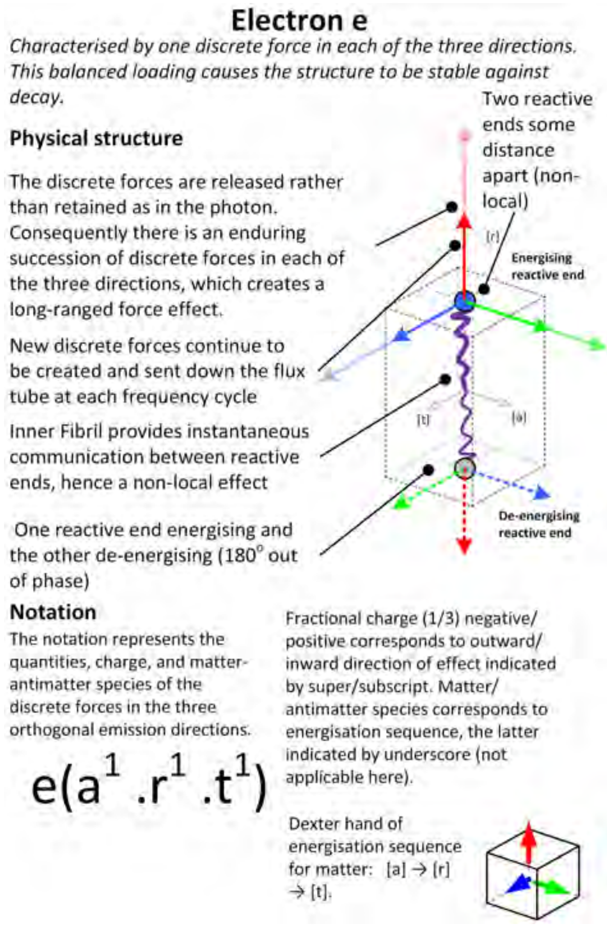

Figure 1. The representation of the electron's internal and external structures. It is proposed that the particle has three orthogonal discrete forces, energised in turn at each reactive end. Adapted from [9].

Table 1. Applications of the cordus theory. Adapted from [10] and [11].

Phenomenon explained	Key concept	Reference
Wave-particle duality in the double slit device	One reactive end passes through each slit.	[7]
Derivation of optical laws from a particle perspective	Includes derivation of reflection and refraction laws, and Brewster's Angle from particle basis.	[7]
Prediction of particle structures	Electron, proton, neutron, neutrino species, photon	[9] [12] [13] [14] [15]
Explanation of the decay processes and prediction of a deeper decay model	Dependency identified on neutrino species loading	[13] [14]
Explanation for the selective spin characteristics of neutrinos whereby the direction of spin is correlated with the matter-antimatter species	Spin direction arises from reaction between incomplete discrete force emissions from the particle, and the background fabric.	[14]
Explanation for particle spin and derivation of the electron g factor g = 2	Cordus particle structure naturally causes g = 2	[10]

Continued

Explanation for the annihilation process	Description of the discrete force changes involved in remanufacture of these particle identities. Includes a conceptual explanation of the difference between otho- and para-positronium decay rates (ortho and para refer to spin combinations of the bound electron and anti-electron/positron).	[16]
Provision of a mechanics for pair production	Rearrangement of discrete forces changes the particle identity.	[17]
Explanation of process of photon emission	Excess energy in the electron changes its span, which is opposed by bonding constraints.	[18] [19]
Synchronous interaction	Synchronous interaction between discrete forces of different matter particles causes the strong nuclear force	[20]
Predicted structure of atomic nuclei and explanation of stability for nuclides H to Ne	Protons and neutrons are arranged in a nuclear polymer. The rules for this arrangement, and for the bridge neutrons, are inferred and are qualitatively consistent with observed stability/instability/non-existence of all nuclides in this range.	[21] [22]
Prediction of a mechanism for asymmetrical baryogenesis	Predicts a decay path for remanufacture of the antielectron to the proton. This also solves the asymmetrical leptogenesis problem.	[12]
Origin of entropy	Fabric increases the Irreversibility of geometric position of particle.	[23]
A theory for time as an emergent property of matter rather than a universal attribute	Time arises from the interaction between the frequency of a particle and the local density of the fabric.	[24]
Nature of the vacuum and the cosmological horizon	Vacuum comprises fabric of discrete forces from massy particles.	[25]
Origin of the finite speed of light	Determined by fabric density, hence variable with epoch of universe and local distribution of mass.	[26]
Quantitative derivation of the relativistic Doppler and the Lorentz factor	Derivation accomplished from a particle perspective. Identifies fabric density as a covert variable.	[6]
A mechanism for how a particle detects and moves in a field gradient	"The operation of force is proposed to occur from the interaction between the energisation sequence of the particle, with the field gradient, resulting in discrete displacement motions of the particle. Specifically the particle sub-structures sweep through a volume of space during their energisation cycle. This locus is warped by the incoming field, hence preferentially displacing the particle along the gradient."	[11]
Unification of fundamental interactions	"All the interactions can be attributed to the discrete force emissions from the particle, more specifically from the different attributes thereof. Thus the electrostatic appears to arise from the direct linear effect of the discrete forces; magnetic from bending of the flux tube; gravitation from handed energisation sequence; strong from the synchronisation of emissions; and weak from rearrangement of discrete force emissions hence remanufacturing of particle identity."	[8]

that direction. Rather, the conceptual initiator arose from [8] [11] which propose mechanisms for how force operates at a fundamental level. The connection between force and motion might not be an obvious one, but the useful starting point was the observation that theoretical prediction that force was an emergent effect for a deeper process of displacement of the reactive ends [8], *i.e.* that displacement was the primary effect. Acting on this theory, and extending it on logical grounds, lead to the theory presented here. Implications for motion were drawn from the force theory, and elaborated into lemmas (indicated §). Then these were applied to develop a theory for motion. Finally, the theory was tested for how it explained other phenomena.

In this context a lemma is a theorised principle, in the form of a proposition. They are not necessarily proven but rather are tentatively accepted as correct, and then used as subsidiary propositions for the further development of the theory. Lemmas are used throughout the construction of the cordus theory. There is an expectation that lemmas in one part of the theory will not contradict those in other parts. So far this has been preserved. Hence the lemmas provide the logical consistency across the theory. Confidence in the lemmas arises to the extent that the resulting theory gives satisfactory explanations of other known phenomena. Hence the application to other areas as shown in the latter part of the results.

3. Results

3.1. Mathematical Representation of Motion Parameters

Consider a text particle, e.g. an electron. Per the cordus theory, it has two reactive ends, and these take alternate turns to energise. At energisation, the reactive end makes a discrete field emission. The following premises are used to develop a theory for motion under this NLHV architecture.

Lemma §1: Potential energy of discrete field emissions has a $\sin^2(\theta/2)$ *function*

In this theory fractional charge (which corresponds to colour charge in QM), is represented by an emission in one [*i*] of the three directions $[a, r, t]$, see [8] [11]. Hence an electron with a total charge of 1 has fractional charge energisation in all three directions, and this is represented as $e[a^1, r^1, t^1]$. The discrete force, or more specifically its potential energy U, varies between 0 and 1 over a full cycle. The shape function for this is $\sin^2\theta_i/2$ [8] [11]. For the individual axes, the shape functions are offset at thirds of the phase angle θ, and expressed as:

$$U_i = Q\sin^2\frac{\theta_i}{2} \quad (1)$$

$$\begin{gathered}\text{For } [a] \text{ component: } \theta_i = \theta S_p \\ \text{For } [r] \text{ component: } \theta_i = \left(\frac{\theta}{2} + \frac{1\pi}{3}\right)S_p \\ \text{For } [t] \text{ component: } \theta_i = \left(\frac{\theta}{2} + \frac{2\pi}{3}\right)S_p\end{gathered} \quad (2)$$

where

Q is magnitude, assumed unity for simplicity

S_p is matter/antimatter species, represented as 1 or −1 respectively (sign convention).

Implications—Even during the sinusoidal null emissions in one axis, the other axes are populated. The flux tube represents the aggregation of the discrete forces. Consequently there are no breaks in the flux tube, which supports an assumption made in the relativistic Doppler part of the theory [6].

Lemma §2: *Ability for reactive end to move is complementary to energisation*

The mobility of reactive ends is assumed to be related to their degree of de-energisation. This is a key assumption in this part of the theory. A reactive end is assumed to be immobile at the phase of maximum energisation (which corresponds to maximal emission strength of discrete forces), and is maximally mobile when de-energised. The mobility of the reactive end to move is complementary to its emission state. Hence for potential energy $U_i = Q\sin^2\frac{\theta_i}{2}$, the Mobility M_i is:

$$M_i = \cos^2\frac{\theta_i}{2} \tag{3}$$

and ranges from 0 to 1.

Lemma §3: *The reactive end moves in a circular orbital motion around its mean position*

The mobility is important for reasons relating to *mobility* and external *perturbation.* First, it leads to the conclusion that the reactive end of a stationary fundamental particle moves in a circular locus around its mean centre. This orbital motion arises because the vector sum of the mobility in the three directions [*a*,*r*,*t*], results in a circular orbit. We propose that this motion is causal to the emission of the discrete forces U_i. This has the consequence that the vector normal to the orbital plane is the same as the mathematical representation of the discrete force emission. Hence, for an electron with discrete forces $e\left[a^1, r^1, t^1\right]$ the normal to the orbital is [1, 1, 1] in the [*a*, *r*, *t*] directions. The corollary is that there is a correspondence between particle identity, which is represented by discrete force emission portfolio [12], and the orbital motion of the reactive end. This correspondence further implies that an emission in say the [*a*] direction corresponds to an orbit in the [*r*, *t*] plane.

The position of the reactive end in its orbit is given by:

$$RE_i = R_{RE}\cos\left(\theta_i\right)C_h \tag{4}$$

where

R_{RE} is the orbital radius, being a small unknown value,

θ_i is per Equation (2).

C_h is sign of charge and takes the values 1 or −1 for negative or positive charge respectively (cordus sign convention).

The second outcome is that the mobility also represents the susceptibility of the reactive end to external perturbation. This occurs via incremental distortion of the orbit, under a field or acceleration [11]. This displacement is not constant through the energisation cycle, because of the phase dependency on the mobility.

For the case of gravitation, this has been shown to eventuate as a distorted spiral locus, see [11]. A formulism for displacement follows later.

Lemma §4: *Continuity of motion is stored as shear in the fibril*

A body that is in motion will continue with that motion unless acted on by an external force (Newton's law). However at a fundamental level it is odd that a body, once it has been put in motion, should continue that motion indefinitely. What preserves velocity? This lemma represents the proposition that the continuity of motion is stored as shear in the fibril itself. The fibril is that substructure that connects the two reactive ends. It is proposed that once this internal shear is created, by an initial external interaction, it is preserved, and the particle continues with that velocity. At this point the physical nature of this shear is not elucidated—we merely propose its existence and show its implications for motion.

Specifically, the process is anticipated as follows.

1) Initial acceleration of the particle arises by external discrete forces causing the reactive end to shift its energisation location in a translational displacement.

2) This requires a change in energisation timing for the reactive end, hence a change in frequency of the fibril. This also changes the span of the fibril, since frequency and span are inversely proportional. It may be necessary for the particle to emit excess energy, hence bremsstrahlung (see below).

3) The translational displacement of the reactive end, as set up by the external acceleration force, is stored in the fibril. We hypothesise it is stored as a type of shear force.

4) This shear is applied continuously to both reactive ends, which respond to it to the extent that they can, *i.e.* to the extent that they are *not* responding to external discrete forces (when they are de-energised). As the emissions of the two reactive ends are complementary, this means that there is no moment when the shear is ineffective in moving one or other of the reactive ends forward.

5) The amount of internal shear can be added to or reduced by further external interactions at the reactive ends. Hence the store of velocity is accumulated or reduced as the particle experiences various episodes of acceleration.

6) A shear component may also be created in the roll direction of motion (with respect to the fibril span), and this is proposed to correspond to circular polarisation.

Acceleration is the process of establishing this shear, by initially prescribing the translational displacement of the reactive ends. At each subsequent energisation cycle this shear is preserved, even after the accelerating force is removed. The shear is zero for stationary particles. A formulism for shear is given below.

Lemma §5: *Displaced motion of reactive depends on mobility and shear*

The orbital positional coordinates of the reactive end $\left[RE_a, RE_r, RE_t\right]$ have an added translational motion due to the velocity shear, and this is called the displacement. This is a deviation away from the circular orbit of the reactive end.

The displacement s_i of the reactive end in each of the three axes is determined from the integral of the mobility, with the product of the shear τ, hence:

$$s_i = \tau \int \cos^2 \frac{\theta_i}{2} \mathrm{d}\theta = \tau \left(\frac{\theta_i}{2} + \frac{1}{2} \sin \theta_i \right) \tag{5}$$

The motion displacement for a nominal shear is shown for the three axes, in Figure 2.

Consider linear motion in the $[a]$ direction. The integral of s_a from Equation (4), over one energisation cycle of 2π gives the total distance S_a moved by the particle in one cycle:

$$S_a = \tau\pi \tag{6}$$

This may also be expressed as

$$S_a = v/f \tag{7}$$

where v is the magnitude of the mean particle velocity, and f is its frequency. Hence

$$\tau = v/(\pi f) \tag{8}$$

Thus the fibril shear is proportional to the velocity and inversely proportional to the frequency (or energy).

The frequency for the electron of 511 keV, per the relativistic formulation [27] is $\omega = 7.81\text{E}20\ \text{s}^{-1}$, hence the period is 8.04505E-21s, and the frequency is 1.24E+20 Hz. With a velocity $0.1c$, the shear per Eqn 8 is

$$\tau = \frac{v}{\pi f} = 7.68 \times 10^{-14} \frac{\text{m}}{\text{cycle}} \tag{8b}$$

In what follows, much larger values are used, e.g. $\tau = 0.5$, for illustrative purposes.

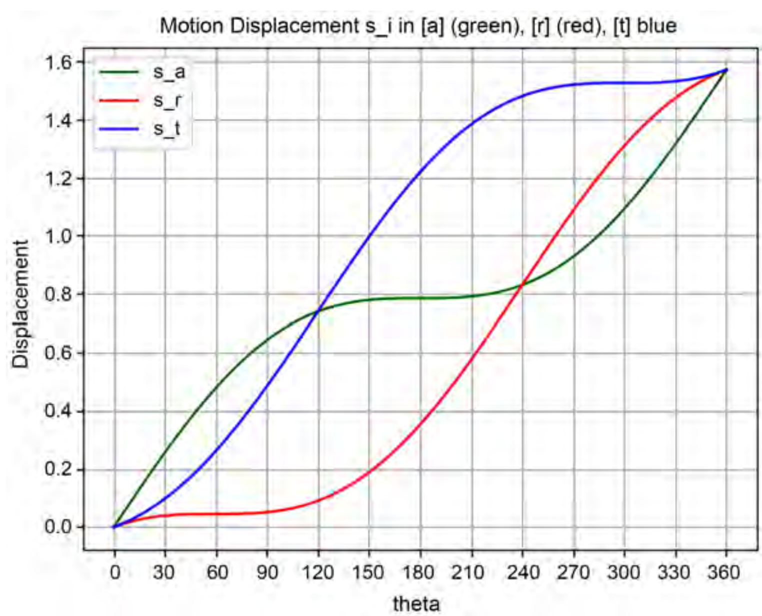

Figure 2. Motion displacement shear $\tau = 0.5$ for the three axes, for an electron. The total displacement per cycle is $P_a = \tau\pi$.

3.2. Motion Parameters

Hence for each of the directional axes [a], [r], and [t] there are a set of parameters that define the motion state: potential energy of the emissions in that direction U_i; mobility; position of the reactive end in its orbit (for a stationary particle); and motion displacement during the cycle s_i which is in response to the velocity shear τ. These parameters are shown in **Figure 3**, for $\tau = 0.5$.

The displacement parameter s_i is of the greatest interest since it describes the deviated locus of the reactive end, and hence the motion of the particle over multiple cycles. Note that it is an incremental motion, characterised by having a stationary or dwell period.

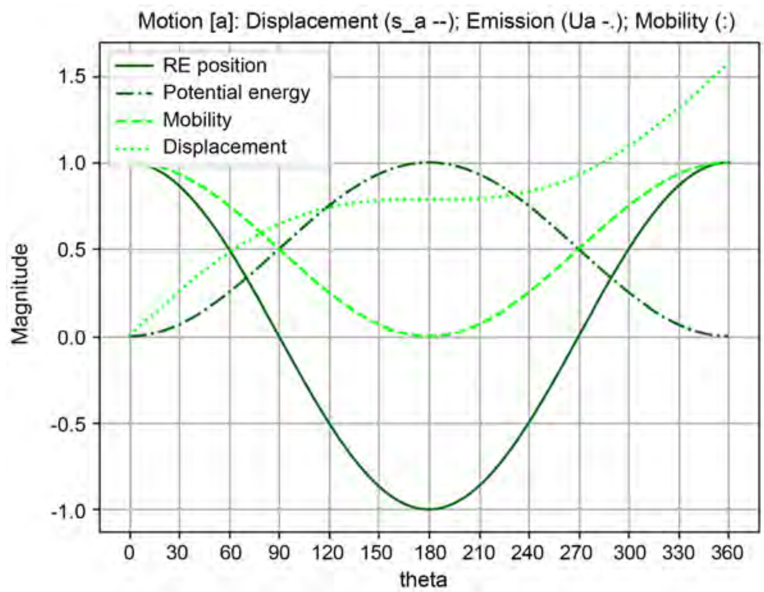

(a)

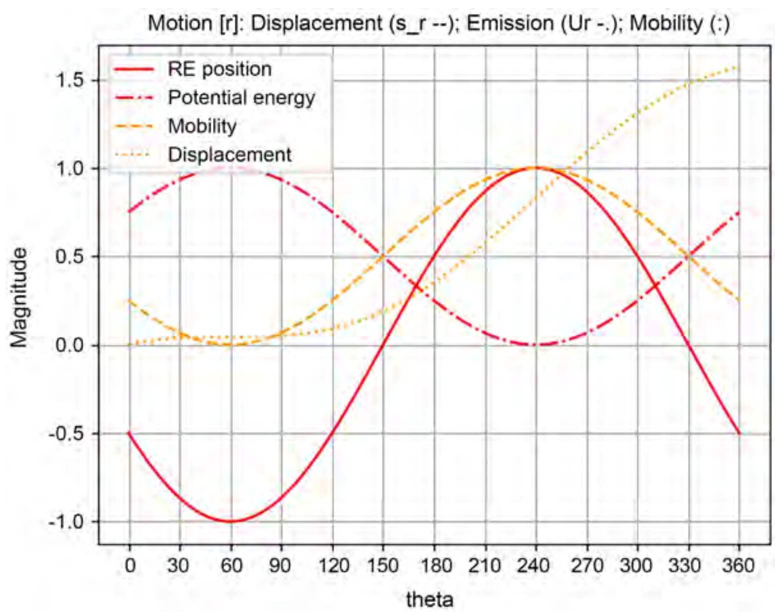

(b)

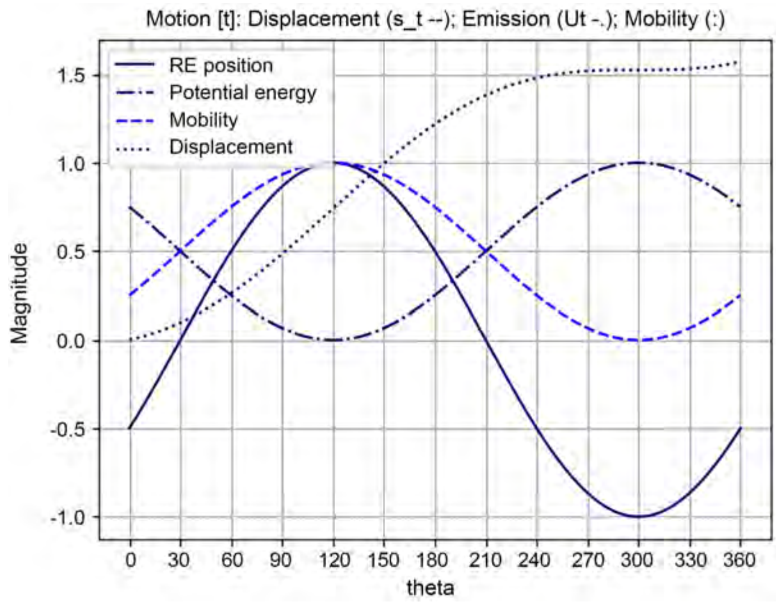

(c)

Figure 3. Motion parameters of the reactive end in the [*a*], [*r*], and [*t*] directions, as a function of energisation, for an electron with $\tau = 0.5$. (a) Motion parameters of the reactive end in the [*a*] direction. (b) Motion parameters of the reactive end in the [*r*] direction. (c) Motion parameters of the reactive end in the [*t*] direction.

3.3. Motion in One Direction

An interesting effect is observed when examining the emissions in one axis, say [a], as a function of location. There are several aspects to this, as follow.

3.3.1. Compressed Pulse of Emissions—The Discrete Force

Both the strength of the emissions U_a and the displaced position of the reactive end s_a depend on the phase angle, but differently. Consequently if emissions are plotted against the displacement, then a localised effect is apparent, see Figure 4. The emissions strengthen rapidly while the displacement stalls, creating a peak.

The result is the emissions are compressed into a pulse during motion, at least when one axis is considered. This confirms and expands on the idea in the early works of the theory, where the emissions were premised to comprise a "discrete force" travelling in a flux tube [6]. Depending on which functionality one wishes to emphasise, the emissions can be thought of as either smooth or discrete. Parts of the theory that use the smooth emission concept are the theory for the relativistic Doppler [6], whereas the discrete concept is apparent in the explanation for asymmetrical baryogenesis [12] and the remanufacture of particle identity more generally (decay) [14] [28]. Either perspective is suitable for the synchronous (strong) interaction [20] and the explanation of nuclear structure [21] [22]. Note that the pulse effect depends on the energisation phase θ, and also the velocity, though this is not apparent in the figure as the data have been normalised.

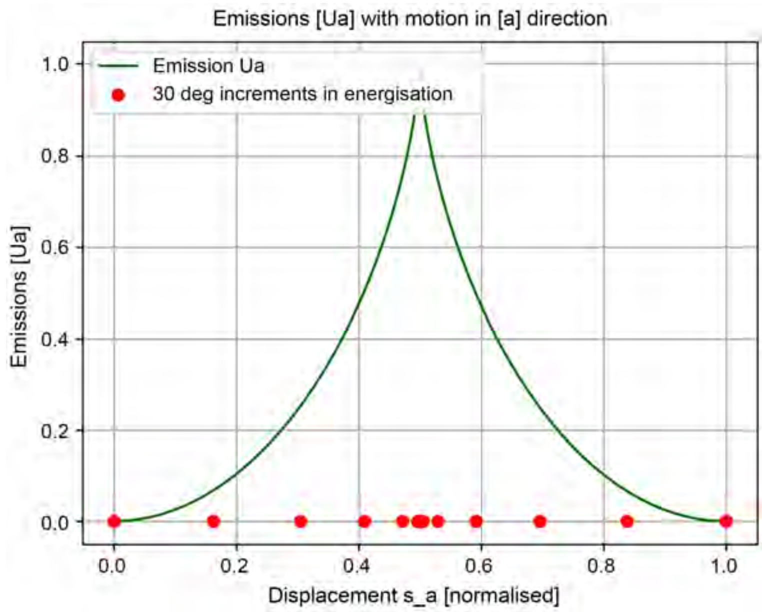

Figure 4. Emissions in $[a]$ as a function of displacement in the same direction. Displacement has been normalised by dividing by $P_a = \tau\pi$. Red dots indicate sample locations of the reactive end, and show how it initially moves quickly, slows to a momentary stop, and then quickens its displacement again.

3.3.2. Gait Locomotion of Two Reactive Ends

Up to here all the analysis has been on one reactive end only. An interesting observation is obtained when examining both reactive ends, see Figure 5. This shows that the one reactive end quickly advances while the other is tending towards being stationary. As the fibril connects the reactive ends, it means that the fibril itself takes oblique angles during the motion. As the energisation alternates, so each reactive end in turn has an opportunity to move forward. An equivalent explanation is that the particle moves by partially tunnelling its de-energised reactive end forward at each energisation cycle. This is consistent with another part of the theory that explained the operation of interferometer partial mirrors [29]. As the reactive end moves, it drags the fibril with it, hence causing yaw on the fibril, and a zig-zag motion of the particle.

Thus velocity, in this interpretation, is discrete translational displacement per frequency cycle. In contrast classic physics tends to see velocity as a continuous motion, and quantum theory sees it as an intrinsic (or mathematical) property of the particle, and also implies it is continuous (albeit uncertain).

We refer to this motion as *gait,* as it is similar to the bipedal gait of human locomotion, where one foot is fixed to the ground while the other does the toe off, swing-through, and heel strike. Conceptually there need be no issue with the idea that a gait locomotion can result in an overall velocity that is approximately continuous.

Note that the emissions of the two reactive ends (A and B) are complementary. The potential energy in the emissions of A are of the form $UA_r = \sin^2(\theta/2)$ while those at the B reactive end are $UB_r = \cos^2(\theta/2)$ and this sums to unity.

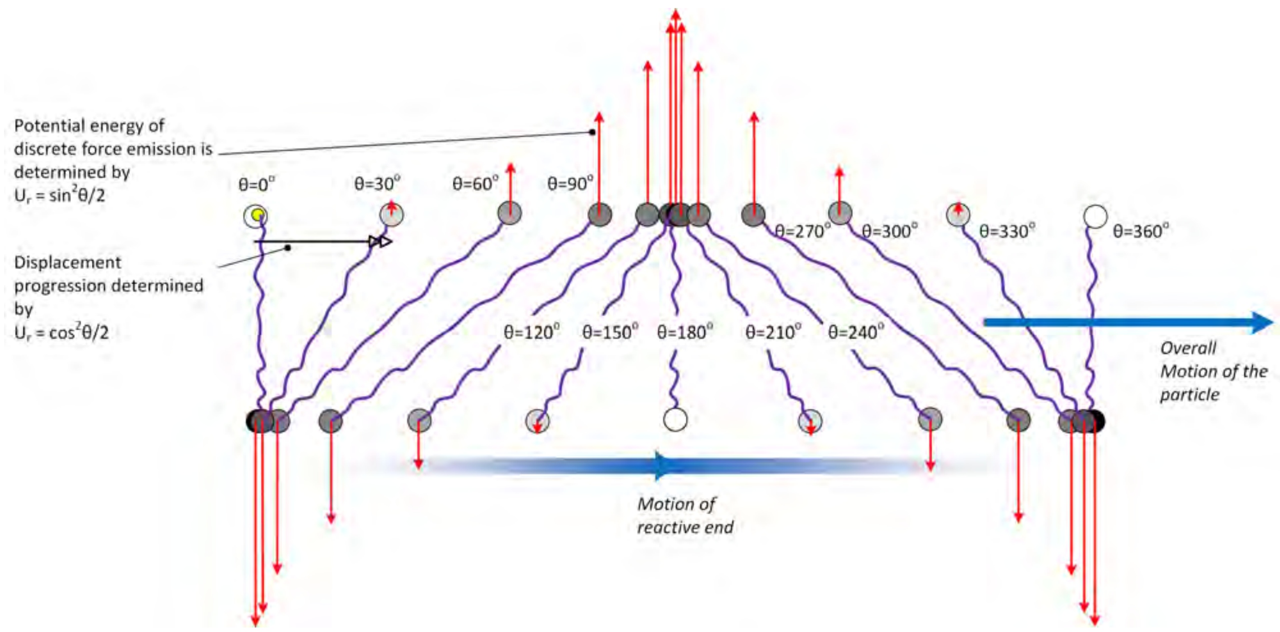

Figure 5. Energisation phase determines the potential energy of a reactive end and also its displacement progression, resulting in a pulse of emissions.

3.3.3. Regression of the Flux Tube

As the particle moves forward the discrete force emissions propagate out into space at the local speed of light, over a spherical front. Over one gait cycle the particle itself moves forward a distance S_a. Meanwhile the discrete forces have moved radially outward to a distance of c/f where c is the speed of light. Consequently the locus of the flux tube trails (regresses) behind the particle. This is similar to the light cone concept in relativity. On average this angle is given by

$$\beta = \tan^{-1} v/c \tag{9}$$

where β is measured from the normal to the velocity. Hence for a stationary particle $\beta = 0^\circ$ and for one travelling at the speed of light $\beta = 90^\circ$. However since the motion of the particle is non-uniform, the location from which the emission occurs needs to be taken into account. The result is a bent locus of the emitted field, see Figure 6 (dashed line).

Thus the flux tube for a moving particle trails the motion with an average orientation angle determined by its velocity and the local speed of light (which in turn is affected by the fabric density $\varnothing$, but with many small jogs corresponding to the phase where the energised reactive end stalls in its forward motion. This is consistent with the magnetism part of the theory, where the interaction is proposed to be communicated to remote moving particles by this distortion of the flux tube, see [11]. This variability of potential energy U_a is propagated out into space with the flux tube. Thus a remote particle will receive a compressed pulse of electrostatic field, with the jogs in the flux tube conveying information about the motion of the basal particle (magnetism). The three phases of the emissions $[U_a, U_r, U_t]$ convey the gravitational information [8].

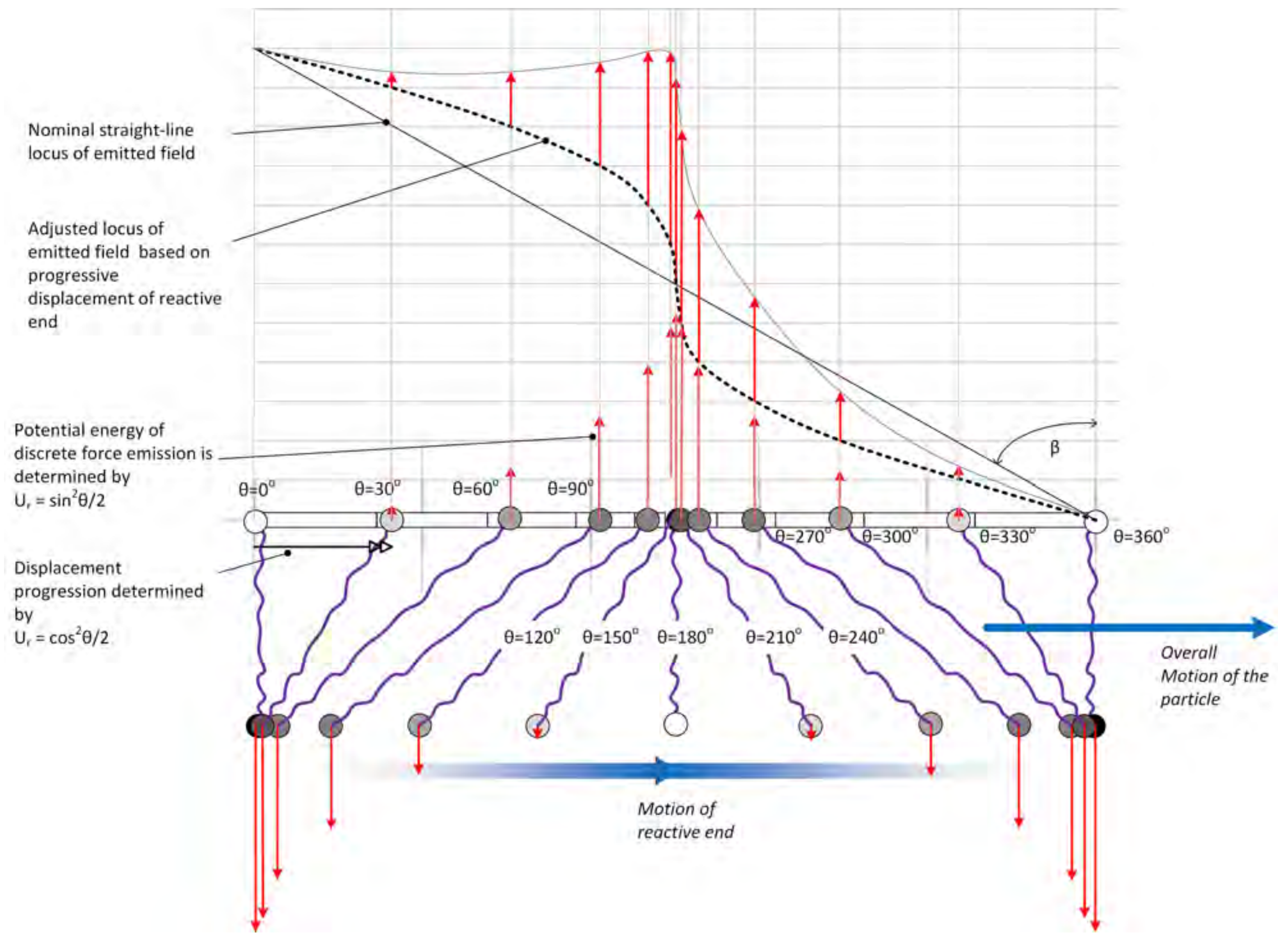

Figure 6. Locus of emitted discrete field in the radial (r) direction.

3.4. Orbit Motion of Reactive end during Translational Motion

For each of the directional axes [a], [r], and [t] there are a set of parameters that define the motion state: potential energy of the emissions in that direction U_i; mobility; position of the reactive end in its orbit (for a stationary particle); and motion displacement during the cycle s_i which is in response to the velocity shear τ.

At the end of the energisation cycles the motion displacement s_i does not undo the effect (as occurs with the orbital), but instead accumulates. Thus over multiple cycles the displacement accumulates, see Figure 7.

Motion in the [a] direction corresponds to no change in the orbital positions in the [r] and [t] directions, and the overall effect is a spiral motion of the reactive end, see Figure 8. This is not a smooth helix, because of the aforementioned dwell part way through.

The idea of the reactive end moving in a circular orbit goes some way to providing a physical explanation for particle frequency. A key principle in QM is that of particles having a relationship between frequency & energy ($E = hf$), and wavelength & momentum ($p = h/\lambda$), hence wave particle duality. Within QM there are two different formalisms for frequency, based on relativistic and

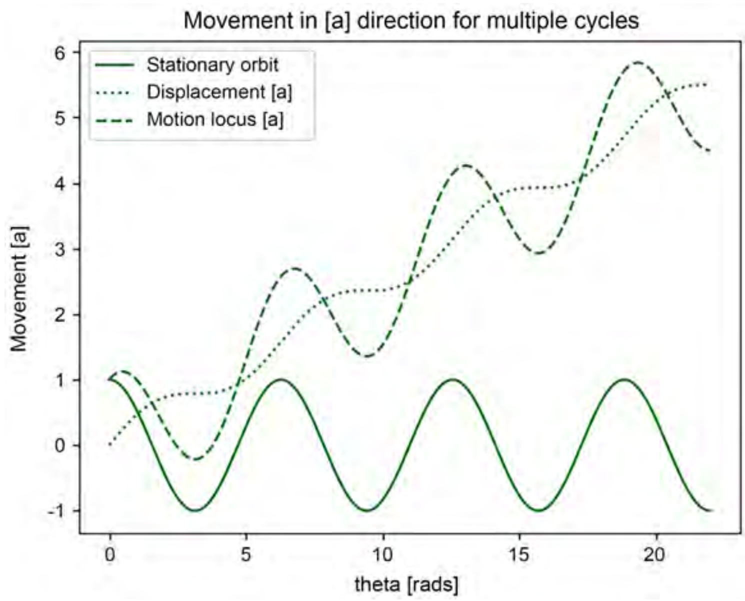

Figure 7. Cumulative displacement in the [a] direction over multiple energisation cycles, for an electron with $\tau = 0.5$ and $R_{RE} = 1$.

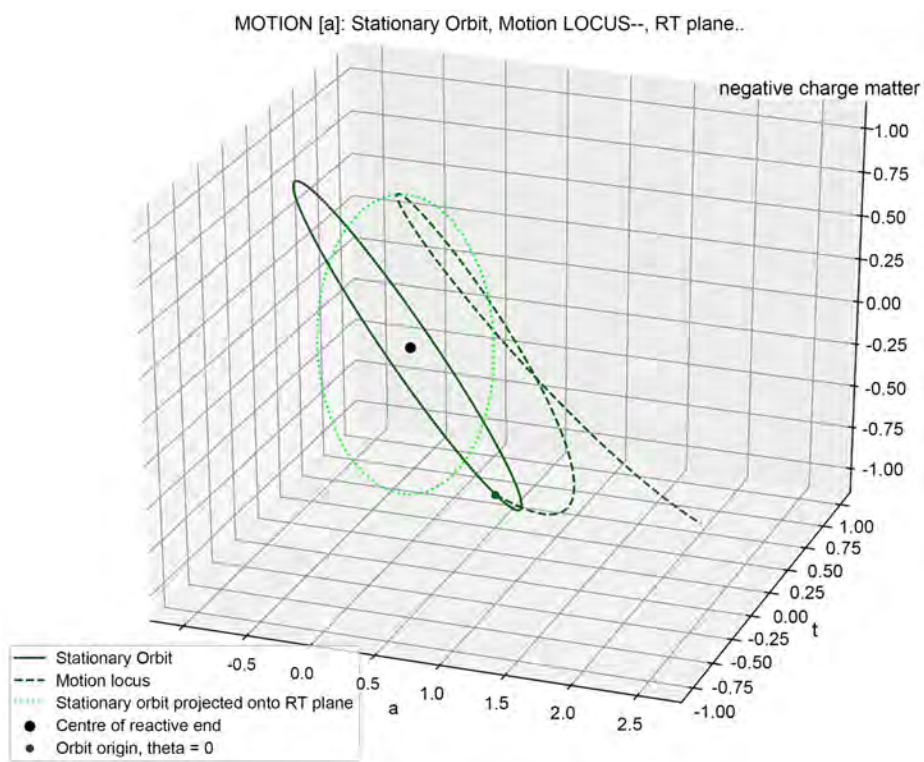

Figure 8. Motion of the reactive end over one energisation cycle, showing the spiral nature of the movement, for an electron with $\tau = 0.5$ and $R_{RE} = 1$. Vertical axis is [r]. Note that the helix angle is not constant, but rather is a periodic variable.

Schrödinger nonrelativistic considerations. The relativistic one is believed to be more accurate [27]. The frequency of the electron for the relativistic version is =7.81E20 s^{-1}, hence the duration of one cycle is 8.04505E-21s. However there is no physical description for frequency within QM, which is understandable since QM assumes 0D point particles. The present theory provides an explicit representation for frequency as the periodic energisation of the reactive ends, and the concurrent circular motion of the reactive end.

3.5. A Note on Time

The analysis has been with energisation as the variable, rather than time. Degree of energisation θ is the proxy for time. The reasons for this are somewhat complex because the theory integrates both the relativistic and quantum concepts of time, as follows.

In this theory time at the macroscopic scale is an emergent property of matter [24]. Specifically time arises from the energisation sequence of particles. It is emergent because particles emit discrete fields as part of their energisation, and hence an observer will experience a fabric of discrete forces from the surrounding spatial distribution of matter. In turn this fabric affects the macroscopic passage of time, by obstructing the emissions of the particles in the observer's own timepiece whether that be a mechanical, biological, atomic, or any other type of clock. Thus time dilation occurs in regions of higher fabric density $\varnothing$, or higher gravitational field [6] [24].

This raises a deeper question: What determines the frequency of the particle? As one critic of this theory observed, "time cannot be defined as oscillation frequency of a particule, because frequency itself requires time" [30]. However we believe the answer is that the frequency is intrinsic to the type of particle, and is traced back to leptogenesis [12]. Hence an electron with discrete force structure of $e\left[a^1, r^1, t^1\right]$ will always have the same rest mass and frequency when measured in the situation of Earth, irrespective of what locus through space and other fabric densities that electron took to get here. In non-Earth situations where the fabric density is different, the frequency of the electron is expected to change [6]. However this will not be detectable from within the same situation, because all the particles in that situation will be likewise affected.

Hence at the particle level it is useful to ignore the effect of fabric density and instead consider the energisation sequence as the origin of time. The theory does not extend to describe the mechanism that regulates the energisation. At the macroscopic level of general relativity, the precise energisation details are less important than the malleability of particle frequency when subject to different fabric density, hence time dilation. At this level the single direction of time becomes apparent, due to entropic interactions between particles [23]. Also, at this level time can be approximated as a continuous phenomenon, as opposed to a discrete one. While the behaviour within a particle is coherent, at a macroscopic scale time is more obviously represented by the relatively slow non-coherent molecular interactions such as mechanical and physiological processes. There is no conceptual difficulty accommodating personal cognitive time and the simultaneity of interactions with other people in this model.

3.6. Application of the Theory to Other Motion Phenomena

3.6.1. Ponderomotive Force

The ponderomotive force moves a charged particle—of either sign—towards the weak field area when exposed to an inhomogeneous oscillating electromagnetic field. The mathematical derivation is well-established. The physical explanation per the current theory is that the orbital motion of the reactive end always has a component in the direction of the gradient of the external field, *i.e.* the reactive end moves up-gradient and down at each orbit. In this way the reactive end is able to sample the gradient of the external field [11]. The oscillating external field is neutral in its effect but its existence causes the reactive end to have more difficulty expressing its own discrete forces. This difficulty is greater at that part of the orbit experiencing the stronger field, e.g. closer to the source. Hence the reactive end favours that part of the orbit where it experiences less external harassment, and moves in the direction of weaker field. Thus the particle moves towards the weak field region.

The bending of light in a gravitational field could be considered an inverse ponderomotive force. The explanation is as above, except the photon has the oscillating field [15] and it experiences more resistance to motion in regions of higher external field gradient (or higher fabric density).

3.6.2. Linear Momentum

As shown above, this theory offers an explanation for a body continuing with velocity until acted on by an external force (Newton's law). However it is not immediately obvious—from an ontological perspective—why momentum should be the product of velocity and mass, and why this should be conserved. Derivation of the classical momentum equation from Newton's 3rd law for a collision is based on the two bodies experiencing the same impulse, *i.e.* the product of reaction force and time duration. The theory provides a physical explanation of this at the particle level.

Consider two cordus particles in a collision. Call the moving one the protagonist, and the stationary one the antagonist. We propose that momentum may be understood as the force response that an antagonist particle must make if it is to arrest the motion of the protagonist particle. The protagonist particle has a pulse of force emissions (see above) over a period of time (one frequency cycle). The antagonist particle is subject to all of this (namely $\int U \mathrm{d}t$), and must deal with it. The faster the protagonist moves the shorter the available interaction time and hence the antagonist has to mount a proportionally greater force response. Also, the emissions of the protagonist are increased by having more discrete forces, which relates to mass. In this theory, particle identity, and therefore also rest mass, is determined by the portfolio of discrete forces emitted by a particle [12] [31]. The more numerous these emissions the greater the mass. Hence both velocity and mass are included in the momentum formulation.

The explanation for why momentum is the product, rather than some other function of velocity and mass, is that the velocity of a particle arises from the fibril shear and its mass by the number of discrete forces, and there is no co-dependency between these variables. Both contribute in linear proportion to the momentum.

3.6.3. Mass and Momentum of the Photon

What about the momentum of the photon? The question relates to how a particle without mass also has momentum. This phenomenon may be explained in the cordus theory by noting that the photon emits discrete forces differently to massy particles: it emits only one discrete force (not a set of three), it emits and then withdraws its discrete force (rather than let it propagate further out into space), and while one reactive end emits the other withdraws (oscillatory reactive end behaviour) [29]. The absence of a mass property therefore arises because the photon's discrete force lacks the (*a*, *r*, *t*) energisation sequence, hence lacks the handed torsional effect that is necessary for mass and gravitation [11].

The apparent mass effect arises because when a photon strikes and is absorbed by a massy particle [18] such as an electron, the energy in the photon goes into the energisation of the recipient electron: specifically the frequency increases [19]. That corresponds to more rapid energisation of the electron. Since particle mass is determined by the number of discrete force emissions *and* the frequency thereof, the overall effect is to increase the mass of the recipient particle.

3.6.4. Bremsstrahlung Radiation under Deceleration

When moving under deceleration the gait of the particle has to be shortened. This is because the decelerating force acts at the reactive ends and causes them to be dislocated (retarded) in their progression. To shorten the gait involves the energisation cycle of the reactive end being truncated, so that some discrete force emissions cannot be completed. This abandonment of energisation requires the corresponding discrete forces to be expunged from the particle. They are instead released as independent discrete forces, which is a photon. The mechanism for this emission at the sub-particle level is shown in **Figure 9**. Several of these principles were adopted from [18] [19], with one important difference: in the bremsstrahlung case it appears that the photon reactive ends may detach sequentially, rather than simultaneously as in [18] [19].

The span of the photon is parallel to that of the electron. The gait theory of motion, with its inclined fibril, naturally concludes that the photon would be emitted in the forward arc. Furthermore, the higher the energy of the electron, the greater its frequency and the less inclined its fibril ($\beta \to 0^\circ$ in Equation (9)), so the photons ought to be emitted in a narrower forward cone. This is indeed what is observed in practice, with photon emission direction being increasing concentrated in the forward direction as electron energy increases [32].

The cordus theory suggests that if the bremsstrahlung electrons were all controlled for the orientation angles of the fibril [10], then the photon emissions ought to be directionally anisotropic in a bi-lobed distribution.

A neutral particle does not emit bremsstrahlung. The tentative explanation in the cordus theory is that the neutral particle only exists because it comprises two

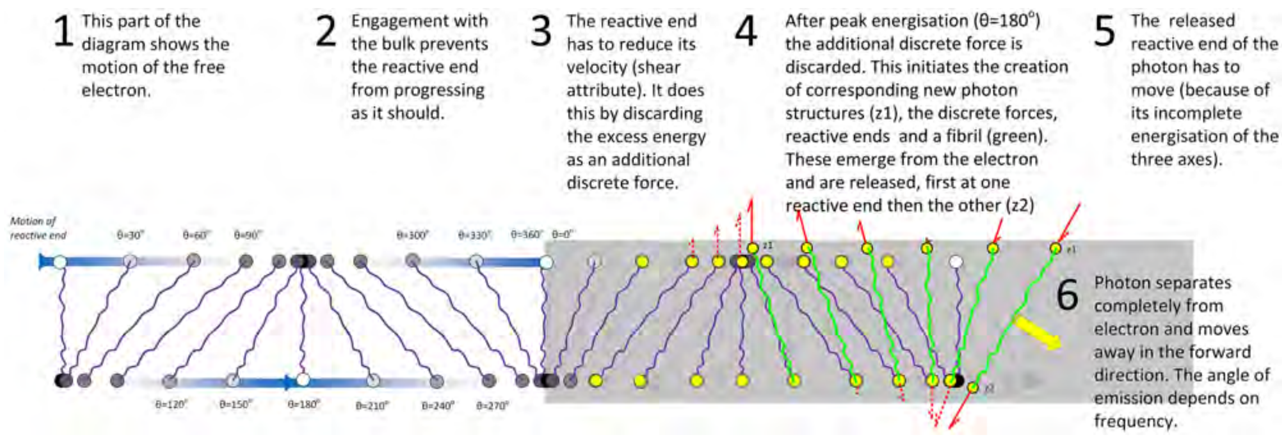

Figure 9. Proposed process whereby a photon is emitted from the electron in bremsstrahlung. The shortening of the electron gait results in photon emission.

or more fundamental particles of opposite charge, with their reactive ends co-located and synchronised in emissions. For an example of this applied to the neutron see [14] [20]. In this theory, charge sign is represented by medially vs. distally directed emissions for positive and negative charge respectively. Hence, the bremsstrahlung emission is proposed to be internally short-circuited: that of the negative discrete force is opposite in effect to that of the positive, so the whole emission is self-contained within the particle. The member particles accommodate the deceleration distress experienced by the other.

4. Discussion

4.1. Findings

The main finding is that, under this theory, the motion of a particle involves each reactive end taking a spiral-like locus, with the reactive ends being in opposite states of energisation. When viewed in one axis only, the motion appears as a gait, with each reactive end moving forward in turn. During motion, the emissions are compressed into a pulse or discrete force, at least when one axis is considered. These findings substantiate other parts of the cordus theory which assumed the existence of discrete forces (e.g. in the synchronous interaction binding the atomic nucleus [20] [22]) and of the flux tube (e.g. the relativistic considerations [6]).

We propose that the verification of the theory is provided by two mechanisms. First, the paper shows how the theory is consistent with observable motion phenomena (ponderomotive force, linear momentum, mass and momentum of the photon, bremsstrahlung radiation). This part of the work provides a descriptive treatment of the phenomena, which contributes to a potentially improved understanding of the underlying effects. The second mechanism of justification is provided by the wider theory, which provides multiple points of comparison with existing empirical observable phenomena. It also provides explanations for phenomena that are poorly understood by existing theories, e.g. asymmetrical baryogenesis [12], and nuclide stability [21]. Moreover, these explanations are coherent across all parts of the theory. Furthermore, it provides a single framework that covers aspects of particle, wave, and gravitational phenomena [8]. No claim is made that these justifications are at the level of proof, nonetheless they do provide a degree of confidence that the theory has sufficient merit to be considered as a candidate new theory of physics.

4.2. Contrast to Existing Theories

The philosophical basis of the cordus theory is that of physical realism—that physically observed attributes arise from physical substructures to the particle. This is different to the premise of quantum mechanics, where the fundamental particle is a zero dimensional (0-D) structure and its observables are attributed to intrinsic variables. As shown here, the idea of a particle having two ends leads to the idea that particle motion involves the reactive ends moving non-continuously. This is somewhat unexpected. Nonetheless the idea has several plausible aspects.

First, for any one reactive end, the position and velocity are conjugate variables, being derivatives of action. This is consistent with the Heisenberg uncertainty principle, hence the results are conceptually consistent with quantum mechanics. This is further reinforced by observing that the cordus theory predicts a potential energy of the reactive ends of the form $\sin^2\theta_i/2$ (Equation (1)), with the other reactive end taking $\cos^2\theta_i/2$. This is significant as the total energy in the particle is unity. This type of relationship is broadly consistent with QM.

Second, the idea of the reactive end moving with an orbital motion provides a physical explanation for frequency that is consistent with QM (which lacks a physical explanation for frequency). This orbital motion is related to the energisation cycle of the fibril and hence to the frequency of the particle itself.

Third, the flux tube with its three energisation components is consistent with prior cordus work that derived the relativistic Doppler from flux tube considerations [6]. Hence the theory accommodates both those great theories of physics, gravitation and quantum mechanics [8].

Fourth, the theory is qualitatively consistent with the observed behaviour of emissions in bremsstrahlung, specifically the forward direction of emission, and the narrower cone of emission with higher frequency.

Finally, the concept has some similarity with de Broglie's idea of the pilot wave [1] [2], in that one might consider the cordus theory as approximately equivalent to linear locus with a superimposed wave component.

Thus the gait locus of particle motion, while it seems strange at first, is compatible with other theories of physics, and with other developments in the cordus theory.

4.3. Critique and Future Work

While the motion of the particle is evident in the gait of the reactive ends, at a still deeper level the velocity of the particle is proposed to be a property of the shear in the fibril. The fibril is the structure that carries this property and causes the other structures (reactive ends and their emissions) to behave accordingly. At this time the theory does not anticipate how the internal shear interaction is physically based. It seems to imply a still deeper structure. In the case of quantum mechanics there is reason to believe that no deeper structure is permissible within that theory [33], though it can be argued that constraint merely arises because QM assumes from the outset that particles are 0-D points. In the case of the cordus theory there appears to be at least one level deeper, and potentially more.

The mathematical representation of the energisation and position of the reactive ends is a welcome development, since a common critique of previous reviewers of the theory has been the lack of a mathematical formulism. However, more remains to be done since there are other variables that need inclusion, see [10]. The number of such variables is similar to that of string theory. Hence the cordus theory may be compatible with string theory, but if so the correspondence of variables between them is not easy to establish. To fully describe a cordus particle it seems necessary to use a combination of continuous and discrete parameters, and it is not clear how this may be achieved.

5. Conclusions

The findings are that, under the assumptions of this theory, the motion of a particle occurs by each reactive end making an irregular spiral displacement in three dimensional space. The motion comprises a movement phase and a brief immobile phase.

This work makes several original conceptual contributions. The first is the conceptual contribution of offering a novel theory of particle motion. The existing literature on particle motion at the fundamental level is sparse. There has been a general assumption that particles, whether classical or quantum, move with a continuous (even if uncertain) velocity. The present gait theory suggests that at the deeper level this apparent continuity is made up of a more complex spiral locus of the particle. Another contribution is the derivation of a formulism for the energisation and mobility of the reactive ends, based on a set of plausible lemmas. This leads to an explicit relationship for the orbital motion of reactive end during translational motion, and hence the prediction of an irregular spiral motion of the particle. Further contributions are the provision of explanations for several physical phenomena: ponderomotive force, the nature of momentum, and bremsstrahlung radiation. Specifically, the theory explains why photon emission would be increasing concentrated in the forward direction with increased electron energy. Another novel contribution of a broad kind is that this theory provides a means to bridge quantum mechanics and special relativity, because it accommodates both particle uncertainty and field transmissions.

Acknowledgements

This work builds on earlier conceptual papers commencing with [7]. The contribution made by those authors to the development of the initial particle concept is acknowledged with gratitude.

Conflicts of Interest

The author declares no conflicts of interest regarding the publication of this paper.

References

[1] de Broglie, L. (1929) The Wave Nature of the Electron, in Nobel Lecture. Nobel Prize in Physics.

[2] Bohm, D. and Bub, J. (1966) *Reviews of Modern Physics*, **38**, 453-469. https://doi.org/10.1103/RevModPhys.38.453

[3] Das, A., *et al.* (2020) *Physical Review E*, **102**, Article ID: 062130.

[4] Shen, H.Z., *et al.* (2018) *Physical Review A*, **97**, Article ID: 042121.

[5] Wojnar, R. (2001) *Acta Physica Polonica*, *Series B*, **32**, 333-349.

[6] Pons, D.J., Pons, A.D. and Pons, A.J. (2018) *Journal of Modern Physics*, **9**, 500-523. https://doi.org/10.4236/jmp.2018.93035

[7] Pons, D.J., *et al.* (2012) *Physics Essays*, **25**, 132-140. https://doi.org/10.4006/0836-1398-25.1.132

[8] Pons, D.J. (2020) *Journal of Modern Physics*, **11**, 1598-1619. https://doi.org/10.4236/jmp.2020.1110100

[9] Pons, D.J. (2015) Internal Structure of the Electron (Image Licence Creative Commons Attribution 4.0). Wikimedia Commons, (Creative Commons Attribution 4.0 International License). https://commons.wikimedia.org/wiki/File:Internal_structure_of_the_electron.jpg

[10] Pons, D.J., Pons, A.D. and Pons, A.J. (2019) *Journal of Modern Physics*, **10**, 835-860. https://doi.org/10.4236/jmp.2019.107056

[11] Pons, D.J. (2020) *Journal of Modern Physics*, **11**, 1560-1575. https://doi.org/10.4236/jmp.2020.1110097

[12] Pons, D.J., Pons, A.D. and Pons, A.J. (2014) *Journal of Modern Physics*, **5**, 1980-1994. https://doi.org/10.4236/jmp.2014.517193

[13] Pons, D.J., Pons, A.D. and Pons, A.J. (2015) *Applied Physics Research*, **7**, 1-11. https://doi.org/10.5539/apr.v7n1p1

[14] Pons, D.J., Pons, A.D. and Pons, A.J. (2014) *Applied Physics Research*, **6**, 50-63. https://doi.org/10.5539/apr.v6n2p28

[15] Pons, D.J. (2015) Internal Structure of the Photon (Image Licence Creative Commons Attribution 4.0). Wikimedia Commons, (Creative Commons Attribution 4.0 International License). https://commons.wikimedia.org/wiki/File:Internal_structure_of_the_photon.jpg

[16] Pons, D.J., Pons, A.D. and Pons, A.J. (2014) *Applied Physics Research*, **6**, 28-46. https://doi.org/10.5539/apr.v6n2p28

[17] Pons, D.J., Pons, A.D. and Pons, A.J. (2015) *Journal of Nuclear and Particle Physics*, **5**, 58-69. https://doi.org/10.1155/2015/651361

[18] Pons, D.J. (2015) *Applied Physics Research*, **7**, 14-26. https://doi.org/10.5539/apr.v7n2p1

[19] Pons, D.J., Pons, A.D. and Pons, A.J. (2016) *Journal of Modern Physics*, **7**, 1049-1067. https://doi.org/10.4236/jmp.2016.710094

[20] Pons, D.J., Pons, A.D. and Pons, A.J. (2013) *Applied Physics Research*, **5**, 107-126. https://doi.org/10.5539/apr.v5n6p23

[21] Pons, D.J., Pons, A.D. and Pons, A.J. (2015) *Physics Research International*, **2015**, Article ID: 651361. https://doi.org/10.1155/2015/651361

[22] Pons, D.J., Pons, A.D. and Pons, A.J. (2013) *Applied Physics Research*, **5**, 145-174. https://doi.org/10.5539/apr.v5n6p23

[23] Pons, D.J., Pons, A.D. and Pons, A.J. (2016) *Journal of Modern Physics*, **7**, 1277-1295. https://doi.org/10.4236/jmp.2016.710113

[24] Pons, D.J., Pons, A.D. and Pons, A.J. (2013) *Applied Physics Research*, **5**, 23-47. https://doi.org/10.5539/apr.v5n6p23

[25] Pons, D.J. and Pons, A.D. (2013) *The Open Astronomy Journal*, **6**, 77-89. https://doi.org/10.2174/1874381101306010077

[26] Pons, D.J., Pons, A.D. and Pons, A.J. (2016) *Applied Physics Research*, **8**, 111-121. https://doi.org/10.5539/apr.v8n3p111

[27] Zürcher, U. (2016) *European Journal of Physics*, **37**, Article ID: 045401. https://doi.org/10.1088/0143-0807/37/4/045401

[28] Pons, D.J., Pons, A.D. and Pons, A.J. (2015) *Applied Physics Research*, **7**, 1-13. https://doi.org/10.5539/apr.v7n1p1

[29] Pons, D.J. (2020) *Optics*, **1**, 243-254. http://viXra.org/abs/2009.0004 https://doi.org/10.3390/opt1030018

[30] Lacina, K. (2014) *Applied Physics Research*, **1**, 26-34.

[31] Pons, D.J., Pons, A.D. and Pons, A.J. (2014) *Physics Essays*, **27**, 26-35. https://doi.org/10.4006/0836-1398-27.1.26

[32] Faw, R.E. and Shultis, J.K. (2003) Radiation Sources. In: Meyers, R.A., Ed., *Encyclopedia of Physical Science and Technology*, Third Edition, Academic Press, New York, 613-631. https://doi.org/10.1016/B0-12-227410-5/00636-0

[33] Colbeck, R. and Renner, R. (2011) *Nature Communications*, **2**, 5. https://doi.org/10.1038/ncomms1416

Scientific Research Publishing

Journal of Modern Physics, 2021, 12, 1954-1959
https://www.scirp.org/journal/jmp
ISSN Online: 2153-120X
ISSN Print: 2153-1196

Koide Lepton Relation Explained by Lepton Radius (Compton Wavelength)/4

T. R. Mongan

84 Marin Avenue, Sausalito, CA, USA
Email: tmongan@gmail.com

How to cite this paper: Mongan, T.R. (2021) Koide Lepton Relation Explained by Lepton Radius (Compton Wavelength)/4. *Journal of Modern Physics*, **12**, 1954-1959.
https://doi.org/10.4236/jmp.2021.1214111

Received: November 12, 2021
Accepted: December 14, 2021
Published: December 17, 2021

Abstract

The intriguing Koide relation between lepton masses, $Q_1 = \frac{m_e + m_\mu + m_\tau}{\left(\sqrt{m_e} + \sqrt{m_\mu} + \sqrt{m_\tau}\right)^2} \approx 2/3$, involving electron mass m_e, muon mass m_μ, and tau mass m_τ, was first presented in 1982. The reason why $Q_1 \approx 2/3$ has long been unclear. However, describing Standard Model fermions as spheres with radius (Compton wavelength)/4, allows only three fermions in each charge state and avoids the infinite energy density of point particles. Then the Koide parameter $Q_1 \approx 2/3$ because the electron Compton wavelength is more than 200 times the muon and tau Compton wavelengths. A tau mass equivalent of 1776.98 MeV, within experimental error bars, would result in $Q_1 = 2/3$. The analysis is discussed in the context of efforts to extend the Standard Model of particle physics.

Keywords

Koide Relation, Standard Model Fermions, Extending the Standard Model

1. Introduction

People have wondered about the nature of fundamental particles for centuries. Our best model of fundamental particles at present is the Standard Model of particle physics that identifies the fundamental particles in our universe as twelve spin 1/2 point particles. Those twelve fundamental fermions, all with spin angular momentum $\hbar/2$ where $\hbar$ is the reduced Planck's constant, are comprised of three charge e leptons, three charge $\frac{2e}{3}$ quarks, three charge $-\frac{e}{3}$ quarks, where e is the electron charge, and three massless neutrinos with zero charge. Unfortunately, we know the Standard Model is incomplete, because observations [1] of neutrino oscillations show that neutrinos must have non-zero mass.

The quantum mechanical uncertainty principle tells us we cannot discern any structure within a particle of mass m that has dimensions smaller than the Compton wavelength $l = \frac{\hbar c}{mc^2}$. That does not mean there can be *no* structure with dimensions less than the Compton wavelength, but only that we can't directly observe it. We can make progress by assuming [2] fundamental fermions in the Standard Model have radius (Compton wavelength)/4, even though we can't directly observe objects of that size. That assumption avoids the problem of the infinite densities of point particles and it has consequences relevant to the Koide relation [3] between lepton masses.

The mass and pressure distribution inside fermions with radius (Compton wavelength)/4, involving their volume $\sim l^3$, their surface area $\sim l^2$, and their diameter $l/2$, results in cubic equations [2] for fermion Compton wavelengths l, allowing at most three particles in each charge state. Describing the mass and pressure distribution with surface and linear elements requires minimum surface shell thicknesses and axial core radii on the order of the Planck length $l_P = \sqrt{\frac{\hbar G}{c^3}}$. The total particle mass is then the sum of the mass equivalents of pressure, $m/2$, in the volume, the mass equivalent of surface pressure $\frac{\pi}{4} S l^2$, and the core mass Ll. So $\frac{4}{3}\pi\rho\left(\frac{l}{4}\right)^3 = \frac{4}{3}\pi\frac{\rho}{2}\left(\frac{l}{4}\right)^3 + 4\pi S\left(\frac{l}{4}\right)^2 + 2L\left(\frac{l}{2}\right)$. The discriminant Δ of the resulting cubic equation for fermion Compton wavelengths $Al^3 - Bl^2 - Cl = 0$, with $A = \frac{\pi}{96}\rho$, $B = \frac{\pi S}{4}$, and $C = 2L$, is $\Delta = B^2C^2 - 4AC^3$. Since the discriminant Δ of the cubic equation for fermion wavelengths is positive regardless of the sign of B, the cubic equation in l has three real roots corresponding to three fermion Compton wavelengths in each charge state. So, if one were to ask why there are only three lepton masses in the Koide lepton relation, the answer would be that describing Standard Model fermions as objects with radius (Compton wavelength)/4 allows only three leptons.

The background presented above regarding fermions with radius (Compton wavelength)/4 provides some insights into the otherwise somewhat puzzling Koide relation between lepton masses. First, it explains why only three lepton masses can be involved. Second, as shown in the following, the Koide parameter $Q_1 \approx 2/3$ is a consequence of the fact that the electron Compton wavelength is more than 200 times the muon and tau Compton wavelengths.

The following analysis is based on Particle Data Group 2020 data [4] specifying Standard Model fermion masses to six significant figures and the six significant figure value $\hbar c = 197.327\ \text{MeV}\cdot\text{F}$, where $1\ \text{F} = 1\times10^{-13}\ \text{cm}$, from CODATA 2021 [5] and NIST Reference on Constants, Units, and Uncertainty. This precision is necessary to show why the Koide parameter Q_1 is so close to

2/3.

2. Koide Q and Lepton Wavelengths

The lepton mass equivalents[4] $m_e = 0.510999$ MeV, $m_\mu = 105.658$ MeV, and $m_\tau = 1776.86$ MeV define the lepton Compton wavelengths by $l = \hbar c / mc^2$. The lepton wavelengths $l_e = 386$ F, $l_\mu = 1.87$ F, and $l_\tau = 0.111$ F then determine three parameters l_e, l_{avg}, and θ_1 related to the three roots of the cubic equation [2] in l that describe the axial, surface, and volume energy distribution within leptons. Then, as seen below, the Koide parameter $Q_1 \approx 2/3$ because the electron Compton wavelength is more than 200 times the muon and tau Compton wavelengths, and a tau mass equivalent of 1776.98 MeV, within experimental [4] error bars, would result in $Q_1 = 2/3$.

Written in terms of Compton wavelengths, Koide's parameter is $Q_1 = \dfrac{\left(\frac{1}{l_e} + \frac{1}{l_\mu} + \frac{1}{l_\tau}\right)}{\left(\frac{1}{\sqrt{l_e}} + \frac{1}{\sqrt{l_\mu}} + \frac{1}{\sqrt{l_\tau}}\right)^2}$. Solutions to the cubic equation [2] in l for leptons with radius $l/4$, specifying the axial, surface, and volume energy distributions in leptons, are projections on the l axis of vertices of a Nickalls [6] equilateral triangle centered on average lepton wavelength $l_{avg} = \frac{1}{3}\left(l_e + l_\mu + l_\tau\right) = 129.375$ F. Those Nickalls wavelengths [6] are $l_e = l_{avg} + R_1 \cos\theta_1$, $l_\mu = l_{avg} - \frac{1}{2} R_1 \cos\theta_1 + \frac{\sqrt{3}}{2} R_1 \sin\theta_1$, and $l_\tau = l_{avg} - \frac{1}{2} R_1 \cos\theta_1 - \frac{\sqrt{3}}{2} R_1 \sin\theta_1$, where $\tan\theta_1 = \dfrac{l_\mu - l_\tau}{\sqrt{3}\left(l_e - l_{avg}\right)}$, $\theta_1 = 0.00394944$, and $R_1 = \dfrac{l_e - l_{avg}}{\cos\theta_1} = 256.773$ F, resulting in $Q_1 = 0.666661$. The electron Compton wavelength l_e is much greater than the muon Compton wavelength l_μ and the tau Compton wavelength l_τ, because the electron mass m_e is much less than the muon mass m_μ and the tau mass m_τ, resulting in the angle $\theta_1 \ll 1$. So, $Q_1 \approx 2/3$ results from electron mass less than 1% of muon or tau mass.

The scale of the equilateral triangle specifying lepton wavelengths is determined by the Nickalls radius R_1 of the circle circumscribing the triangle centered at $l_{avg} = 129.375$ F, and the orientation of the Nickalls triangle is determined by the angle θ_1 between the l axis and a line between the center of the circle and the vertex corresponding to the largest Compton wavelength. Koide's parameter Q_1 is very sensitive to θ_1. Fixing R_1 at 256.773 F and l_{avg} at 129.375 F, an increase in θ_1 by only 0.007% to $\theta_1 = 0.003944701$ increases Koide's Q_1 to $Q_1 = 0.6666666$. That increase in θ_1 does not change the electron mass m_e or the muon mass m_μ, but it does increase the tau mass m_τ slightly to 1776.98 MeV, a result within PDG 2020 [4] error bars.

Analogous Koide parameters can be identified for quarks and neutrinos. Quark masses $m_u = 2.16$ MeV, $m_c = 1270$ MeV, and $m_t = 173$ GeV, with charge $2e/3$, and $m_d = 4.67$ MeV, $m_s = 93$ MeV, and $m_b = 4180$ MeV, with charge $-e/3$, consistent with PDG 2020 data [4], result in $Q_{2/3} = 0.85$ and $Q_{-1/3} = 0.73$. If fundamental fermions are Godel solutions [2] to Einstein's equations and electron neutrino vacuum energy density = (cosmic vacuum energy density), $m_{e\nu} = 0.00136$ eV. Neutrino oscillation data [1] then estimate $m_{\mu\nu} = 0.00858$ eV and $m_{\tau\nu} = 0.0508$ eV, with neutrino mass sum 0.061 eV about half Vagnozzi's upper bound [7] 0.12 eV, and $Q_0 = 0.48$.

3. Concluding Remarks

None of the results and conclusions in the preceding discussion, except those related to neutrino mass estimates, are affected by the following remarks. However, we can go further in considering the nature of Standard Model fermions by identifying them with Godel solutions to Einstein's equations rotating with angular velocity ω, with an average matter density ρ equal to the average fermion mass density, pressure $\frac{1}{2}\rho c^2$ from negative vacuum energy density $-\frac{1}{2}\rho c^2$, and an effective internal gravitational constant $G_f = \frac{\omega^2}{4\pi\rho}$. If half of any fundamental fermion charge is located at radius (Compton wavelength)/4 on the axis of rotation, fermion rotation does not cause radiative loss of energy from accelerated charge. The orientation of the fermion rotation axis is unknown until the z component of fermion angular momentum is measured, so the fermion mass will appear sinusoidally distributed on a disk of radius (l/4) perpendicular to the line of sight.

Three positive Compton wavelengths in each charge state require negative surface mass equivalent density S and positive mass L per unit core length. Negative S results from positive vacuum energy density $\frac{1}{2}\rho c^2$ within the shell that is opposite the negative vacuum energy density $-\frac{1}{2}\rho c^2$ in the volume. Then the negative pressure equivalent mass inside the shell counters the positive pressure equivalent mass in the volume. So, with no net pressure at the fermion surface, no force acts to increase or decrease fermion size, as necessary for stable fundamental fermions as Godel solutions within our universe. The sum of fundamental fermion mass components is $\frac{\pi}{48}\rho l^3$, with surface mass component $-\frac{\pi}{32}\rho l_{avg} l^2$ and core mass component $\frac{\pi}{64} l\left(l_{avg}^2 - \frac{R^2}{4}\right)$. So, the surface mass multiple of the total mass is $-\frac{3}{2}\frac{l_{avg}}{l}$ and the core mass multiple of the total mass is $\frac{3}{4}\frac{l_{avg}^2 - \frac{R^2}{4}}{l^2}$. The surface mass and core mass multiples increase in magnitude with decreasing l because smaller fermion volumes at smaller l decrease the volume occupied by positive pressure from negative vacuum energy density of Godel solutions, but the magnitude of the ratio (surface mass)/(core mass) $= -\frac{2ll_{avg}}{l_{avg}^2 - \frac{R^2}{4}}$ increases with l.

The internal gravitational constant G_l for fundamental fermions with radius $l/4$, identified as Godel solutions to Einstein's equations, is determined by Godel's relation $\omega = 2\sqrt{\pi G_l \rho}$ with the fermion matter density $\rho = \frac{48\hbar}{\pi c^2 l^4}$ and the angular velocity ω of the Godel solutions. Fermions with radius $l/4$ and core radius r have moment of inertia $I = \frac{2}{5}\frac{m}{2}\left(\frac{l}{4}\right)^2 + \frac{2}{3}\frac{\pi}{4}Sl^2\left(\frac{l}{4}\right)^2 + \frac{1}{2}Llr^2$. The last term in I is negligible because $r \ll l$, so the resulting internal fundamental fermion gravitational constant is $G_l = \frac{3c^3l^4}{\hbar\left(l - l_{avg}\right)^2}$.

The angular velocity of the fermion spheres is $\omega = \frac{\hbar}{2I} = \frac{8c}{0.2l - l_{avg}}$ and the tangential speed v_T of points on the spherical shell equator as a multiple of the speed of light is $\frac{v_T}{c} = \frac{\omega l}{4c} = \frac{2l}{0.2l - l_{avg}}$. Closed time-like curves can exist within the Godel solutions corresponding to the lowest mass fermions in each charge state, where $\frac{v_T}{c} > 1$. Such closed time-like curves would be unacceptable in Godel cosmologies, because they seem to prevent evolution of the cosmos in time. However, they are not problematic in the case of first generation Standard Model fermions that do not evolve in time from their creation to annihilation.

Classical physics idealizes the force of gravity between extended bodies as the force between point masses concentrated at the center of mass of each body. The mathematical construct corresponding to the center of mass of extended Standard Model fermions provides a link to the idealization of point particles in quantum mechanics. At the instant of particle-antiparticle creation, the centers of mass of the respective Godel solutions to Einstein's equations coincide and their spin axes are oppositely aligned. Correspondingly, at the instant of particle-antiparticle annihilation, the centers of mass of the respective Godel solutions to Einstein's equations coincide and the spin axes are oppositely aligned.

This description of Standard Model fermions as Godel solutions to Einstein's equations is fully consistent with experimental evidence. Any unfamiliar characteristics of this description of Standard Model fermions should not be a reason for abandoning the model, given the equally unfamiliar (at the time) aspects of quantum mechanical description of atoms, and early indications from general relativity of the existence of black holes.

Future work should focus on efforts to understand the interactions of various Godel solutions to Einstein's equations bearing half of any associated charge at radius (Compton wavelength)/4 on their axis of rotation. Such a simple combination of ideas from general relativity and quantum mechanics may provide further insight into the nature of elementary particles, but it is certainly *not* the long sought unification of general relativity and quantum mechanics. Any such unification must face the fundamental difficulty that general relativity can be seen as a theory *of* space, while quantum mechanics is a theory describing events within space.

Conflicts of Interest

The author declares no conflicts of interest regarding the publication of this paper.

References

[1] Capozzi, F., Lisi, E., Marrone, A., Montanino, D. and Palazzo, A. (2016) *Nuclear Physics B*, **908**, 218. https://doi.org/10.1016/j.nuclphysb.2016.02.016

[2] Mongan, T.R. (2021) *Journal of Modern Physics*, **12**, 983-987. https://doi.org/10.4236/jmp.2021.127060

[3] Koide, Y. (1982) *Lettere al Nuovo Cimento*, **34**, 201-205. https://doi.org/10.1007/BF02817096

[4] Zyla, P.A., *et al.* (2020) *Progress of Theoretical and Experimental Physics*, 083C01.

[5] Tiesinga, E., *et al.* (2021) *Journal of Physical and Chemical Reference Data*, **50**, 033105. https://doi.org/10.1063/5.0064853

[6] Nickalls, R.W.D. (1993) *The Mathematical Gazette*, **77**, 354. https://doi.org/10.2307/3619777

[7] Vagnozzi, S. (2019) Cosmological Searches for the Neutrino Mass Scale and Mass Ordering. Stockholm University, Stockholm.

Journal of Modern Physics, 2021, 12, 1960-1965
https://www.scirp.org/journal/jmp
ISSN Online: 2153-120X
ISSN Print: 2153-1196

Multidimensional Effects on Diffusion of a Particle in Tilted Periodic Potentials

Huanhuan Luo, Zhanwu Bai

Department of Mathematics and Physics, North China Electric Power University, Baoding, China
Email: 2678025575@qq.com, baizhanwu@126.com

How to cite this paper: Luo, H.H. and Bai, Z.W. (2021) Multidimensional Effects on Diffusion of a Particle in Tilted Periodic Potentials. *Journal of Modern Physics*, **12**, 1960-1965.
https://doi.org/10.4236/jmp.2021.1214112

Received: November 8, 2021
Accepted: December 19, 2021
Published: December 22, 2021

Abstract

This study investigates the diffusive motion of a Brownian particle in a 2D tilted periodic potential, where bias force is exerted in the x direction. The dimension effect is revealed by simulating the Langevin equation. The diffusion coefficient in x and y directions is a nonmonotonic function of the bias force, and a massive enhancement is observed in x and y directions in comparison with the case without a tilt in x direction. The underlying physical mechanism is explored.

Keywords

Surface Diffusion, Tilted Periodic Potential, Dimensionality, Langevin Simulation

1. Introduction

Many physical situations can be described by the diffusion of a Brownian particle in a tilted periodic potential; such situations include Josephson junctions [1], rotating dipoles in external fields [2], rotation of molecules in solids [3], superionic conductors [4], charge density waves [5], mode locking in laser gyroscopes [6], diffusion of atoms and molecules on crystal surfaces [7], particle separation by electrophoresis [8]. For the diffusion of an overdamped Brownian particle in a tilted periodic potential, an exact analytical expression for the effective diffusion coefficient is derived for arbitrary potentials and arbitrary strengths of the thermal noise [9]. The effective diffusion coefficient in a critically tilted periodic potential may be, in principle, arbitrarily enhanced in comparison with the potential-free thermal diffusion. A study has shown that in the underdamped case the diffusion coefficient is increased exponentially by a decrease in temperature in a certain interval of bias force [10], which originates from the correlation time of velocity increases exponentially with an increase in the inverse temperature. The nonmonotonic behavior of the effective diffusion index and superballistic diffusion are observed [11] when the noise intensity is weak and the external force is close to the critical value at which local minima of the potential just vanish. Lévy particles exist in either a running state or a long-tailed behind state, the distance at which the two-state centers increase with time plays a definitive role in superballistic diffusion. Langevin simulation has shown that for super-ohmic damping and certain parameters, the diffusive process of a particle in a titled periodic potential sequentially undergoes four time regimes: thermalization, hyperdiffusion, collapse, and asymptotical restoration [12]. A reformational ballistic diffusive system is considered a marginal situation that does not exhibit the collapsed state of diffusion. The diffusion properties of a vibrational motor, in which an additional time-dependent driving brings the system out of equilibrium and the other time-periodic driving fills the role usually played by noise, are investigated in [13]. The diffusion coefficient exhibits a nonmonotonic function of bias force due to the coexisting attractors, and an enhancement of diffusion phenomenon was observed. The analytical form of the effective free energy function in the model of entropic resonance is changed with addition of a bias force in a periodic potential, as shown in [14].

For surface diffusion problem, at least two degrees of freedom are concerned. Several multidimensional effects have been investigated. Based on the previous research on one-dimensional periodic potential, this paper extends to two-dimensional, thus highlighting the innovation. Molecular dynamics simulations conducted based on the Bhatnagar-Gross-Krook model have shown that the x-y coupling suppresses a large proportion of long jumps causing a decrease in the diffusion coefficient for all values of damping [15]. This effect can be attributed to the narrowing of the saddles with respect to the well bottom. Two kinds of approximation schemes, namely quasi-2D approximation and effective potential approach, have been applied to predict the 2D diffusion rate of a particle [16]; the results of these schemes are qualitatively in agreement with the numerical results. The 2D diffusion rate constant over noise intensity shows a nonmonotonic behaviors function of noise intensity, in contrast to the monotonic behavior in 1D case [17] [18]. In the present work, the dimensional effect in a tilted periodic potential is investigated.

2. Model

We consider a Brownian particle diffusing in a 2D coupled periodic potential under the influence of Gaussian white noise; the particle is contact with a heat bath at temperature T which provides fluctuation and dissipation. The dynamics of the process is governed by the following Langevin equations

$$\begin{aligned} &\dot{x} = v_x,\, m\dot{v}_x + m\gamma v_x + \frac{\partial U}{\partial x} = f_x + \xi, \\ &\dot{y} = v_y,\, m\dot{v}_y + m\gamma v_y + \frac{\partial U}{\partial y} = \xi, \end{aligned} \tag{1}$$

where U is a 2D coupled periodic potential, given by

$$U = U(x, y) = u_0 [\cos x + \cos y] + u_1 \cos x \cos y, \tag{2}$$

and ξ is a zero mean Gaussian white noise satisfying the fluctuation-dissipation theorem

$$\langle \xi(t) \xi(t') \rangle = 2m\gamma k_B T \delta(t - t'), \tag{3}$$

where f_x is a constant force exerted in the x direction, m is the mass of the Brownian particle, γ is the damping coefficient, and k_B is the Boltzmann constant. The profile of the 2D tilted periodic potential $V(x, y) = u_0 [\cos x + \cos y] + u_1 \cos x \cos y - f_x x$ is plotted in **Figure 1**. What we wish to investigate is the difference between the above-mentioned model and the 1D tilted periodic potential, and how the the bias force in x direction f_x influences the diffusion in y direction.

3. Langevin Simulation Results and the Underlying Physical Mechanisms

Langevin and the Fokker-Planck equations are most popular approaches for investigating surface diffusion. Although several analytical methods for the solution of 1D Langevin and Fokker-Planck equations are available [19], making any analytical progress is usually difficult on a set of multidimensional coupled equations. We simulate the Langevin Equation (1) by the second-order Runge-Kutta algorithm. In the calculation, the natural unit ($m = 1$, $k_B = 1$), the dimensionless parameter $V_0 = 1$, and the time step $\Delta t = 10^{-3}$ are used. The results are stable for time steps in the vicinity of the one we used. The test particles start from the a potential well and have zero velocity. The number of test particles $N = 2 \times 10^5$ is used to describe the surface diffusion motion of a Brownian particle. A quantity of fundamental interest in surface diffusion is the diffusion coefficient, which is defined as

$$D = \lim_{t \to \infty} \left\langle \left(\Delta \vec{r}(t) \right)^2 \right\rangle \Big/ 2dt = \lim_{t \to \infty} \left[\left\langle \left(\Delta x(t) \right)^2 \right\rangle + \left\langle \left(\Delta y(t) \right)^2 \right\rangle \right] \Big/ 2dt, \tag{4}$$

where d is the spatial dimension. The mean square displacement $\left\langle \left(\Delta \vec{r}(t) \right)^2 \right\rangle$ reveals a good linear relation at long times.

Figure 2 shows the influence of the tilt in x direction on the diffusion in y direction. The purpose of this figure is twofold. First, it presents a comparison of cases with and without tilt. Second, it displays a nonmonotonic relation of the diffusion coefficient with the tilt. The diffusion coefficient increases when the bias force is exerted. The physical mechanism is as follows: the particle with a high velocity in y direction accelerates in x direction, leading to a much larger resultant velocity; consequently, the particle can across the potential barrier in y direction along a direction between x and y axes, and the running state in y direction is formed. The coexistence of the locked state and running state results in rapid diffusion. Such a physical picture is confirmed by the velocity distribution in y direction (**Figure 3**). We can see that the number of particles with high

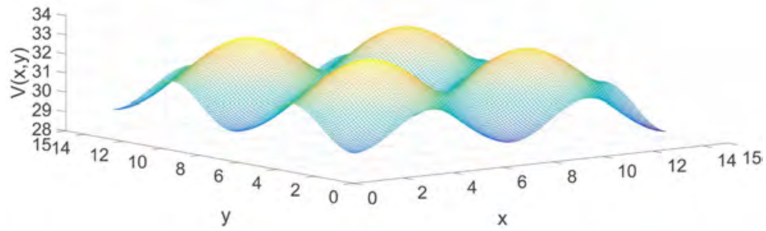

Figure 1. The profile of the 2D tilted periodic potential.

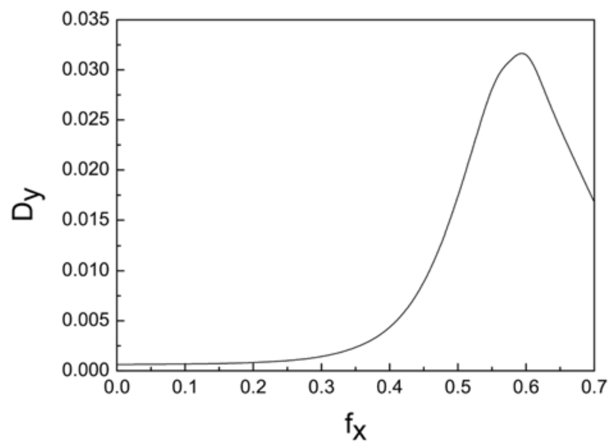

Figure 2. Diffusion coefficient in y direction versus the bias force in x direction. Where $T = 0.3$, $V_b = 1$, $\gamma = 0.2$.

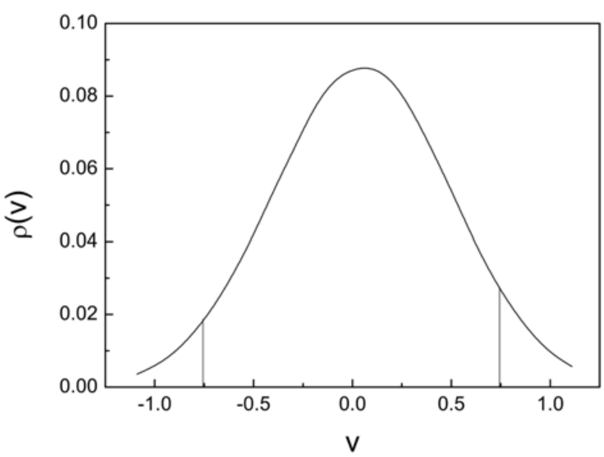

Figure 3. Velocity distribution in y direction. Where $T = 0.2$, $V_b = 1$, $\gamma = 0.2$, $f_x = 0.5$, and time $t = 300$.

positive velocities is obviously greater than that with negative values. The non-monotonic dependence on bias force can be explained as follows: as the bias force increases, the resultant velocities tend to x direction, and the number of particles in running state in y direction decreases gradually. These phenomena imply that the diffusion in one direction can be controlled by exerting a force in another direction. A comparison of the diffusion coefficient for x direction in two and one dimensions is shown in Figure 4. The dependence of the diffusion

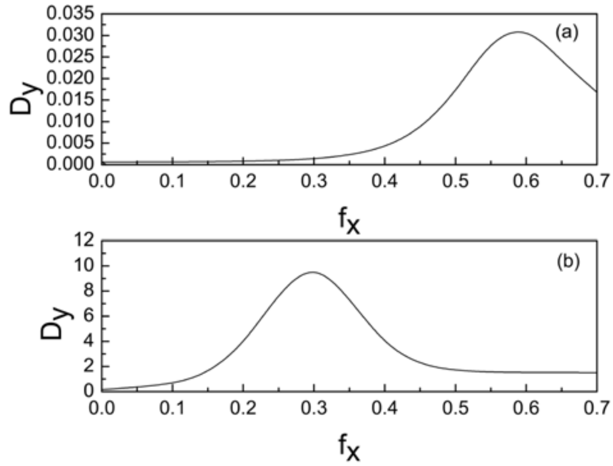

Figure 4. Diffusion coefficient in x direction versus the bias force in x direction. Where $T = 0.3$, $V_b = 1$, $\gamma = 0.2$, (a) for 2D case; (b) for 1D case.

coefficient on the bias force presents a nonmonotonic relation. In contrast to the diffusion coefficient arriving its maximum when $f_x < f_{xc}$ (f_{xc} is the critic tilt where the potential barrier vanishes, here $f_{xc} = 0.5$) in the 1D case, the maximum is achieved when $f_x > f_{xc}$ in two dimension case. The coexistence of the locked state and running state leads to a rapid diffusion, the locked state survives under $f_x > f_{xc}$ in the 2D case due to the diffusion in y direction and coexistence of the locked state and running state. The massive enhancement of the diffusion coefficient in x direction in the 2D case is attributed to the coexistence of the locked state and running state in y direction benefits the maintenance of locked state for x direction. For periodic potential without bias force, the particle wanders in various directions before it jumps along x direction, leading to a slower diffusion in the 2D case compared with that in the 1D case [15]. However, the rapid diffusion in tilted periodic potential in y direction that comes from the coexistence of locked state and running state benefits the maintenance of locked state for x direction. In addition, the coexistence of two states leads to rapid diffusion in medium to long periods.

4. Conclusion

We studied the diffusive motion of a particle moving in a 2D tilted periodic potential, where bias force is exerted in x direction. The diffusion coefficients were presented as nonmonotonic functions of bias force. The dimensionality is embodied in the interplay of the diffusion in x and y directions. Hence, it is possible to control the diffusion in one direction by applying force in the vertical direction. Bias force helps the particle form a running state in y direction, and leads to rapid diffusion, which benefits the maintenance of locked state in x direction, and leads to a rapid diffusion in this direction. The diffusion coefficient in x direction in the 2D tilted periodic potential exhibits massive enhancement compared with that in the 1D tilted periodic potential.

Conflicts of Interest

The authors declare no conflicts of interest regarding the publication of this paper.

References

[1] Barone, A. and Paterno, G. (1982) Physics and Applications of the Josephson Effect. Wiley, New York. https://doi.org/10.1002/352760278X

[2] Reguera, D., Rubi, J.M. and Pérez-Madrid, A. (2000) *Physical Review E*, **62**, 5313. https://doi.org/10.1103/PhysRevE.62.5313

[3] Georgievskii, Y. and Burshtein, A. (1994) *The Journal of Chemical Physics*, **100**, 7319. https://doi.org/10.1063/1.466876

[4] Fulde, P., Pietronero, L., Schneider, W.R. and Strässler, S. (1975) *Physical Review Letters*, **35**, 1776. https://doi.org/10.1103/PhysRevLett.35.1776

[5] Gruner, G., Zawadowski, A. and Chaikin, P.M. (1981) *Physical Review Letters*, **46**, 511. https://doi.org/10.1103/PhysRevLett.46.511

[6] Schleich, W., Cha, C.S. and Cresser, J.D. (1984) *Physical Review A*, **29**, 230. https://doi.org/10.1103/PhysRevA.29.230

[7] Frenken, J.W.M. and Van der Veen, J.F. (1985) *Physical Review Letters*, **54**, 134. https://doi.org/10.1103/PhysRevLett.54.134

[8] Ajdari, A. and Prost, J. (1992) *Proceedings of the National Academy of Sciences of the United States of America*, **88**, 4468-4471. https://doi.org/10.1073/pnas.88.10.4468

[9] Reimann, P., Van den Broeck, C., Linke, H., Hänggi, P., Rubi, J.M. and Pérez-Madrid, A. (2002) *Physical Review E*, **65**, Article ID: 031104. https://doi.org/10.1103/PhysRevE.65.031104

[10] Marchenko, I.G. and Marchenko, I.I. (2012) *EPL*, **100**, 50005. https://doi.org/10.1209/0295-5075/100/50005

[11] Lü, K. and Bao, J.-D. (2007) *Physical Review E*, **76**, Article ID: 061119. https://doi.org/10.1103/PhysRevE.76.061119

[12] Zhang, J.M. and Bao, J.-D. (2017) *Physical Review E*, **95**, Article ID: 032107. https://doi.org/10.1103/PhysRevE.95.032107

[13] Guo, W., Du, L.C. and Mei, D.C. (2014) *Journal of Statistical Mechanics*, **2014**, Article No. 04025. https://doi.org/10.1088/1742-5468/2014/04/P04025

[14] Burada, P.S., Schmid, G., Reguera, D., *et al.* (2009) *EPL*, **87**, 50003. https://doi.org/10.1209/0295-5075/87/50003

[15] Elkoraychy, E., Kotri, A., Mazroui, M., Sbiaai, K. and Saadouni, K. (2015) *Modern Physics Letters B*, **29**, Article ID: 1550090. https://doi.org/10.1142/S0217984915500906

[16] Bao, J.D. (2001) *Physical Review E*, **63**, Article ID: 061112. https://doi.org/10.1103/PhysRevE.63.061112

[17] Festa, R. and Galleani d'Agliano, E. (1978) *Physica A*, **90**, 229-244. https://doi.org/10.1016/0378-4371(78)90111-5

[18] Gunther, L., Revzen, M. and Ron, A. (1979) *Physica A*, **95**, 367-369. https://doi.org/10.1016/0378-4371(79)90062-1

[19] Risken, H. (1989) The Fokker-Planck Equation. Springer-Verlag, Berlin. https://doi.org/10.1007/978-3-642-61544-3

Journal of Modern Physics, 2021, 12, 1966-1974
https://www.scirp.org/journal/jmp
ISSN Online: 2153-120X
ISSN Print: 2153-1196

Some Consequences of a Simple Approach for Constructing a Theory of a Relativistic Fermi Gas

Roberto Lopez-Boada[1], Luis Grave de Peralta[2,3*]

[1]Science and Wellness Department, Broward College, Pembroke Pines, FL, USA
[2]Department of Physics and Astronomy, Texas Tech University, Lubbock, TX, USA
[3]Nano Tech Center, Texas Tech University, Lubbock, TX, USA
Email: *luis.grave-de-peralta@ttu.edu

How to cite this paper: Lopez-Boada, R. and Grave de Peralta, L. (2021) Some Consequences of a Simple Approach for Constructing a Theory of a Relativistic Fermi Gas. *Journal of Modern Physics*, **12**, 1966-1974.
https://doi.org/10.4236/jmp.2021.1214113

Received: November 25, 2021
Accepted: December 20, 2021
Published: December 23, 2021

Abstract

It is shown how to build a simple but exact theory of a relativistic Fermi gas at 0 ˚K, which is based in a recently reported analytic formula for the energies of a relativistic spin-0 particle in a box. A white dwarf star is then simulated as a sphere filled with a relativistic Fermi gas. The Chandrasekhar mass limit is simply obtained using this model. We then discuss, using the proposed approach to relativistic quantum mechanics, how the interplay between the special theory of relativity, quantum mechanics, and gravity determines the stability of the matter.

Keywords

Quantum Mechanics, Relativistic Fermi Gas, Relativistic Quantum Mechanics

1. Introduction

The theory of a non-relativistic Fermi gas is commonly discussed in the context of the theory of metals in solid state physics [1]. The theory of a non-relativistic Fermi gas is built from a well-known analytical expression, which gives the energies of a non-relativistic spin-0 particle in a three-dimensional infinite well (particle in a box) [2]. The Pauli exclusion principle is used, in the non-relativistic theory of a Fermi gas at 0 ˚K, for taking care of the fermion nature of the particles forming a Fermi gas [1] [2]. However, this relatively simple theory cannot be directly extended to the relativistic domain [3] [4]. This is because no such analytical expression was known, until recently, for the energies of a relativistic spin-0 particle in a box. In this work, we show, for the first time, how a simple but precise theory of a relativistic Fermi gas can be constructed. We use for this a recently reported analytical expression for the energies of a relativistic particle in a box [5] [6] [7] [8]. As it is shown in the **Appendix**, this analytical expression was obtained by solving a surprising Schrödinger-like but quasi-relativistic wave equation; therefore, using the same mathematical techniques required for obtaining the non-relativistic formula [2] [5] [6] [7] [8] [9].

In what follows, first, in Section 2, some results of such a simple theory of a relativistic Fermi gas, at a 0 ˚K temperature, are presented. While the consequences for solid state physics of this theory will be presented elsewhere, here, in Section 3, these results are used, for the first time, for obtaining in an alternative way, simple but precise, the Chandrasekhar mass limit of Fermi gas stars. Then, in Section 4 is presented a discussion about how the interplay between quantum mechanics, Newtonian gravity, and special relativity determines the stability of the matter. Finally, the conclusions of this work are given in Section 5.

2. The Approach

The theory of a non-relativistic Fermi gas, formed by N non-interacting fermions with spin-1/2, is based on the knowledge of the analytic expression of the energies corresponding to a 0-spin particle trapped in an infinite well (particle in a box), which can be easily calculated using the Schrödinger equation [1] [2]. The fermion nature of the particles is included by considering the Pauli exclusion principle, which is purely quantum in nature, and implies that only two fermions can simultaneously be at the same quantum state [1] [2].

Only recently, an analytic expression giving the energies of a spin-0 particle trapped in an infinite well was reported [5] [6] [7] [8]. This result was obtained using the GPPP (Grave de Peralta-Poirier-Poveda) method [5] [6] [7] [8] [9]. A fast review of the GPPP method is described for self-suffice reasons in the **Appendix**. It is worth noting that, first, there is an excellent agreement between the energies calculated using the analytic formula [5] [6] [7] [8], and the energies numerically calculated using the Dirac equation [10]. Second, it is well understood the relationship between the GPPP method and the Dirac equation [11]. Consequently, we can now construct a simple but exact theory of Fermi gases, which is valid from the non-relativistic to the ultrarelativistic regime. For doing this, we just need to repeat the same steps often follows for constructing the non-relativistic theory of a Fermi gas but using the new energy formula. We should start by substituting the non-relativistic formula for the energies of a quantum particle of mass m in a cubic box of size L [1] [2]:

$$E_{|\boldsymbol{n}|} = \frac{\pi^2\hbar^2}{2mL^2}|\boldsymbol{n}|^2, \quad \boldsymbol{n} = \left(n_x, n_y, n_z\right), \quad n_{x,y,z} = 1, 2, \cdots \tag{1}$$

by the corresponding formula for a relativistic particle [5] [6] [7] [8]:

$$E_{|\boldsymbol{n}|} = \frac{\pi^2\hbar^2}{(\gamma+1)mL^2}|\boldsymbol{n}|^2 = (\gamma-1)mc^2. \tag{2}$$

In Equations (1) and (2), $\hbar$ is the reduced Plank constant [1] [2], and γ is the especial relativity Lorentz factor [5]-[12]:

$$\gamma = \sqrt{1 + \frac{p_{|\boldsymbol{n}|}^2}{m^2 c^2}} = \sqrt{1 + |\boldsymbol{n}|^2 \pi^2 \left(\frac{\lambda\!\!\!^-_C}{L}\right)^2}, \ \lambda\!\!\!^-_C = \frac{\hbar}{mc}. \tag{3}$$

In Equation (3), p is the magnitude of the linear momentum of the particle in the box, and (c) is the speed of the light in the vacuum. In the non-relativistic limit, $L \gg \hbar/mc$; therefore $\gamma \approx 1$ and then Equation (2) coincides with Equation (1). In the ultrarelativistic limit, $L \ll \hbar/mc$; therefore $\gamma \gg 1$, thus Equation (3) also gives the correct relation between E and p for an ultrarelativistic particle [3] [4]:

$$E_{|\boldsymbol{n}|} = p_{|\boldsymbol{n}|} c, \ \ p_{|\boldsymbol{n}|} = \frac{|\boldsymbol{n}|}{L} h. \tag{4}$$

In the thermodynamic limit, $N \gg 1$, each quantum state corresponds to a point in the "n-space" with energy given by Equation (2) [1]. In the ground state of the Fermi gas at 0 ˚K, all the energy levels up to the Fermi energy (E_F) level are occupied, and all the higher levels are empty [1]. The ground state is then represented by a three-dimensional isotropic and uniform Fermi sphere. Therefore, the number of states in the Fermi sphere and its radius are related by the following equation [1]:

$$N = 2 \times \frac{1}{8} \times \frac{4}{3} \pi |\boldsymbol{n}_F|^3 \Rightarrow |\boldsymbol{n}_F| = \left(\frac{3N}{\pi}\right)^{1/3}. \tag{5}$$

In Equation (5), the factor of two expresses the two spin states, and the factor of 1/8 expresses the fraction of the sphere that lies in the region where all $n_{x,y,z}$ are positive. Substituting Equation (5) in Equation (2), and replacing L^2 by $V^{2/3}$, we obtain a formula for E_F:

$$E_F = \frac{\hbar^2 \left(3\pi^2\right)^{2/3}}{(\gamma+1) m} \left(\frac{N}{V}\right)^{2/3} = (\gamma - 1) mc^2, \ \gamma = \sqrt{1 + \left(3\pi^2\right)^{2/3} \lambda\!\!\!^-_C{}^2 \left(\frac{N}{V}\right)^{2/3}}. \tag{6}$$

It is straightforward to show that Equation (6) gives the correct values of E_F in both the non-relativistic and the ultrarelativistic limits [1] [3] [4]. Moreover, Equation (6) is valid in all this range. The rest of the theory of a Fermi gas is constructed from the analytic formula for E_F [1]. For instance, the total energy of the Fermi gas when it is in its ground state at 0 ˚K is:

$$E_T = \frac{\hbar^2}{m} \left(\frac{3\pi^2}{V}\right)^{2/3} \int_0^N \frac{(N')^{2/3}}{\gamma + 1} \mathrm{d}N' \approx N \theta E_F. \tag{7}$$

The integral in Equation (7) can be easily calculated in the non-relativistic (θ = 3/5) and the ultrarelativistic (θ = 3/4) limits. Consequently, Equation (7) with θ slowly changing from 3/5 to 3/4 gives the exact value of E_T in the relativistic and ultrarelativistic limits [1] [3] [4], and it is a good approximation to E_T in between these limits. The degeneracy pressure of the Fermi gas is then calculated as [1] [3] [4]:

$$P = -\frac{\partial E_T}{\partial V} \propto \begin{cases} \left(\frac{N}{V}\right)^{\frac{5}{3}}, & \text{non-relat} \\ \left(\frac{N}{V}\right)^{\frac{4}{3}}, & \text{ultrarelat} \end{cases} \tag{8}$$

We should emphasize here that the existence of the degenerate pressure in a Fermi gas is a purely quantum effect.

3. The Chandrasekhar Mass Limit

Using the Fermi gas as a model, it is possible to calculate the Chandrasekhar limit, *i.e.*, the maximum mass any white dwarf star may have (without significant thermally generated pressure) without collapsing into a black hole or a neutron star. The latter is a star mainly composed of neutrons, where the collapse is also avoided by neutron degeneracy pressure [13] [14].

A simple model for a Fermi gas star, formed by $N \gg 1$ spin-1/2 particles of mass m, is a spherical star of radius r formed by a Fermi gas of total mass $M_S = Nm$ and constant density $\rho = M_S/V$, with $V = (4/3)\pi r^3$. Using this model, the total kinetic energy of the gas (associated to the degeneracy pressure) is E_T as given by Equation (7). Consequently, when including the Newtonian gravitational energy [13], we obtain for the total energy of the star (E_S):

$$E_s(r) = E_T(r) - \alpha_G \frac{GM_S^2}{r}. \tag{9}$$

In Equation (9), G is the gravitational constant, and the parameter α_G is equal to 3/5 = 0.6 for a constant density sphere, but it takes slightly different values depending on the details of de internal structure of the star ($\rho(r)$). Using Equations (6) and (7), substituting V by $(4/3)\pi r^3$, and rearranging Equation (9), we obtain:

$$E_s(r) = \theta a \frac{M_S^{5/3}}{(\gamma+1) r^2} - \alpha_G \frac{GM_S^2}{r}, \quad a = \left(\frac{3\pi}{4}\right)^{2/3} \frac{\hbar^2}{m^{8/3}}, \quad \gamma = \sqrt{1 + \frac{a}{c^2} \frac{M_S^{2/3}}{r^2}}. \tag{10}$$

Or alternatively:

$$E_s(r) = \theta \left(\sqrt{1 + \frac{a}{c^2} \frac{M_S^{2/3}}{r^2}} - 1 \right) M_S c^2 - \alpha_G \frac{GM_S^2}{r}. \tag{11}$$

The radius of the Fermi gas star can be then estimated as the values of r for which $E_S(r)$ has a local minimum. When the particles forming the gas move at non-relativistic speeds, it is easier to use Equation (10) with $\gamma = 1$. Solving the equation $dE_S/dr = 0$, we obtain:

$$r = \frac{\theta a}{\alpha_G G M_S^{1/3}} = \left[\left(\frac{3\pi}{4}\right)^{2/3} \frac{\theta}{\alpha_G} \right] l_P \left(\frac{m_P}{m}\right)^3 \left(\frac{m}{M_S}\right)^{1/3}. \tag{12}$$

For obtaining Equation (12), we used the following relations involving the Plank's length (l_P) and mass (m_P):

$$\frac{\hbar^2}{Gm^{8/3}} = \frac{\hbar^2}{Gm^3} m^{1/3}, \quad \frac{\hbar^2}{Gm^3} = l_P \left(\frac{m_P}{m}\right)^3, \quad l_P = \sqrt{\frac{\hbar G}{c^3}}, \quad m_P = \sqrt{\frac{\hbar c}{G}}. \tag{13}$$

Therefore, a non-null radio, which decreases monotonically when M_S increases, exists for any star mass. This indicates the existence of an equilibrium between the centrifugal influence of the degeneracy pressure (a purely quantum mechanical effect) and the crushing gravitational force in the massive star. In contrast, when the particles forming the gas move at ultrarelativistic speeds, we can use either one of Equations (10) and (11) with:

$$\gamma \approx \frac{\sqrt{a}}{c} \frac{M_S^{1/3}}{r} \gg 1. \tag{14}$$

For obtaining:

$$E_S(r) \approx \left(\theta c \sqrt{a} M_S^{4/3} - \alpha_G G M_S^2\right) \frac{1}{r}. \tag{15}$$

Consequently, $E_S \to -\infty$ when $r \to 0$; *i.e.*, the star collapses, when:

$$M_S > M_{Ch} = \left(\frac{\theta}{\alpha_G}\right)^{3/2} \sqrt{\frac{3\pi}{4}} \left(\frac{m_P}{m}\right)^2 m_P. \tag{16}$$

We obtained an excellent agreement with the Chandrasekhar mass limit ($M_{Ch} \approx 1.43$ solar masses) [3] [11] [12], when taking $m \approx 1.992$ times the Hydrogen mass (m_H), and $\alpha_G \approx 0.4725$. Finally, using Equations (11) and (13), and solving the equation $\mathrm{d}E_S/\mathrm{d}r = 0$, we obtain:

$$r = \beta \left[\left(\frac{3\pi}{4}\right)^{2/3} \frac{\theta}{\alpha_G}\right] l_P \left(\frac{m_P}{m}\right)^3 \left(\frac{m}{M_S}\right)^{1/3} \sqrt{1 - \left(\frac{M_S}{M_{Ch}}\right)^{4/3}}. \tag{17}$$

The dependence of r (in solar radii) on M_S (in solar masses) corresponding to Equation (17) is shown as a continuous red curve in **Figure 1**. We used here the same values of m, and α_G reported above. The parameter $\beta = 7$ was needed for qualitatively matching previously reported radius-mass relations [3] [14]. This indicates that the inclusion of effects related to the internal structure of the stars are needed for making detailed quantitative calculations [3] [13] [14]. Nevertheless, the overall picture discussed in this Section is correct, and the collapse ($r \to 0$) of the ultrarelativistic Fermi gas star in now evident when $M_S \to M_{Ch}$. Clearly, Equation (17) coincides with Equation (12) in the non-relativistic limit, *i.e.*, when $M_S \ll M_{Ch}$. The dependence of r on M_S corresponding to Equation (12) is shown as a discontinuous blue curve in **Figure 1**. Note that the gravitational collapse of a Fermi start can only be predicted when the effects of the especial relativity are included in the model.

4. Stability of the Matter

The curves shown in **Figure 1** describe the stability of huge cosmological objects formed by numerous quantum particles. However, these curves streakily resemble other curves that were obtained while describing the stability of elemental

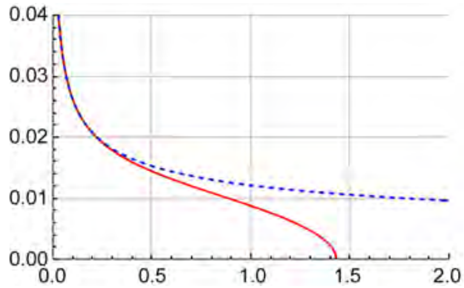

Figure 1. Radius-mass relations in a Fermi gas star model, relativistic (continuous red curve) vs non-relativistic (discontinuous blue curve).

particles and atoms [5]. It has been shown that a good estimate of the size of a Hydrogen-like atom, which is formed by an electron of mass m_e bounded to a nucleus of charge Ze, where e is the absolute value of the electron charge, can be obtained as the value of r minimizing the energy of the electron in the atom (E), which is given by the following expression [5]:

$$E(r) \approx \frac{\hbar^2}{(\gamma+1)m_e r^2} - \frac{Ze^2}{4\pi\epsilon_0 r}, \quad \gamma = \sqrt{1+\left(\frac{\lambda_C}{r}\right)^2}. \tag{18}$$

Equation (18) is like Equation (10) but with the relativistic quantum mechanics term, $E_T(r)$, substituted by the relativistic quantum mechanics kinetic energy of the electron, and the gravitational energy of the Fermi gas substituted by the Coulombic energy of the electron in the atom [2] [5] [15].

It is not then surprising that the dependence of the size of the atom (r) on Z, as shown in **Figure 2(a)**, resembles the curves plotted in **Figure 1**. In this case, a non-relativistic description (continuous blue curve) predicts atoms with any value of Z should all be stable. However, when special relativity in included in the model (red points), and $Z < 137$, the electrical force between the nucleus and the electron tends to collapse the atom but pure quantum mechanical effects stabilize it. In contrast, atoms with $Z > 137$ are unstable (the electron collapses to the nucleus, $r \to 0$) and thus these atoms should not exist [5]. Indeed, no atom with $Z >$ 118 has ever been observed.

The following hypothesis, explaining why there are not elemental quantum particles with a mass larger than the Plank mass [5] [16], is much more closely related with the previous discussion about the fate of Fermi gas stars. If an elemental particle of mass m were able to interact gravitationally with itself, due the spread of its mass density through its wave function [5] [16] [17], the energy of the free particle could be estimated using the following equation [5] [16]:

$$E(r) \approx \frac{\hbar^2}{(\gamma+1)mr^2} - \frac{Gm^2}{r}. \tag{19}$$

With γ given by Equation (18). The value of r that minimizes Equation (19) was found solving the equation $\mathrm{d}E/\mathrm{d}r = 0$ [5] [16]:

$$r = a_D\sqrt{1-\left(\frac{m}{m_P}\right)^4}, \quad a_D = l_P\left(\frac{m_P}{m}\right)^3. \tag{20}$$

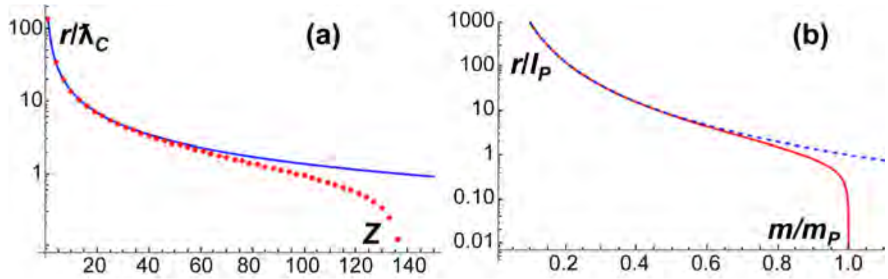

Figure 2. (a) Calculated radii of hydrogen-like atoms in λ_C (reduced Compton wavelength) units as a function of Z for (continuous blue curve) $\gamma \approx 1$ and (red points) $\gamma \gg 1$. (b) Calculated radii of the radius of a quantum particle, in Plank units, as a function of m in Plank units for (discontinuous blue curve) $\gamma \approx 1$ and (continuous red curve) $\gamma \gg 1$.

In contrast, for the non-relativistic case; *i.e.*, using Equation (19) with $\gamma = 1$, it was found that $r = a_D$ [5] [16]. As shown in **Figure 2(b)**, a non-relativistic description (discontinuous blue curve) predicts elemental particles with any mass are possible. The dependence of r (in Plank units) on m (in Plank units) corresponding to Equation (20) is plotted in **Figure 2(b)** as a continuous red curve. When special relativity is included in the model, and $m < m_P$, gravity tends to collapse the particle, but pure quantum mechanical effects stabilize it. However, $r \to 0$ when $m \to m_P$; thus, as it is well known, no elemental particles with mass larger than the Plank mass could exist [5] [16]. Moreover, **Figure 2(b)** shows that, close to the particle collapse, the size of the particle is ~ a_D. This factor also appears in Equations (12) and (17). A comparison of Equations (17) and (20), and **Figure 1** and **Figure 2(b)**, reveals the transition from stable to instable is more abrupt for a single particle than for a Fermi gas star.

The stability of atoms, the so-called stability of the first kind [18], disappears when the combined effects of special relativity and electrostatic overcome the stability provides by quantum mechanics effects, thus producing the collapse of superheavy atoms. The stability of single quantum particles, a kind of zero-order stability, disappears when the combined effects of special relativity and gravity overcome the stability provided by quantum mechanics effects, thus producing the collapse of elemental particles. While elemental quantum particles with a mass larger than the Plank mass may not exist [5], massive cosmological bodies formed by an extremely large number of quantum particles do exist. The stability of the white dwarfs and neutron stars is an instance of the so-called stability of the second kind [18]. This stability also disappears when the combined effects of special relativity and gravity overcome the quantum effects, associated to the Pauli exclusion principle, that makes the stability possible.

5. Conclusion

We have shown that the analytical expression of the energies of a relativistic spin-0 particle trapped in a cubic box, which can be obtained using the GPPP approach (as shown in the **Appendix**), can be used as the foundation of a simple but exact theory of a Fermi gas, which is valid from the non-relativistic to the ultrarelativistic regimes. For instance, we were able to obtain the Chandrasekar mass limit using this approach and, due to the simplicity of our approach, we were able to illustrate the interplay between gravity, quantum mechanics, and special theory of relativity that determines the stability of matter.

Conflicts of Interest

The authors declare no conflicts of interest regarding the publication of this paper.

References

[1] Kittel, C. (2005) Introduction to Solid State Physics. 8th Edition, J. Wiley & Sons, New York.

[2] Griffiths, D.J. (2018) Introduction to Quantum Mechanics. 3rd Edition, Prentice Hall, New York. https://doi.org/10.1017/9781316995433

[3] Greiner, W., Neise, L. and Stöcker, H. (1997) Thermodynamic and Statistical Mechanics. Springer-Verlag, New York.

[4] Landau, L. and Lifshits, E.M. (1970) Statistical Physics. 2nd Edition, Pergamon Press, Oxford.

[5] Grave de Peralta, L., Poveda, L. and Poirier, B. (2021) *European Journal of Physics*, **42**, Article ID: 055404. https://doi.org/10.1088/1361-6404/ac0ecc

[6] Grave de Peralta, L. (2020) *The European Journal of Physics*, **41**, Article ID: 065404. https://doi.org/10.1088/1361-6404/aba7dc

[7] Grave de Peralta, L. (2020) *Results in Physics*, **18**, Article ID: 103318. https://doi.org/10.1016/j.rinp.2020.103318

[8] Grave de Peralta, L. (2020) *Journal of Modern Physics*, **11**, 196-213. https://doi.org/10.4236/jmp.2020.112012

[9] Grave de Peralta, L. (2020) *Scientific Reports*, **10**, Article No. 14925. https://doi.org/10.1038/s41598-020-71505-w

[10] Ruiz-Columbié, A., Farooq, H. and Grave de Peralta, L. (2021) *Journal of Modern Physics*, **12**, 1358-1374. https://doi.org/10.4236/jmp.2021.1210085

[11] Grave de Peralta, L. and Farooq, H. (2021) *Journal of Modern Physics*, **12**, 1145-1159. https://doi.org/10.4236/jmp.2021.128068

[12] Christodeulides, C. (2016) The Special Theory of Relativity. Springer, New York.

[13] Morison, I. (2008) Introduction to Astronomy and Cosmology. Wiley, London.

[14] Kutner, M.L. (2003) Astronomy, a Physical Perspective. 2nd Edition, Cambridge University Press, Cambridge. https://doi.org/10.1017/CBO9780511802195

[15] Walker, J., Resnick, R. and Halladay, D. (2014) Fundamentals of Physics. 10th Edition, J. Wiley & Sons, New York.

[16] Poveda, L.A., Ruiz-Columbié, A. and Grave de Peralta, L. (2021) Relativistic Corrections to the Diósi-Penrose Model. http://arxiv.org/abs/2103.00994

[17] Diósi, L. (1984) *Physics Letters A*, **105**, 199. https://doi.org/10.1016/0375-9601(84)90397-9

[18] Lieb, H.E. and Seiringer, R. (2010) The Stability of Matter in Quantum Mechanics. Cambridge University Press, New York. https://doi.org/10.1017/CBO9780511819681

[19] Grave de Peralta, L., Poirier, B. and Poveda, L.A. (2021) APS March Meeting U71-00234.

Appendix

The Poirier-Grave de Peralta equation [5] [19]:

$$i\hbar\frac{\partial}{\partial t}\Psi=\left[\frac{\hat{p}^2}{(\hat{\gamma}+1)m}+V\right]\Psi,\ \hat{\gamma}=\sqrt{1+\frac{\hat{p}^2}{m^2c^2}},\ \hat{p}=-i\hbar\nabla. \tag{A1}$$

is fully Lorentz-covariant [5]. It can be shown that for a particle in the box, Equation (A1) exactly reduces to solving the following Schrödinger-like equation [5] [19]:

$$i\hbar\frac{\partial}{\partial t}\Psi=-\frac{\hbar^2}{(\gamma+1)m}\nabla^2\Psi+V\Psi. \tag{A2}$$

In Equation (A2), γ is not an operator but the parameter (GPPP approach) [5]:

$$\gamma=\sqrt{1+\frac{2}{mc^2}E_{Sch}},\ E_{Sch}=\left\langle\psi_{Sch}\left|\frac{\hat{p}^2}{2m}\right|\psi_{Sch}\right\rangle. \tag{A3}$$

In Equation (A3), E_{Sch} and ψ_{Sch} are the energy and wavefunction, respectively, of the particle in a box calculated by solving the Schrödinger Equation [2]. Clearly, Equation (A2) is the Schrödinger equation when $\gamma = 1$. Moreover, Equation (A2) can be solved as the Schrödinger equation is solved [5] [6] [7] [8] [9]. For a particle in the box [5]:

$$E_{|\boldsymbol{n}|}=\frac{\pi^2\hbar^2}{(\gamma+1)mL^2}|\boldsymbol{n}|^2,\ \gamma=\sqrt{1+\frac{2}{mc^2}E_{Sch}}. \tag{A4}$$

Equations (2) and (3) follows directly from the substitution of $E_{Sch} = E_{|n|}$ given by Equation (1) in Equation (A4). It should be noted that there is an excellent correspondence between the energy values calculated using Equations (2) and (3), and the numerically calculated energies using the Dirac's equation [10].

Journal of Modern Physics, 2021, 12, 1975-2002
https://www.scirp.org/journal/jmp
ISSN Online: 2153-120X
ISSN Print: 2153-1196

Evolution of Life Forms in Our Universe

Robert M. L. Baker Jr.[1], Bonnie Sue Baker[2], Jeannie Hall Moller Fontana[1]

[1]Gravwave LLC, Palm Desert, USA
[2]Transportation Sciences Corporation, Palm Desert, USA
Email: drrobertbakerjr@gmail.com, bonniesuebaker@gmail.com, jeanniefontanamd@gmail.com

How to cite this paper: Baker Jr., R.M.L., Baker, B.S. and Fontana, J.H.M. (2021) Evolution of Life Forms in Our Universe. *Journal of Modern Physics*, **12**, 1975-2002.
https://doi.org/10.4236/jmp.2021.1214114

Received: November 11, 2021
Accepted: December 24, 2021
Published: December 27, 2021

Abstract

Paraphrasing Descartes: A *Life form* entity "*thinks*" therefore it exists. Our research method is to take *evolution* to be change or adjustment in order for the entity to "survive." Such evolutionary "adjustments" are expected to occur after the Life form entity has evolved into a thinking "cyborg" or "humanoid" Life form. That is a life forms whose intellectual and physical capabilities are extended beyond normal by a combination electronic, organic and mechanical means. Ultimately an *Accelerated Evolutionary* adjustment is expected to be to be accomplished by a physical modification of "cyborg" or "humanoid" Life form entities by themselves or by other such entities. Here we define a humanoid as a cyborg self-controlled by an electronic artificial brain that has "freewill". The major law for all life forms resident in our Universe be they amoebas, fungus, bugs, or bunnies, human or non-human humanoids is survival of the fittest. We speculate that humans are not the only life form that has been, is, or will be present in our Universe—but due to the necessity of survival, no matter how they started out, inevitably their most probable destiny is to wind up as spheres of living-thinking, mental material orbiting a star or galaxy. The most fit life forms require the most effective protection or shield against "predators" ranging from viruses, bacteria, parasites, dangerous life forms, etc. essentially protection or shield against ANY adversarial or dangerous life form or environmental danger such as radiation. The effectiveness of such a shield is directly proportional to their resistivity to predators and other dangers and inversely proportional to their area; the smaller the predator's "target" the better. In the future such Life form entities may be "built not born" or adjusted by other entities. It is proposed that manipulative appendages such as human limbs e.g., arms, legs, hands, etc. will disappear and possibly evolve into "mind-controlled" or "thinking-controlled", artificial-intelligence implemented external mechanisms and devices. How would life forms evolve to maximize volume, required to house their increased mental capabilities consisting of cognitive/microelectronic material of the highest possible density, and minimize surface area for protection? Since the sphere is the geometric figure exhibiting the largest volume to area ratio, their shape would be spherical. Life forms could, therefore, evolve into spherical "artificial" planets orbiting stars or galaxies—powered by "starlight". We will not, however, consider directly the incorporation of multiple Life forms in the same sphere. Science fiction is utilized only to illustrate concepts.

Keywords

Evolution, Cyborg, Humanoid, Brain Communication, Life Form, Cosmology, Magnetic Nanoparticles

1. Introduction

This paper investigates the *evolution* of life forms in our Universe. Paraphrasing Descartes: A *Life forms* entity "*thinks*" therefore it exists. We take *evolution* to be change or adjustment in order for the entity to "survive." Such evolutionary "adjustments" are expected to occur after the Life form entity has evolved into a thinking "cyborg" or "humanoid" Life form. A humanoid is a cyborg self-controlled by an electronic artificial brain that has "free will". That is a life form whose intellectual and physical capabilities are extended beyond normal by a combination electronic, organic and mechanical means. Ultimately an *Accelerated Evolutionary* adjustment is expected to be to be accomplished by the physical modifications of "cyborg" or "humanoid" Life form entities by themselves or by other such entities. We will greatly reduce our paper's scope to carbon-based chemical activities of the organic animal variety, inclusive of, but not restricted to Homo sapiens. The major law for all life forms resident in our Universe be they amoebas, fungus, bugs, or bunnies, human or non-human humanoids is survival of the fittest. (Or, more generally, life forms more suited to the environment are more likely to survive) as suggested by [1] Charles Darwin (1859), [2] Herbert Spencer (1852) and others. We will utilize Homo sapiens simply as an example to speculate on how life forms will evolve. We speculate that humans are not the only life form that has been, is, or will be present in our Universe—but due to the necessity of survival, no matter how they started out, inevitably their most probable destiny is to wind up as spheres of living-thinking, mental material: life forms orbiting around and nourished by radiation from stars and/or galaxies. That is our speculation or model. We are therefore suggesting a "Working Hypothesis", which is defined (*Wikipedia*) as a hypothesis that is provisionally accepted as a basis for further research in the hope that a tenable theory will be produced, even if the *hypothesis* ultimately fails or is significantly modified (Isaac Newton's *Principia Mathematica*, as significantly modified by Einstein, is an example). It is essentially an encouragement for further research.

The more fit life forms require the most effective protection or shield against "predators" ranging from viruses, bacteria, parasites, dangerous other life forms… essentially protection or shield against ANY adversarial or dangerous life form or environmental danger such as harmful radiation. The effectiveness of such a shield is directly proportional to their resistance to predators and other dangers, such as harmful radiation, and inversely proportional to their area. That is, the smaller their exposed area, the smaller a target they present to any and all predators and dangers such as radiation. Resistance of the shield will be determined by the characteristics of the predators or environmental dangers encountered and for this study is not considered to be a major issue. For example, their shield may be variable in absorption from near black body (for absorption of radiant energy to power them) to high reflectivity of harmful radiation, particles, or projectiles, etc.

The most fit life form will have maximized *imagination*[1]. Maximum *imagination* is functionally defined as the entity who can best define *imagination.* A circular definition or argument of course somewhat similar to the circular orbit of the entity around a star or galaxy. In this regard. Science Fiction is utilized to illustrate concepts, especially in section 4.

Whether or not Life form civilizations will winnow down to one or a few is another issue not directly addressed herein. It may well be that ultimately life forms congregate into subgroup civilizations in order to implement and foster collective activities. Friendship with other life forms, which is involved in the formation of subgroup civilizations and on the winnowing down of Life form civilization's number, may be a thing that affects a life form's psychological and or physical health and wellbeing. Friendship is extremely complex—in fact, too complex to analyze properly. For example, the demands that maintaining a life form's relationships with other life forms makes on the brain's computing power is so great that the number of friends Homo sapien life forms can have at any one time might currently be, very roughly limited to around 150. British evolutionary anthropologist Robin Dunbar (who works at the *University of Oxford*) in Malcolm Gladwell's Book, *The Tipping Point*, stated that there are different layers of friendship or fellowship, depending on how close you are with someone, which is impossible to analyze in great detail. We will, therefore, not analyze directly the incorporation of multiple Life forms in the same sphere.

As mentioned in the Introduction, all life forms are expected to become electronic, organic or mechanism-enhanced or "cyborgs" or "humanoids" and in the future we may be "built not born" or adjusted or modified by other entities. It is proposed in Section 1 that manipulative appendages such as human limbs e.g., arms, legs, hands, etc., after thousands or millions of years of non-use, will disappear and evolve into "mind-controlled" or "thinking-controlled", artificial-intelligence-implemented external mechanisms and devices. An example is shown

[1]Albert Einstein is reported to have stated: "*Imagination* is more important than knowledge. For knowledge is limited to all we now know and understand, while *imagination* embraces the entire world, and all there ever will be to know and understand." The most FIT life form will have maximized *imagination*. Maximum *imagination* is functionally defined as the entity who can best define *imagination.* A circular definition or argument of course, but possibly somewhat similar, imaginatively, to the circular orbit of a Life form entity around a star or galaxy. In any event, the more fit life form will have a large amount of knowledge and be "quick thinking", but even more importantly exhibit the most imagination.

in Figure 1 and Figure 2, in which an artificial arm and hand take control of an external device.

Figure 2, first-ever successful mind-controlled robotic arm without brain implants in 2019, using novel sensing and machine learning techniques, Bin He and his lab (He, B. 2020) have been able to access signals deep within the brain, achieving a high resolution of control over a robotic arm.

https://www.youtube.com/watch?v=UkZquERzoOo.

All such controls and communications will be by mind and between similar life forms mind to mind. Such controls and communications are not anticipated to involve significant external systems such as antennas, but only devices "internal" to a given life form. How would life forms evolve to maximize volume, required to house their increased mental capabilities consisting of cognitive/electronic material of the highest possible density, and minimize surface area for protection—that is be a smaller target for predators? Since, as previously mentioned, the sphere is the geometric figure exhibiting the largest volume to area ratio, their shape would be spherical. Please see Figure 3 for a science-fiction picture of such a life form.

Figure 1. An artificial arm and hand take control of an external device. From Figure 2 of [3] Baker and Baker (2016).

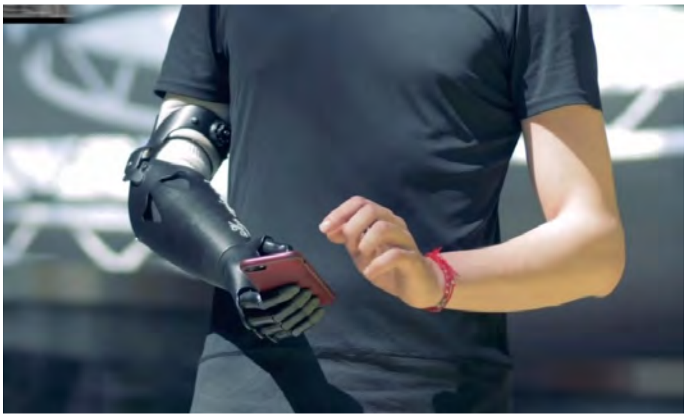

Figure 2. Breakthrough in non-invasive mind-control of robotic limbs ([4] He, B., 2020).

Figure 3. Fictional picture of a spherical life form the 1953 Science-Fiction Movie "Invaders from Mars."

We believe that life forms will evolve into spheres composed of living mental material whose size will be determined by their density needed to properly function, environment, and the local gravitational field. That is, the sphere's mass will need to allow necessary movement and be "sustainable" in the sphere's local gravitational field. For their sustenance or energy, Life forms would, therefore, evolve into spherical "artificial" planets composed of high-density living mental material orbiting stars or galaxies—nourished and powered by "starlight." Their inter-Life form and inter-stellar communications, to be discussed in Section **2.5,** would be by means of mind-controlled and brain activated transceivers of high-frequency gravitational waves (HFGWs). As discussed in the footnote 1, the most fit life forms are expected to have maximized imagination.

2. Amazing Trends in Life form Evolution

2.1. The Rise of the Cyborg and the Humanoid Spheres

We agree with J. A. Hodgson (as quoted by [5] L. Jones (2021)): "We don't know, but, certainly, human genetic variation is increasing. Worldwide there are roughly two new mutations for every one of the 3.5 billion base pairs in the human genome every year…" says Hodgson. "…which is pretty amazing—and makes it unlikely we will look the same in a million years." We are speculating that the engine of change or adjustment of a life form is adaptation to a (final) form that survives. We believe we can conjecture intelligently on the evolutionary path that survival brings life forms on in our Universe. Notice that we are considering any "life form" not necessarily a specific life form. But one of the primary premises of our conjecture is that "All roads lead to Rome". That is independent of their initial condition, all surviving humanoid life forms in our Universe will eventually reach the same spherical final life form on stellar orbit given about stars or galaxies in a sufficient length of time, such as many billions of years (possibly hundreds of billions of years as will be mentioned in Section 4). Because it is such an amazing and dramatic anatomical change predicted for life forms after their reconfiguration to humanoids, we have and will continue to emphasize (perhaps over emphasize) the eventual change from limbed creatures to a spherical form quite frequently,

As was mentioned in [3] Baker and Baker (2016) "…advance has been taking shape over the past several millennia, but most dramatically over the last few decades. Broadly speaking this amazing advance is the introduction of electronic components into the human body and especially into the brain." As a specific example of such advancement is the actual mind control of a mechanical hand shown in **Figure 4**. Here we see an actual Homo sapien life form whose mind, via an electronic interface, controls a mechanical hand to feed herself a candy bar and can feel the bar via haptic feedback[2]!

Prosthetic in **Figure 5** enables a wide range of daily activities, such as zipping a suitcase, shaking hands, and petting a cat[2].

Figure 4. An actual Homo sapien person whose mind, via an electronic interface, controls a mechanical hand to feed herself a candy bar. From **Figure 2** of [3] Baker and Baker (2016).

Figure 5. Inflatable robotic hand gives amputees real-time tactile control. Please see: https://www.itproportal.com/features/future-of-artificial-intelligence-for-2020.

[2]Haptic feedback is the use of *touch* to communicate with users. Most people know the feeling of a vibration in a mobile phone or the rumble in a game controller—but haptic feedback is much more than that. [32] (Robert Blenkinsopp, 2020).

As pictured in Figure 6, *Ai-Da* is the world's first ultra-realistic artist robot powered by AI and named after Ada Lovelace, the first female computer programmer in the World. She is a humanoid with human facial features and a robotic body created by the *Oxfordians*, a group of cutting-edge art and technology experts formed in 2020. Please see: https://en.wikipedia.org/wiki/Ai-Da.

In the near future, the clear outcome would be for Homo sapien and, in general ALL "advancing" Life forms in our Universe, eventually to evolve into a combination cybernetic or electronic and biological being: a "cyborg" or even to a "humanoid", a cyborg controlled internally by an organic brain as shown in Figure 6, Figure 7. As the Life form cyborg "controllers" begin to control their ever improving (evolving) cyborg "helpers", the difference between them begins to narrow, a distinction without a difference: For example, the "transformation" or "mental implants" in the mouse brain [6] Vetere G., Tran L. M., Moberg S., *et al.* (2019) and, as will also be mentioned, tagging neurons, the mind-to-mind communication of Figure 8 and the prosthetics examples, of Figure 1 and Figure 5 will essentially **join** the controller and the associated "cyborg" functions.

Figure 6. "Hello, Baker's residence. They are unavailable right now. Please leave your name and number. I am the Baker's Cyborg, Ai-Da, Robot/ Humanoid ID number 823. If you are a Cyborg, please leave your Humanoid ID number and maybe we can get together sometime."

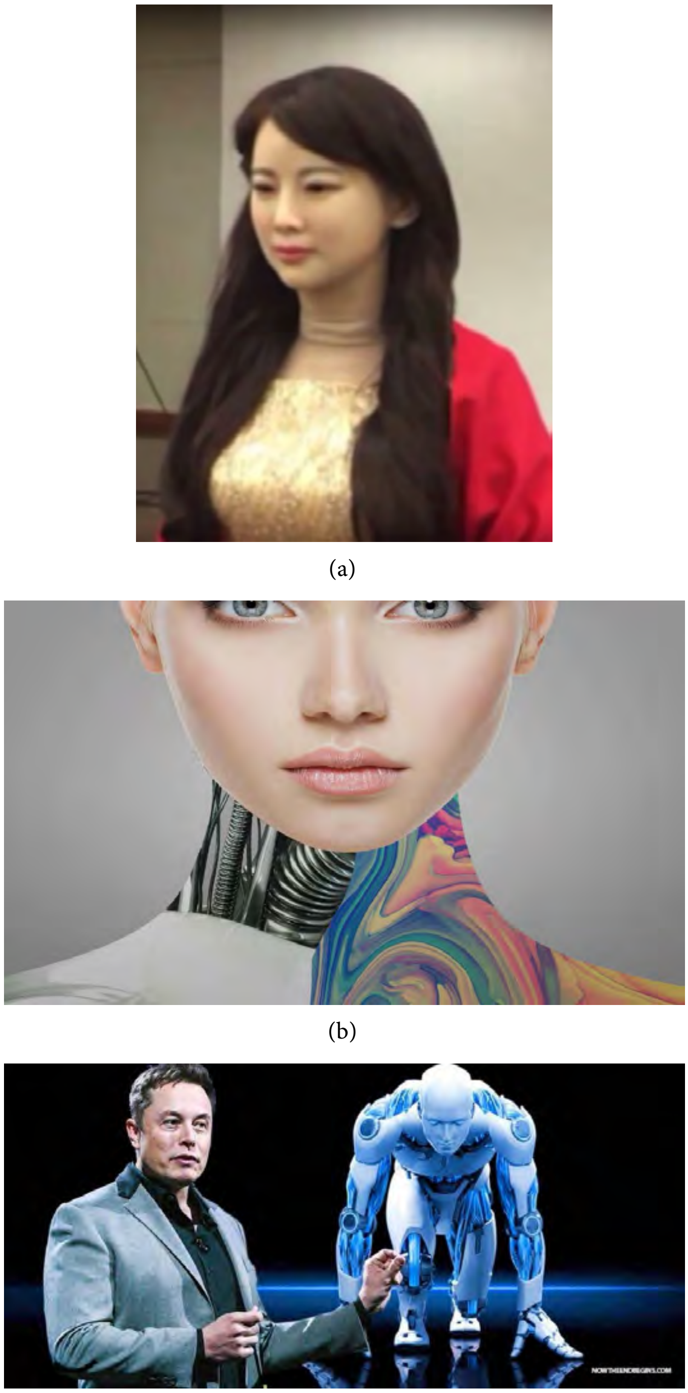

(a)

(b)

(c)

Figure 7. (a) This is the near present-day cyborg, showing the development of machine learning: An AI cyborg. Eventually, more advanced cyborgs may evolve into (b); (b) This is one outcome of the evolution of cyborgs—human features and personality traits programed by a machine learning AI cyborg or humanoid. It is to be completely renovated and evolved to someone like the fictional spherical humanoid in Figure 3; (c) Elon Musk predicts Artificial Intelligence will be better than humans at everything, including sports, in the year 2030.

Figure 8. Brain-to-brain direct communication [20] (Power (2014) and [21] Grey (2016)). Mind Melds and Brain Beams: The Dawn of Brain-to-Brain Communication (https://www.youtube.com/watch?v=SObhSqYglvQ).

Robert F. Service (2013) [7] said in the Journal *SCIENCE* "The beginnings of a cyborg world have already arrived…!" and [8] Manuela Veloso who suggests that we "Embrace a robot-human world" (2015). It is suggested that such cyborg forms of intelligent beings would allow advanced civilizations to endure at least hundreds of thousands of years. In the future, [9] Greene (2017) said, there is a good possibility that humans will find a way to merge with their machines: "We're already finding, on much shorter timescales, [that the] distinction between biological beings and artificial beings is starting to blur," Greene said. "I could see a new kind of hybrid species out of the biological and the synthetic."

What if also an Artificial Memory could be implanted in your or a humanoid's brain? Just imagine an *Artificial Education*—your brain filled with Artificial Knowledge! Experiments reported by [6] Vetere G., Tran L. M., Moberg S., *et al.* (2019) indicate "…we created a fully artificial memory in mice. Similarly to a natural memory…" More recently a Boston College team [10] (Denny, 2020) modified mice's brains with light-sensitive proteins from algae DNA. Denny's team can tag neurons that encode individual memories with glowing molecules. This enables them to see, under a microscope, which cells were active when a mouse learned something, and which cells were active when it remembered something. In addition, once they've labeled a memory neuron or neurons, they can switch it off and on with a laser using a technique called *optogenetics.* This Artificial Education is somewhat like taking *Soma* in the book *Brave New World* to "go" on vacation, while laying down in bed in your home: creates memories of a vacation for you.

However, "Naked Knowledge" may not be as important as we might first think. Naked knowledge of paints, canvases, art history, etc. would not an artist make! Artificial simulation of abstract thinking would probably be extremely difficult to implant in memories as well as muscle-control protocols for physical action, e.g., sports and emotions like love, feelings and hate or dislike. Perhaps these mental functions are involved in other parts of the brain not analyzed like the basolateral amygdala portion observed in the just referenced study. Although implanted in memory hypnotically, the fictional conditioned response of the soldiers in the movie "Manchurian Candidate" (1962) was "Raymond Shaw is the kindest, bravest, warmest, most wonderful human being I've ever known in my life" according to the story they all still did not like him! Also suggested by Frank J. Tipler (http://www.franktipler.com/) in 1994. So, BEWARE: one must take extreme care about whose rendition of history or any other "facts" is being implanted in your or any life form's brain[3].

2.2. Artificial, Accelerated Evolution

One probable evolving Life form (e.g., cyborg or humanoid) would involve the replacement or repair of their "parts" especially if they were largely composed of electronic components as we predict for human life forms in the future. Such cyborgs and humanoids would be essentially *immortal* or at least very long-lived until they are replaced or significantly repaired.

An almost obvious development would be "*Life form Evolution*" that is, replacement parts could also be the installation of improved or upgraded parts—in fact, complete change or adjustment of the design of all future "*models*" of one "*line*" of humanoids. Such adjustment amounts to *Accelerated Evolution* and *humanoids building humanoids.* We now embark on the treacherous trail of considering "judgment", "consciousness", "personality", "freewill," etc. in order to predict humanoid evolution. Again, we invoke our paraphrase of Descartes: "A *Life form* entity 'thinks' therefore it exists." Thus the design of the most survivable *humanoid* entity boils down to the definition of "thinks." And that boils down to imagination ("knowledge" is just an implant in an organic or electronic-brain part of a humanoid entity). So, EVOLUTION is by survival of the Life form entity or entities having the BEST IMAGINATION. Therefore, we leave it to you, dear reader, to suggest what Life form entity would have the best *imagination* leading to its survival and we make a full circle. Figuratively speaking, that *circle is the orbit about our star.*

2.3. The Specific Steps of Life form Evolution

The following compact summaries of the evolutionary steps of life forms in our Universe, specifically humanoids, are all based on survival of the fittest.

1) When all operations of life forms, such as locomotion and control of devices as shown in **Figure 1**, **Figure 2**, **Figure 4** and **Figure 5**, are accomplished by mind-control, perhaps in a few hundred or millions of years, the fit Life form entities will eliminate their hands, arms and legs as completely unessential encumbrances.

2) The most efficient manner in which needed energy can be collected and delivered to a humanoid will be to place the humanoid or humanoid civilization on orbit, artificial planets about a long-lasting stellar energy source. The radiant

[3]Naked Knowledge speaks to the importance of the Turing Test: a machine can still, to this day in 2021, not tell you what an orange actually TASTES like unless a human gives it the information to state.

energy from that energy source would probably be delivered by photovoltaic conversion.

3) The more survivable fit life forms will seek protraction from pernicious predator entities, radiation, micrometeorites, etc. by the humanoids assuming a smaller surface or target area and a higher density internal composition, that is a spherical form composed of very resistant surface material.

Advanced humankind is evolving into a cyborg entity having a complete artificial education. Furthermore, such entities could well be repairable and include technological improvements in their "parts" as time goes by. As mentioned, in a sense cyborgs could be *immortal* and constantly improving, or *evolving*. In any event, it is concluded that the Life form entity's lifespan on our Earth will dramatically increase with the advent of advances in evolutionary cyborg and eventually humanoid technology. Obviously, such an advance would produce a myriad of current problems for humanity such as the necessity for stringent population/birth control and other; new governmental-paradigms to manage not only transition to a huge aging population, but possibly an "ageless" population, mentioned in [3] (Baker and Baker (2016)). Indeed, an "ageless" population, could be free of "earthly human needs and desires" and encounter new, yet to be determined, evolutionary pressures.

2.4. Distinction without a Difference

As discussed the Life form "controllers" begin to control their ever improving (evolving) cyborg "parts," the difference between them begins to narrow a **distinction without a difference:** for example, the "transformation" or "mental implants" in the mouse brain [6] Vetere G., Tran L. M., Moberg S., *et al.* (2019]), the mind-to-mind communication of **Figure 8** and the prosthetics examples, of **Figure 1** and **Figure 5** essentially joining the controller and the associated "cyborg" function to a reasoning or thinking *humanoid* entity is inevitable. Will life forms in the future be "born or built"? Again, we ask the questions: Will they be "assembled" by putting parts together or being grown together or both? Will Life form entities be eternal in the sense of the reparable survivors being the more "experienced" entities? We have suggested that *evolution* and survival of the fittest will take their evolving electronic brains to achieve free-will, imagination and become humanoids. Therefore, the answer to the questions is YES.

The research progress is real, as a mix of biologists, materials scientists, and nanotechnology experts are chipping away at a host of challenges. "I see it as building a seamless interface between cells, tissues, and electronics," says Aleksander Noy, a bio-nano-electronics expert at Lawrence Livermore National Laboratory and the *University of California*, quoted by [7] Service (2013). For now, most of these efforts are focused on providing better health care and quality of life for patients (**Figure 4** and **Figure 5**). Neuro-Engineers at Stanford are using measurements of brain activity to help restore function in people who are paralyzed. Recently, working with a man paralyzed from the neck down, the researchers implanted two arrays of tiny electrodes in a part of his brain responsible for hand movement [11] (Willett, *et al.* (2021)). As the man imagined writing letters, the scientists used machine learning to translate his brain activity into letters on a screen. Using this system, the man could write 90 letters per minute—more than doubling the previous record for typing via brain activity. The pace of the incorporation of enhancing technologies into "man" is on an exponential growth scale.

Over time, we anticipate devices "…that will make us better athletes and soldiers," or even reduce our facial wrinkles! For example, the Electrolift® mask device developed and discussed by [12] Baker (2013) "A few years ago these things were science fiction. But now we are seeing the emergence of real devices and applications," stated [13] Noy (2011). "And fast…" says Zhenan Bao, an organic electronics expert at *Stanford University* in California: "The competition is furious" according to [7] Service (2013). The idea of fusing man and machine has long tantalized humanity. Over the past century, researchers have pioneered myriad efforts to use electronics to measure biological activity and sometimes even alter it. According to Underwood (2013), Geoffrey Ling, a top biotechnology research official at the *Defense Advanced Research Project Agency* (*DARPA*), challenged neuroscientists to do something extraordinary: Develop an implantable device in a human brain that can reverse memory loss. Also UCLA's *Brain Institute* and other universities are developing electronic prostheses that interact with brain regions critical to memory. Victims of stroke may soon have improvement due to brain implants that still allow individual decision making or "thinking" [14] (Ganguly *et al.* (2015). Michael McAlpine, a mechanical engineer at *Princeton University0*, and colleagues [15] (Machens, (2012)) reported in the May 1, 2013 issue of *Nano Letters* [16] (Mannoor (2013)) that they've made the first 3D printed functional organ: a bionic ear that "hears" acoustic sounds and ultrasounds. "We're trying to see if one could introduce augmented functionality that a human wouldn't ordinarily have…" McAlpine says. "Organs from the lab…" appear to be realistic even today as discussed in the June 18, 2015 issue of *Nature* [17] (Marx, 2015).

2.5. Communication

A step in that direction is presented in [18] Hirschberg and Manning (2015). An obvious conclusion is that evolution will produce some form of efficient and unmitigated, *yet editable*, direct brain-to-brain or mind-to-mind intercommunication (**Figure 8**). Certainly, the direct "plug" to one brain that transfers thoughts to control a complex prosthetic device, **Figure 2**, **Figures 4-6**), could eventually be expected to direct thoughts to and from another brain. In another advance a tiny brain transplant helped a blind teacher see letters again [19] (Chappell (2021)).

The nonprofit Battelle team gets even fancier with their "Brain Storm" nano transducers: magnetic nanoparticles wrapped in a piezoelectric shell. The shell can convert electrical signals from neurons into magnetic ones and vice-versa (**Figure 9**). This allows external transceivers to wirelessly pick up the transformed signals and stimulate the brain through a bidirectional highway. The magnetometers can be delivered into the brain through a nasal spray or other non-invasive methods, and magnetically guided towards targeted brain regions. When no longer needed, they can once again be steered out of the brain and into the bloodstream, where the body can excrete them without harm.

It is essential to identify and quantify the means of their interpersonal intercommunication. A step in that direction is presented in [18] Hirschberg and Manning (2015). An obvious conclusion is that evolution will produce some form of efficient and unmitigated, *yet editable* (we really do not want all of our: "thoughts" transmuted to others without editing), direct brain-to-brain or mind-to-mind intercommunication (**Figure 8**). Certainly, the direct "plug" to one brain that transfers thoughts to control a complex prosthetic device, (**Figure 2**, **Figures 4-6**), could eventually be expected to direct thoughts to and from a brain to another. "By creating a more accessible brain-machine interface that doesn't require surgery to use, DARPA could deliver tools that allow mission commanders to remain meaningfully involved in dynamic operations that unfold at rapid speed," (**Figure 10**). Al Emondi, DARPA's program manager for Next-Generation Nonsurgical Neurotechnology, said in a statement: (https://www.bizjournals.com/columbus/news/2019/06/17/battelle-lands-20-4m-to-develop-brainstorm-tech.html The shell can convert electrical signals from neurons into magnetic ones and vice-versa. This allows external transceivers to wirelessly pick up the transformed signals and stimulate the brain through a bidirectional highway. The magnetometers can be delivered into the brain through

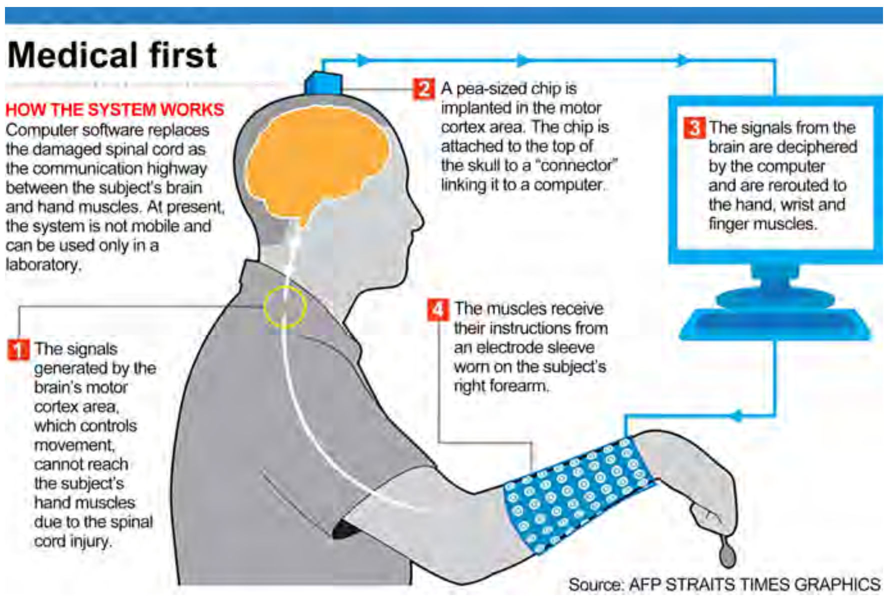

Figure 9. The nonprofit Battelle team gets even fancier with their "Brainstorm" transducers: magnetic nanoparticles wrapped in a piezoelectric shell.

Figure 10. Envisioning the bioengineered soldier of the future through DARPA research programs, Combining DARPA research programs to imagine what super-human capabilities a futuristic soldier could have.
(https://www.bizjournals.com/columbus/news/2019/06/17/battelle-lands-20-4m-to-develop-brainstorm-tech.html)

a nasal spray or other non-invasive methods, and magnetically guided towards targeted brain regions. Please see Figure 11. When no longer needed, they can once again be steered out of the brain and into the bloodstream, where the body can excrete them without harm.

Gravitational waves would be the most appropriate means of communication to a life form other advanced life forms since they are far-reaching and pass through all matter without attenuation. Such waves would necessarily be of high frequency (unlike the very low frequencies of black-hole merger signals) in order to accommodate the largest information bandwidth. Hence they would be High-Frequency Gravitational Waves or HFGWs.

What is the nature of Gravitational Waves themselves? Please examine the following chart in Figure 12 that compares water waves with gravitational waves. Dicusion of the LiBaker High-Frequency Gravitational Wave (HFGW) Detector or receiver and the HFGW generator or transmitter can be found in [22] Baker (2017) pages 121-122 and 93-112, respectively. Advanced models of such transceivers would support Life form communications in future.

2.6. Consider the Early Change of Our Homo Sapien Life Form or Species

According to [23] Haldane (1929) the primitive Earth's atmosphere was essentially reducing, with little or no oxygen. Ultraviolet rays from the Sun induced reactions on a mixture of water, carbon dioxide, and ammonia. Organic substances such as sugars and protein components were synthesized. These molecules "accumulated till the primitive oceans reached the consistency of hot dilute soup." The first reproducing things were created from the *Primordial Sea* (Figure 13) and then moved from the *Hydrosphere* to the *Lithosphere* (Figure 14).

At some point a primordial organism randomly built the mechanisms needed to replicate its genetic structure, thus really becoming the first life form as in Figure 13. This life form or organism would have had only a single gene. Then

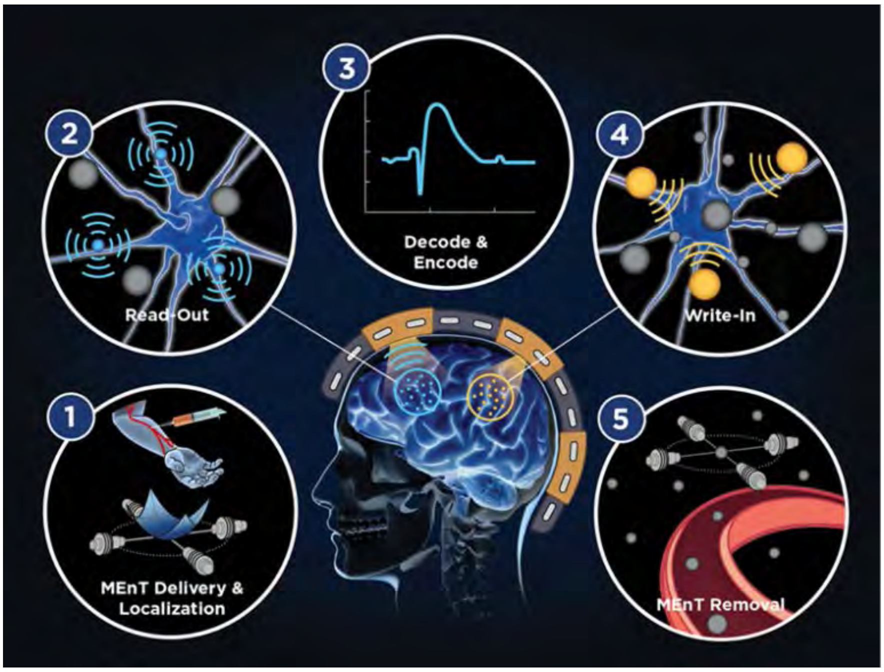

Figure 11. Battelle created this infographic to explain the theory of using magnetic nanoparticles to wirelessly transmit brain signals for outside software to decode.

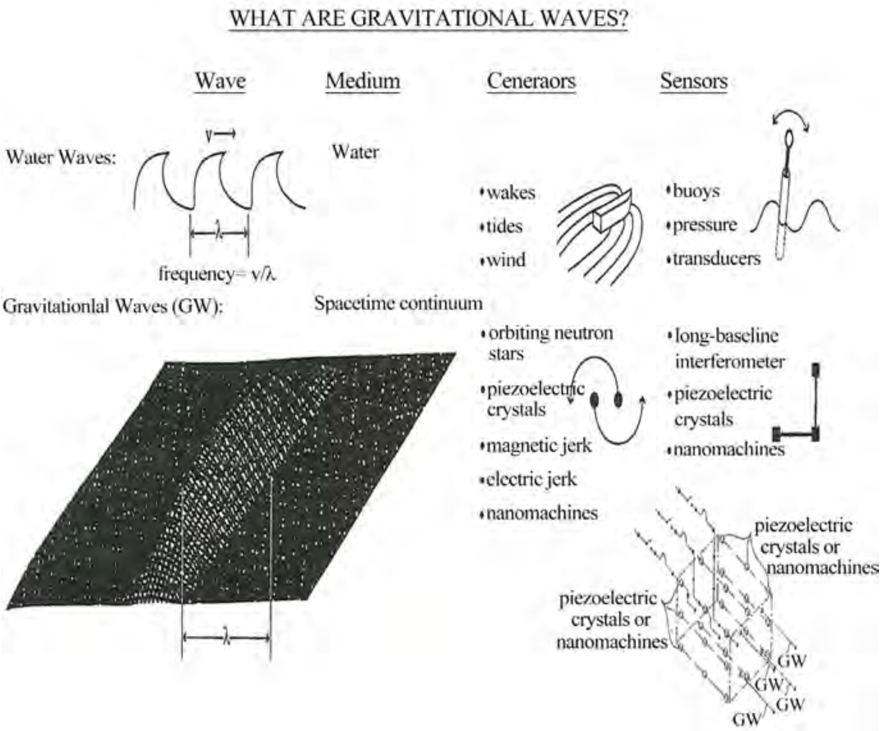

Figure 12. Gravitational waves as described in this diagram are ripples in spacetime, but can be utilized for communications, somewhat like sound or radio waves.

Figure 13. Beginning of life on our Earth in the Primordial Sea. All living beings on the Earth evolved from the "Single Cell" that appeared before the Precambrian Era.

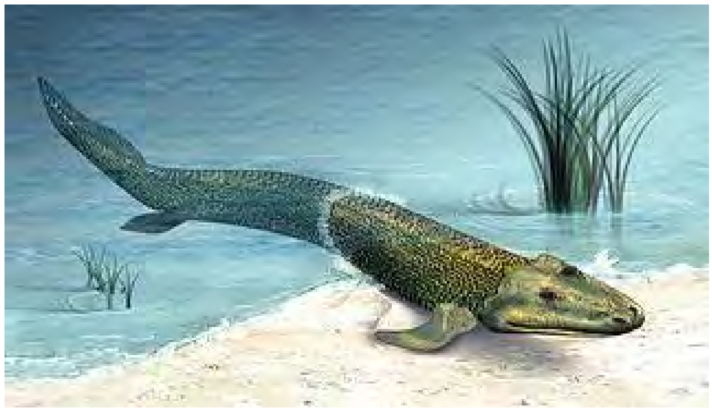

Figure 14. Our Earth's Life form moves from the *Hydrosphere* to the *Lithosphere*.

cosmic rays came down and, so to speak, "shuffled the gene deck" and variants appeared to selectively survive and reproduce according to "survival of the fittest" [1] [2] (Spencer, 1852; Darwin, 1859). Next would come our Earth's human Life form's change in the Biosphere as shown in **Figure 15**. Then human life forms begin to occupy outer space in our Universe as in the space station shown in **Figure 16**. Such a location would be prophetic of the life form's celestial-orbital, final destination and residence described in **Figure 20**.

Maybe not be the "Final" frontier for distant-future life forms in a *Multiverse* (**Figure 17**). Purely speculative signals "adjacent" *Multiverse* are discussed in Section 5 of [3] Baker and Baker (2021).

By the way, a quite different approach to the bigger question of the evolution of our Universe itself is given by [24] Vilenchik, L., and Vilenchik, M. (2019) and by [30] Baker (2020) in his "Rollout Theory".

3. Past Progress and Adjustment Motivated by Survival

3.1. Recent Possible Adjustments

Life forms will need to adjust to any change in their environment in order to

Figure 15. Our Earth's human Life form's change in the Biosphere.

Figure 16. Some of human life forms occupy Outer Space: "The Final Frontier".

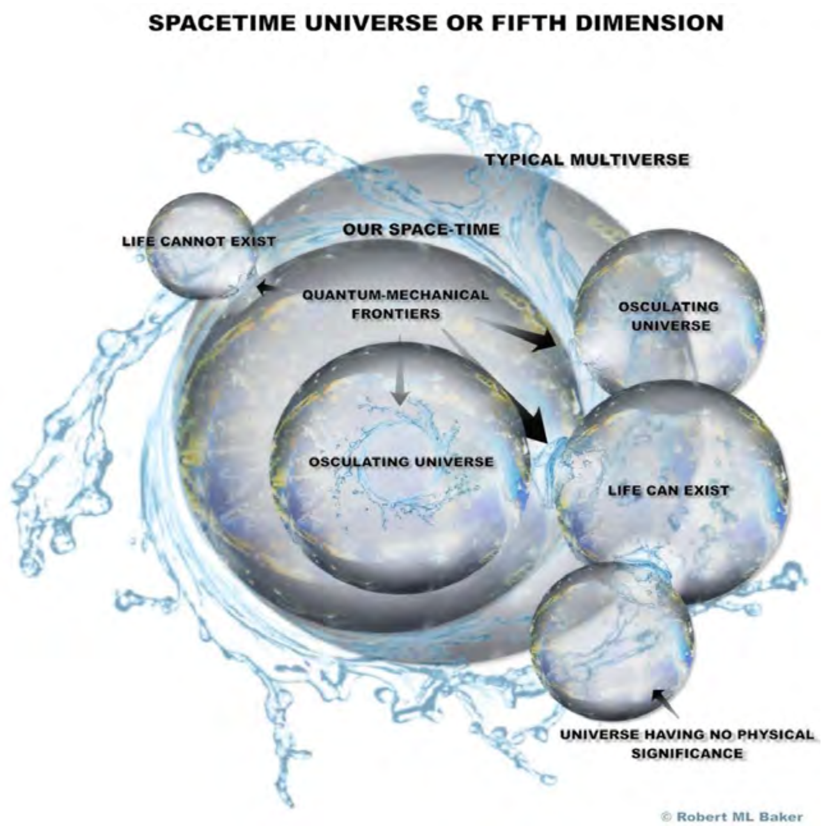

Figure 17. May not be the "Final" frontier for distant-future life forms in a Multiverse. From **Figure 15** of [3] (Baker and Baker, 2021).

survive. Assuming there's no catastrophic events such as discussed in the next Section 4, which terminates the majority of life forms on the planet, we hypothesize Homo sapien Life form evolution will continue to select traits to improve survivability. As related to life forms on Earth, Glaciers grow for about 90,000 years and then, mainly due to unavoidable perturbations of the Earth's orbit about the Sun, take one or more 10,000 year periods to collapse or melt during the resulting unavoidable periods of considerable climate change such as global warming. [25] (Berger, 2021, Hays, Imbrie, Shackleton. 1976). Present life forms (humans, other animals. marine life, etc.) themselves, especially Humans, due to their current need to cultivate, transport, prepare, consume, digest and expel "nutritional residue" (sewage) create climate change. This is part of "…anthropogenic global climate change," According to [26] Michael Desai and his colleagues (Desai, 2019), "…the largest (climate change) probably being greenhouse gas produced by these world's food-production systems." There are adverse effects due to our human Life form's industrial activities and their use of contaminants to the atmosphere, lithosphere or, in general to the life form's neighborhood environment. The use of fossil fuels produces some atmospheric contamination and climate change, but their effect are smaller than the climate change caused by the World's food-production systems. As has happened for millions of years, temporary sea-level, atmospheric composition, etc. changes may result, but no major changes or adjustments in Homo sapien life form's structure or operation are expected to occur; at least not over next 20,000 to 30,000 years.

3.2. Mind Boggling Progress and Adjustments

The MEANS of Evolution for some life forms is expected to radically change in the near future. Homo sapiens as well as any and all life forms in our Universe will participate in the "*Cyborg Revolution*" Possibly the first major operational change in life forms, specifically Homo sapien life forms, is exhibited in **Figure 4** and **Figure 5**, that is total mind control of mechanisms and equipment exterior to the life form. For example, turning on lights or an electric motor simply by thinking about the action. This progress, after perhaps thousands of years, would suggest the mind-boggling prospect: that, since they are no longer necessary, evolution would actually eliminate the need for external appendages such as hands and arms. Such appendages would be no longer be of competitive advantage. After tens of thousands or hundreds of thousands of years of non-use it would be reasonable to get rid of such appendages. "Just about everybody who thinks about trait evolution focuses on traits that are beneficial," writes first author [27] David Lahti (2009), a biologist at *Queens College*. "But few people think about traits (or body parts) that are useless, or that are becoming less useful over time will be no longer be of competitive advantage…" for *survival.* At this point, life forms such as human life forms and/or humanoid life forms (**Figure 6**), would be beginning to evolve into mainly "mental material" and commencing their evolution journey over perhaps millions or billions of years into a more secure (and survivable) *spherical form.* Such a Life form is fictionally described in **Figure 3**. We are now discussing time intervals in "Astronomer's time units" of millions and hundred billions of years. Evolution to a spherical form is easier to visualize by specifically, considering the humanoid *Ai-Da* shown in **Figure 6**. In her case the contraction of her parts and mental material to a spherical form could be imagined as a rather straight forward mechanical/electronic modification or rearrangement of her "parts".

What about other life forms existing at this evolutionary time in the "Terrestrial Part" of our Universe (home to the Homo sapien life forms)—the farm animals, pets, fish, birds, butterflies, mycelium, jungle beasts, bugs large and small, bad bacteria, viruses, fungi, *et al.*? If they are unfit to survive or for artificial accelerated evolution, then they will NOT survive (our Universe is NOT a kind or gentle place). As long as they provide, comfort, amusement, service, etc. and do not "bother" the higher intellectual level life forms (in this case very advanced Homo sapiens, cyborgs, humanoids *et al.*), they will NOT evolve relate to or effect in any way the evolutionary path of the evolving advanced forms under consideration. They will, in fact, NOT be members of the elite "*Survivor's Club*"! Whose members are evolving advanced life forms (eventually including cyborgs and humanoids). The early life form *Survivors* essentially exhibited as lined up in the evolutionary parade at the top of **Figure 15** will survive, and the rest will simply be neglected and left to perish. Like everything else in our Universe, all life forms have an opportunity to survive: "Survival of the Fittest" or "Law of the Jungle" Most probably do not become members of the *Survivor*'*s Club* and as we suggest perish.

It is amazing how our brain and body can actually dramatically change in size and function as they might well do over time. **Figure 18** actually shows how minibrains can "grow" crude eyes. This opens up the possibility that cyborg components need not always be electronic, but they could also be organic. Furthermore, the "design" of a life form could be accomplished by a system of controlled growth they cannot feel or love, for example. It's scary to think they will evolve and be able strategize even about things no human "put into them" but that could happen. We just don't know for sure if it will or when it will happen, possibly along a different evolutionary path. As mentioned in the Introduction, we restrict our study to "animals", but if, for example, a microscopic bacteria, fungus (for example a two-billion-year-old mycelium fungus, Helen Briggs, "World's oldest fungus raises evolution questions", *BBC News*, 25, April, 2017), somehow can develop an "intelligence" to "design", mentally remote control ALL its external functions and "install" some functional bacteria "part" and include or grow it in a new "model" of such a *bacteriniod*, then it might somehow participate in the *Survivor*'*s Club* and eventually wind up on stellar orbit! Same goes for *bunnyniods*!

3.3. Life form Sustenance Found on Stellar Orbits

The next gigantic evolutionary step or steps, (each step now requiring hundreds of thousands, millions or perhaps billions of years in Astronomer's time units to accomplish), we suggest is that all life forms will evolve *not* to require "food" for survival. Rather life forms would find nourishment from the energy they collect *directly* from starlight. The most efficient way to accomplish that would be to install life form or Life form civilization on orbits about stars and/or galaxies that the life form and/or Life form civilizations orbit. (In the "Terrestrial Part" of our Universe, it is our star, the Sun.). The concept here is that nourishment or energy that the life forms require will evolve efficiently, *not* from the ancient practice of farming various crops, which collect energy from the Sun to grow, in order to provide the energy our life form's body requires after food preparation of the crops. NO, but energy *directly* from their star's "sunlight" to electrical energy (photovoltaic converted). The days of "hunter-gatherers" and "pastoralism and/or horticulturalism" will be completely over. Therefore a life form's ability to obtain energy directly from a star or stars will not result in any contaminants entering their "neighborhood" from food consumption, processing or waste disposal. A very "clean" Universe is anticipated. Essentially, we will be transformed, over millions if not billions of years, from a spherical blob-like embryo baby material of today, shown in **Figure 19**, to a spherical blob-like ball of embryonic mental material orbiting stars or galaxies shown in **Figure 20**.

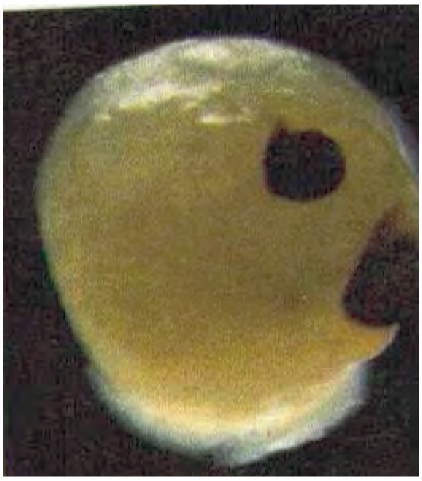

Figure 18. Two cup-shaped protrusions form rudimentary "eyes" in a lab-grown brain tissue. Picture from p 947, *Science* 373, Issue 6558, August 27, 2021.

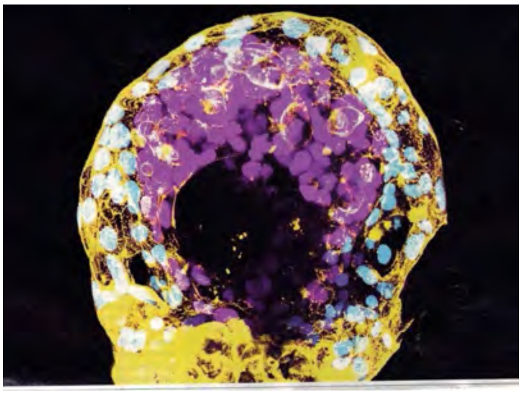

Figure 19. A human embryo of today, grown in the laboratory for 12 days [29] (Powell, (2021)).

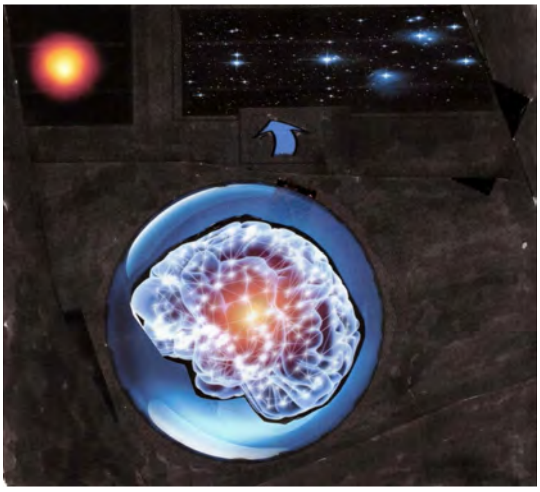

Figure 20. Artistic representation of the ultimate evolution of life-forms in our Universe to become living-thinking, mental material occupying spheres orbiting and nourished by a star or galaxy.

It's hard to imagine that all other life forms will "eat" from starlight, become spheres and disappear off the Earth and other bastions of life in our Universe to orbit stars. And, also to fathom that the same evolution occurs for all other "Earths" in our Universe. We are considering change over millions or even billions of years of years from now. The evolutionary parade on the top part of **Figure 15** is also very hard to imagine and sparked extreme controversy [28] (Larson, 2006): "How could we arise from monkeys much less fish?" But where did our fish fins go? And our Monkey tails—we know we had them since we still have tail bones? However, our evolution is ALL TRUE! Therefore it is not unreasonable to predict that in a few hundred thousand or million years we will become armored spheres, orbiting a star and feeding off its radiation --*Bon Appetite*!.

Actually, we will have "*Accelerated Evolution*" in which we predict "change" can be achieved by manipulation of parts of the eventual "humanoid" life forms populating our Universe, such as *Ai-Da* (shown in **Figure 6**). Of course it is impossible to assert that ALL life forms in our Universe participate in the same evolutionary process, probably not in concert, but it is our best guess.

The period of time for the incubation, development and possible demise of a Life form civilization may be billions of years. As discussed in the "Rollout Theory of our Universe" [25] (Baker, 2020) and "Detection and Determination of the Variation of the Speed of Time" [31] (Baker, Baker and Li, 2021) because of the very high speed of time in our early Universe (extreme red shift stars), millions and billions of "years" as observed by astronomers today may appear to last only seconds today. Plenty of time for the formation and evolution of many Life form civilizations, especially if the speed of time increases since the beginning of our Universe.

As far as locomotion is concerned, a corollary would be the life form's ability to operate vehicles and/or devices to translocate the life form itself as suggested in the science-fiction movie from which **Figure 3** was extracted. There also may be progress in a life form's ability to change, like a chameleon, its protective surface or shield from a shiny surface to reflect unwanted radiation like the Golden Tortoise beetle, to a black body to absorb energetic radiation required for power and "solar-sailing like" translocation. This is somewhat like the *Klingon ships* "cloaking" ability in the science-fiction television show *Star Trek*.

3.4. Proposed Ultimate Specifications of the Life form of Our Species

3.4.1. Shape

Life forms of our human species, and perhaps other non-human life forms, are expected to evolve having a shape to maximize volume, required in order to house their increased mental capabilities consisting of cognitive/micro-electronic or "living organic" material of the highest possible density and locomotion mechanisms, etc. and minimize surface area or their target area they present to any and all predators for protection? Since it is the geometric figure exhibiting the largest volume to area ratio is a sphere its shape would become spherical.

3.4.2. Weight

It is anticipated that the fit, survivable life forms of our species, and perhaps other non-human life forms, would locate themselves in the weightless free-fall of outer space. Therefore, weight would be of no consequence. Their mass might be minimized' for enhanced mobility and in order to house their increased mental capabilities consisting of cognitive/microelectronic material of the highest possible density; and a low-mass propulsive mechanism. Their actual size or dimensions (e. g., diameter since spherical) would be defined by their maximum volume. Although their volume might be considered to be unconstrained, since they are assumed to become on orbit about a star or stars (e.g., orbiting a galaxy), if they present too large of an area, then danger from debris, radiation, predators or other dangers might be increased as their exposed area is increased. Therefore some compromise would be struck.

3.4.3. Locomotion

Since it is anticipated that the fit life forms would locate themselves in the weightless free-fall of outer space, orbiting a star or galaxy, they would not require *locomotion*, except a small amount for orbit-keeping, or mobility for harvesting or collecting food or energy. Nevertheless, *locomotion* would be required in order for the Life form to avoid predators and other dangers. Therefore, they would require some propulsive mechanism such as "solar sailing", electrostatic propulsion or be equipped in order to scoop up materials from the space in their immediate vicinity and electrically accelerating it for propulsion.

4. Demise

("So many ways, so much time" Bobbie Baker, 1936, the "Kiddish Country" and *Battle Cry*, January/February 2019 issue,)

Albert Einstein is reported to have stated: "*Imagination* is more important than knowledge. For knowledge is limited to all we now know and understand, while *imagination* embraces the entire world, and all there ever will be to know and understand."

Following that edict, we will utilize the *imagination* from *Science-Fiction* movies to suggest possible situations resulting in the demise of a Life form civilization:

Very Little Bugs ("War of the Worlds," 2005 ["The smallest among us (microbes) could kill off their entire Martian civilization!"]) ("Andromeda Strain" 1971 [Virulent pandemic, e.g., COVID-9999999, from outer space.])

Very Big Bugs ("Them," 1954 [Giant Ants attack], "Godzilla," 1998)

Lethal Orbital Collision ("When Worlds Collide," 1951,)

Lethal Encounter ("Alien," 1979 [Deadly monsters unleased on other life-form civilizations. By the way, probably it was the author of this horror movie, Dan O'Bannon, who imaginatively reminds us that cyborgs need not always be filled with electronic components, but that organic components {like those in the Movie's character "Ash"} might also do nicely.])

Mental Self Destruction ("Forbidden Planet," 1956 [Mind control of a nightmare monster killed the Krell Life form civilization.])

Extinguishing of Mother Star/Galaxy ("Forbidden Planet," 1956 [Destruction of the central "Mother" planet at Movie's end]) [A star with a mass like our Sun can continue fusing hydrogen for about 10 billion years. On the other hand, if the star, which a more mature spherical Life form has chosen to orbit is very small, with a mass only a tenth that of our Sun, it can keep fusing hydrogen for more than the 100 billion years during the early Universe.]

Overtaken by Cybernetic Devices ("Rise of the Machines, Terminator 3," 2010), ("Westworld," 1973 [Amusement park androids that malfunction and begin killing visitors, could kill off any Life form civilization that enjoys amusement.])

Police, "Robocop," 1987 ("The Day the Earth Stood Still," 1951 [Powerful robot Gort, policing the Universe and destroying ANY "dangerous" Life form civilization it finds.])

Politics ("Survival of the fittest" scientifically determined law {Spencer, 1852; Darwin, 1859} *unavoidably* replaced by an attractive "Welfare State," which has a fatal attraction for and enslaves the electorate by providing "free" goods and services in return for maintaining, by election (tyranny of the majority), a huge and powerful central government. A powerful government that *unavoidably* and ultimately is attracted to and directed by a resourceful, nefarious leader (e.g., Mao Tse Tung, Maduro, Pol Pot, Hitler, Peron, Stalin, Mussolini, Castro, *et al.* leading to the demise of a Life form civilization)

Sports ("Predator," 1987 [Encounter with a creature that has "fun" hunting and killing an entire Life form civilization]), "Hunger Games." 2012 [Promotes the "fun" of killing off a Life form civilization's "people"], "War Games," 1983 [Computer takes over a ballistic-missile system and thinks it's all just a "game" to destroy countries including the "tit-tat toe" game, which the computer finds cannot be won.])

Artificial Intelligence. Elon Musk in the 2018 documentary about artificial intelligence, *Do You Trust This Computer*? "If AI has a goal and humanity just happens to come in the way, it will destroy humanity as a matter of course without even thinking about it, no hard feelings." Musk warns that the creation of superintelligence could lead to an "immortal dictator." That would end a civilization as we know it

Nutrition ("Soylent Green," 1973 ["People live in the streets and line up for their rations of water and Soylent Green. That's a high-protein foodstuff allegedly made from plankton cultivated in the seas. But actually from the bodies of people who die" leading to a demise of a Life form civilization])

Dream "Machines" ("13th floor," 1999 ["A newly completed virtual reality simulation (VR) of 1937 Los Angeles discloses some extraordinary situations."]) (The "Matrix", 1999 [In which intelligent machines have been created to distract humans while using their bodies as an energy source. When computer programmer Thomas Anderson uncovers the truth, he is drawn into a rebellion against the machines along with other Life form civilizations who have been "freed" from the Matrix. But if the programmer fails, then a demise of a life-form civilization would ensue.)

Slow degradation of a life form (Not truly a DEMISE, but gradually withering away to a life form "nothingness." Similar to the famous comment by General Douglas MacArthur: "Old Soldiers never die—they just fade away!").

Suicide or lack of will to go on.

5. Conclusions

It is easier to conclude a simple sequence for Life form Evolution rather than a precise time-ordered sequence. For all Life forms in our Universe, be they amoebas, fungus, bugs, or bunnies, human or non-human humanoids, the simple sequence in time we suggest is:

1) Complete Life form's conversion to a cyborg and/or (for Homo-sapiens)

Humanoid configuration as being the very fittest life form since it would be both repairable and improvable by other life forms.

2) Inclusion in brains exhibiting a communications capability: e.g., brain to brain, brain to machine, brain to HFGW transceiver, etc. communication capability. Thus, the supporting electronic circuits will need to be very close together and electronic "brain" components of minimum volume.

3) Developed and implemented artificial education function.

4) Elimination of the need for external appendages such as hands, arms and legs by cognitive control of locomotion and all external devices and mechanisms.

5) Development and fabrication of minimum target or surface area shields for protection of life form's Predators.

6) Optimum (because of 2) and 5) constraints) for all Life forms to be spherical in shape—no other solid-geometrical shape will be as fit.

7) Direct conversion of stellar radiation ENERGY to the energy needed for the life form to function.

8) Artificial, Accelerated Evolution would involve the replacement or repair of their "parts" especially if they were largely composed of electronic components as we predict for human life forms in the future.

9) Direct conversion of stellar radiation energy to the energy needed for the life form to function.

10) Life form's ability to operate vehicles and/or devices to translocate the life form itself by means of an appropriate propulsion to adjust stellar orbits—artificial planets.

11) Selection and translocation to an appropriate stellar-orbital locations achieved.

BUT what will the Life form do for the justification for its Existence and *for Amusement*?

a) Imagination, leading to curiously, leading to understanding, leading to:

b) Creativity and the justification for its existence. For example, discovering and analyzing in detail our human life form would certainly justify "their" existence!

c) Amusement: for example:

i) Sports (e.g., Bowling),

ii) Games,

iii) Exploration,

iv) Hobbies,

v) Art,

vi) Movies, etc. and, of course,

vii) SEX (returning to the science-fiction movie's aspect of imagination, we suggest the "Orgasmatron" from Woody Allen's movie "Sleeper", 1973).

MAIN CONCLUSION[4]:

Spherical form: As outlined in Section 5, the only reasonable ultimate design that the Life forms in our Universe will take is the one capable of adapting to environmental change by repair and design change by itself or by other life forms. Therefore, the only shape having a minimum volume (exhibiting the minimum inter component distances) and the smallest target area (for protection) is, by the laws of Solid Geometry and Physics, a sphere. Possibly the shape of a liquid drop of any mass or density in gravity-free space is a model. Also we agree with Itai Yanai's and Martin J Lercher's conclusion [33] from Gee's Book: *A* (*Very*) *Short History of Life on Earth*, that "…our Earth will be uninhabitable to even the hardiest organisms, spelling the final doom for Earth-evolved-life unless, perhaps, some earthlings manage to escape into space first." We agree, but we believe that the earthling will probably escape and inhabit spheres orbiting stars and galaxies!

Motivation: Other active life forms in our Universe are probably more curious about us (about our human life form) than we are about theirs. That curiosity and resulting creativity would serve to encourage and justify "their" existence! (Consider the curiosity of the little extraterrestrial botanist in the fanciful 1982 Science-fiction movie "ET".) Also "they" would have probably evolved not to just a spherical shape composed of mind or "thinking" and "communicating" matter orbiting a star (**Figure 20**), but to an enormously greater level of intelligence, imagination1 and observational capability than have we! Therefore, let's reformulate our search for extraterrestrial life from looking for their signals to striking up a conversation by greatly enhancing our ability to propagate a "Hello There. How Are You?" Signal. But Beware: please see [3] "Application of High-Frequency Gravitational Waves to the Cataclysmic Event of Our First Encounter with Intelligent Extraterrestrial Beings".

Acknowledgements

The authors express their appreciation for the editing and most helpful com-

[4]Will the ultimate life form be male or female or both? The authors remain undecided!

ments provided by Mellissa King, MBA. Senior Fellow Advocacy & Public Affairs, regenerative medicine foundation, Jan 2021-present, Chief Operating Officer, *brain window*, *INC*, Medical device company and Jeremy Horne, philosopher extraordinary.

Conflicts of Interest

The authors declare no conflicts of interest regarding the publication of this paper.

References

[1] Darwin, C. (1859) The Origin of the Species. Digital Edition, Goldstein, London.

[2] Spencer, H. (1852) A Theory of Population (Anonymous). *The Hayworth Papers*, March 20.

[3] Baker, Jr., Robert, M.L. and Baker, B.S. (2016) *Journal of Applied Mathematics and Physics*, **4**, 110-129. https://doi.org/10.4236/jamp.2016.41015

[4] He, B., Yuan, H., Meng, J. and Gao, S. (2020) Neural Engineering. 3rd Edition, Springer Nature, Berlin.

[5] Jones, L. (2021) What Will Humans Look like in a Million Years. https://www.bbcearth.com/news/what-will-humans-look-like-in-a-million-years

[6] Vetere, G., Tran, L.M., Moberg, S., Steadman, P.E., Restivo, L., Morrison, F.G., Ressler, K.J., Josselyn, S.A. and Frankland, P.W. (2019) *Nature Neuroscience*, **6**, 933-940. https://doi.org/10.1038/s41593-019-0389-0

[7] Service, R.F. (2013) *Science*, **340**, 1162-1165. https://doi.org/10.1126/science.340.6137.1162

[8] Veloso, M. (2015) *Nature*, **521**, 415-418. https://doi.org/10.1038/521415a

[9] Greene, B. (2017) Year Million. *Life Science Newsletter*, May 15. https://www.livescience.com/59115-year-million-series-explores-future-of-humanity.html

[10] Denny, C. (2020) Modifications of a Mouse's, Brain. *Boston College Magazine*, Spring.

[11] Willett, F.R., Avansino, D.T., Hochberg, *et al.* (2021) *Nature*, **593**, 249-254. https://doi.org/10.1038/s41586-021-03506-2

[12] Baker, Jr. and Robert, M.L. (2013) About Face, Economic Round Table, the California Club, Los Angeles. PowerPoint Presentation, May 2.

[13] Noy, A. (2011) *Advanced Materials*, **23**, 807-822.

[14] Gulati, T., Won, S.J., Ramanathan, D.S., Wong, C.C., Bodepudi, A., Swanson, R.A. and Ganguly, K. (2015) *The Journal of Neuroscience*, **35**, 8653-8661. https://doi.org/10.1523/JNEUROSCI.5007-14.2015

[15] Machens, C.K. (2012) *Science*, **338**, 1156-1157. https://doi.org/10.1126/science.1231865

[16] Mannoor, M.S., Jiang, Z., James, T., Kong, Y.L., Malatesta, K.A., Soboyejo, W.O., Verma, N., Gracias, D.H. and McAlpine, M.C. (2013) *Nano Letters*, **13**, 2634-2639. https://doi.org/10.1021/nl4007744

[17] Marx, V. (2015) *Nature*, **522**, 373-377. https://doi.org/10.1038/522373a

[18] Hirschberg, J. and Manning, C.D. (2015) *Science*, **349**, 261-266. https://doi.org/10.1126/science.aaa8685

[19] Chappell, B. (2021) *The Journal of Clinical Investigation*, **131**, e1511331.

[20] Power, S.A. (2014) *Science*, **345**, 262. https://doi.org/10.1126/science.1255866

[21] Grey, R. (2016) Could We Soon "Speak" Telepathically? Mind-Reading Computer Deciphers Words from Brainwaves before They Are Spoken. *Daily Mail*. https://www.dailymail.co.uk/sciencetech/article-3386875/Could-soon-speak-telepathically-Mind-reading-computer-deciphers-words-brainwaves-spoken.html

[22] Baker, Jr. and Robert, M.L. (2017) Gravitational Waves, the World of Tomorrow, a Primer. 3rd Printing, Infinity Publishing, West Conshohocken.

[23] Haldane, J.B.S. (1929) *The Rationalist Annual*, **148**, 3-10.

[24] Vilenchik, L. and Vilenchik, M. (2019) *Journal of High Energy Physics*, *Gravitation and Cosmology*, **5**, 884-898. https://doi.org/10.4236/jhepgc.2019.53044

[25] Berger, A. (2021) *Climate of the Past*, **17**, 1727-1733. https://doi.org/10.5194/cp-17-1727-2021

[26] Desai, M. (2019) *Nature*, **575**, 275.

[27] Lahti, D.C., Johnson, N.A., *et al*. (2009) *Trends in Ecology and Evolution* (*TREE*), **24**, 487-496. https://doi.org/10.1016/j.tree.2009.03.010

[28] Larson, E.J. (2006) Summer of the Gods. Basic Books, New York.

[29] Powell, K. (2021) *Nature*, **597**, 22-24. https://doi.org/10.1038/d41586-021-02343-7

[30] Baker, Jr. and Robert, M.L. (2020) *Journal of High Energy Physics*, *Gravitation and Cosmology*, **6**, 609-622. https://www.scirp.org/journal/jhepgc

[31] Baker, Jr., Robert, M.L., Baker, B.S. and Li, F.Y. (2021) *Journal of Modern Physics*, **12**, 761-780. https://doi.org/10.4236/jmp.2021.126049

[32] Blenkinsopp, R., Young, G.W., Milne, H., *et al*. (2020) *Proceedings of the ACM on Human-Computer Interaction*, **4**, Article No. 81.

[33] Yanal, I. and Lercher, M.J. (2021) *Science*, **374**, 828. https://doi.org/10.1126/science.abm0121

Journal of Modern Physics, 2021, 12, 2003-2030
https://www.scirp.org/journal/jmp
ISSN Online: 2153-120X
ISSN Print: 2153-1196

The Quantum Redshift Effect of Photon

Zhenglong Xu

Wuzhen High School, Tongxiang, China
Email: zhl-xu@126.com

How to cite this paper: Xu, Z.L. (2021) The Quantum Redshift Effect of Photon. *Journal of Modern Physics*, **12**, 2003-2030.
https://doi.org/10.4236/jmp.2021.1214115

Received: November 24, 2021
Accepted: December 28, 2021
Published: December 31, 2021

Abstract

By applying the relevant contents of time-dependent perturbation theory in present quantum mechanics, this paper operates the Hamiltonian operator on the existing steady-state wave function of the hydrogen atoms, creates the formula of the average energy loss per collision of a single photon with a neutral hydrogen atom. Then, by operating the Hamiltonian operator on the wave function of a helium atom, the expression of photon energy loss is extended to each bound electron in the neutral atoms of the general element. Applying theoretical derivation, it concludes that the photon's energy, momentum, and frequency decrease with distance in an exponential attenuation law, or the wavelength increases with distance in an exponential growth law during the propagation in intergalactic space, the photons collide with neutral atoms in the medium. Compared with Hubble redshift law, we discover that these laws conform to the so-called Hubble redshift or cosmological redshift in form and quantity. Therefore, this paper reveals a new physical mechanism—the quantum redshift effect of the photon in astronomy, astrophysics, and cosmology, thus challenging Hubble's law and the Big Bang theory.

Keywords

Hamiltonian Operator, Perturbation Theory, Hubble Redshift, Cosmological Redshift, Quantum Redshift Effect, Hubble Constant

1. Introduction

The Big Bang theory considered the "Redshift" be evidence that the universe is expanding. Whether the redshift is evidence has always been a matter of great debate. The reason for the controversy is that after that explanation, few people have done in-depth research on the physical mechanism of the origin of the redshift, and physicists do not seem to be interested in this question, but rather in dark matter and dark energy. How photons travel through intergalactic space with a redshift is a mystery. Since discovered quasars in the 1950s, the redshift is not entirely consistent with Hubble's law and the so-called cosmological redshift, leading physicists to revisit the origin of redshifts. There have been many theories in history, such as tired light theory, photon aging theory, intrinsic redshift theory, physical constant change theory, new tired light theory. But no one can fully reveal its physical mechanism to convince the Big Bang theorists. So, what way can solve this mystery?

2. The Collision of a Single Photon with a Free Electron

This section attempts to explore the physical mechanism of the origin of redshift employing classical electrodynamics. There are different opinions in astrophysics about whether the intergalactic space medium is neutral gas or plasma gas. Assuming the intergalactic medium is thin plasma rather than a continuum. The electrodynamic treatment of electromagnetic wave propagation in continuous media is not adopted. This paper uses the term "photon" rather than "light"; and utilizes the ideas of the size and shape of a single photon [1]. Suppose a photon collides with an electron in a plasma, how much energy lost the photon does, and what direction the photon travels.

2.1. Relationship between Compton Scattering and Thomson Scattering

Suppose that photons travel from distant galaxies to Earth through intergalactic space, where the medium is a thin plasma that is consisted of electrons and protons. Photons can only collide with a free electron or a free ion, but it is almost impossible to with both simultaneously. Since there is no mutual constraint between electrons and nuclei, the way to deal with photons colliding with charged particles is classical electrodynamics rather than quantum mechanics.

In the energy calculation, the energy lost by the collision of photons with free electrons is much larger than that lost by the collision of free protons. Therefore, only that between the photon and the free-electron is considered, not between photon and proton.

When a single photon collides with a free electron, one of the effects may occur. The first effect is the Compton effect and the second effect is the Thomson effect.

The probability of a Compton effect occurring in a collision between a single photon and a free electron is [1]

$$p_C = \frac{\pi}{2}\frac{\lambda_C}{\lambda} \tag{1}$$

And the probability of the Thomson effect is

$$p_T = \frac{2\lambda - \pi\lambda_C}{2\lambda} \tag{2}$$

Here, λ_C is the Compton wavelength of an electron, and λ is the wavelength of a photon.

Apparently, for photons in the optical band, the wavelength is longer than the Compton wavelength, *i.e.*, $\lambda \gg \lambda_C$. Therefore, the probability of the Compton effect is very low, but the energy lost in each collision is relatively high. When photons in the optical band collide with free electrons, the probability of the Thomson effect is much higher than that of Compton scattering, the energy lost by photons in each collision is relatively low.

The paper "the size and shape of a single photon" deeply discussed the Compton effect, which found that the condition for the Compton effect is: First, the photon wavelength is small enough to meet $\lambda \le \pi\lambda_C/2$; Second, although it does not meet $\lambda \le \pi\lambda_C/2$, the electron is collided by the edge of the photon. Under such conditions, the interaction time cannot reach the photon vibration period that the electron ejects by the photon electric field. In Compton scattering, both the electron and the photon change direction. Therefore, the photon no longer travels in a straight line.

In Compton scattering, if the interaction time between electron and photon reaches one period, *T*, there is no Compton effect. In this case, the Thomson effect will occur.

2.2. Thomson Effect of Single Photon-Single Electron

This section focuses on the Thomson effect when a single photon collides with a free electron.

Suppose the photon propagates along the Z-axis at the velocity *c*, the electric field vibrates along the X-axis, and the mass of the electron is m_e. The charge of the electron is -*e*. The electric field strength of photon is

$$E = E_0 \sin\omega\left(t - \frac{z}{c}\right) \tag{3}$$

where E_0 is the amplitude of photon electric field strength, ω is the angular frequency of photon electric field vibration, and *t* is time.

Assuming that the electron initially rests at the origin of the coordinate OXYZ, the initial position is $x_0 = 0$, the initial speed is $\dot{x}_0 = 0$, omitting $z/c = 0$ in the brackets of the sinusoidal function, the electric field force of the electron acted by the photon is

$$F_e = -eE_0 \sin\omega t \tag{4}$$

When an electron vibrates in the electric field of a photon, electromagnetic radiation will occur. In turn, the radiation acts on the electron, causing the electron to subject a damping force proportional to the moving velocity $\dot{x}$

$$f = -\gamma_0 m_e \dot{x} \tag{5}$$

where γ_0 is the damping coefficient of the electron

$$\gamma_0 = \frac{e^2\omega^2}{6\pi\varepsilon_0 m_e c^3} \tag{6}$$

where ε_0 is the vacuum dielectric constant.

The resultant force on the electron is

$$F = m_e \ddot{x} = -eE_0 \sin \omega t - \gamma_0 m_e \dot{x} \tag{7}$$

Thus, can list the following equation

$$\begin{cases} \ddot{x} + \gamma_0 \dot{x} = -\dfrac{eE_0}{m_e} \sin \omega t \\ x_0 = 0; \dot{x}_0 = 0 \end{cases} \tag{8}$$

By solving this equation, the velocity of the electron is

$$\dot{x} = \frac{eE_0}{m_e \left(\omega^2 + \gamma_0^2\right)} \left[\left(\gamma_0 \sin \omega t + \omega \cos \omega t\right) - \omega \mathrm{e}^{-\gamma_0 t} \right] \tag{9}$$

The displacement of the electron is

$$x = -\frac{eE_0}{m_e \omega \gamma_0 \left(\omega^2 + \gamma_0^2\right)} \left[\left(\omega^2 - \gamma_0^2\right) - \left(\omega^2 \mathrm{e}^{-\gamma_0 t} - \gamma_0^2 \cos \omega t + \omega \gamma_0 \sin \omega t\right) \right] \tag{10}$$

The work done by photon to the electron is

$$W = \int_0^X F_e \mathrm{d}x = \int_0^T F \dot{x} \mathrm{d}t \tag{11-a}$$

$$= \frac{e^2 E_0^2}{m_e \left(\omega^2 + \gamma_0^2\right)} \int_0^T \sin \omega t \left[\left(\gamma_0 \sin \omega t + \omega \cos \omega t\right) - \omega \mathrm{e}^{-\gamma_0 t} \right] \mathrm{d}t \tag{11-b}$$

$$= \frac{e^2 E_0^2}{m_e \left(\omega^2 + \gamma_0^2\right)} \left[\frac{1}{2} \gamma_0 T + \frac{\omega^2}{\omega^2 + \gamma_0^2} \left(1 - \mathrm{e}^{-\gamma_0 T}\right) \right] \tag{11-c}$$

where T is the period of photon vibration [1].

Under the condition of $\gamma_0 \ll \omega$ and $\gamma_0 \ll \omega_0$, take the approximate $\mathrm{e}^{-\gamma_0 T} \approx 1 - \gamma_0 T$, the above formula becomes

$$W = \frac{e^2 E_0^2}{m_e \left(\omega^2 + \gamma_0^2\right)} \left[\frac{1}{2} \gamma_0 T + \frac{\omega^2 \gamma_0 T}{\omega^2 + \gamma_0^2} \right] \tag{11-d}$$

$$= \frac{3e^2 E_0^2}{2 m_e \omega^2} \gamma_0 T \tag{11-e}$$

Use Equation (6), and the above equation becomes

$$W = 2\pi\alpha \frac{\left(\hbar\omega\right)^3}{\left(m_e c^2\right)^2} \tag{11-f}$$

$$= 3 \frac{\sigma_T}{\sigma_P} \cdot \hbar\omega \tag{11-g}$$

Here utilizing the following relationship:

The relationship between the electric field strength of a single photon and the photon frequency [1]

$$eE_0 = \frac{\hbar \omega^2}{c} \tag{12}$$

The fine structure constant

$$\alpha = \frac{e^2}{4\pi\varepsilon_0 \hbar c} \tag{13}$$

The classical electron radius formula

$$r_e = \frac{e^2}{4\pi\varepsilon_0 m_e c^2} \tag{14}$$

The Thomson scattering cross-sectional area of classical electron

$$\sigma_T = \frac{8\pi}{3} r_e^2 \tag{15}$$

The cross-sectional area of linearly polarized photon [1]

$$\sigma_P = \frac{\alpha}{\pi^2} \lambda^2 \tag{16}$$

In the above formulas, $\hbar$ is the reduced Planck constant.

Equation (11-g) shows that the work done by a photon to an electron is equal to the ratio of three times the cross-sectional area of the electron to the cross-sectional area of the photon multiplied by photon energy. Every time a photon and a free electron occur Thomson scattering, the energy lost by the photon is $W = \left(3\sigma_T / \sigma_p\right)\hbar\omega$. It means that the energy lost by the photon is that intercepted by the electron.

In macroscopic electrodynamics, express the formula of Thomson scattering of a beam of light by a single electron as the power of electron scattering as the following:

$$P_T = \sigma_T I_0 \tag{17}$$

where I_0 is the intensity of the incident beam of light. In classical electrodynamics, the light intensity I_0 is independent of photon frequency.

The difference between Equations (11) and (17) represents the difference between a single photon and a beam of light.

Equation (9) shows that when the photon interacts with the electron for a period T, the electron gets the recoil velocity or the recoil momentum in the X-direction; in turn, the photon momentum also changes in the X-direction, which means that the photon no longer propagates in a straight line.

Summary:

1) Because Compton scattering and Thomson scattering will change the direction of photon motion, once Compton scattering or Thomson scattering occurs on the path of propagation to the Earth, it cannot be received by observers on the Earth. Therefore, Compton scattering and Thomson scattering cannot be the cause of extragalactic galaxy redshift.

2) The occurrence of the Compton effect and Thomson effect depends on plasma, so it can infer that the neutral gas dominates the intergalactic medium rather than plasma.

3. Collision of a Single Photon with a Hydrogen Atom

3.1. Size Comparison between Photon and Atom

Photons of different wavelengths have different sizes. For studying the energy loss in the collision between a single photon and an atom, it is necessary to understand several typical photon size parameters. All photons mentioned in this paper are linearly polarized photons.

Here, the electric field size of a photon refers to the length of the photon along the electric field direction, and the formula is [1]

$$L_E = \frac{2}{\pi}\lambda \tag{18}$$

The photon cross-sectional area formula is as Equation (16).

Photons in **Table 1** refer to:

1) The microwave corresponding to the maximum energy distribution of the cosmic microwave background;

2) Infrared corresponding to the maximum energy distribution of human thermal radiation;

3) The most sensitive light of the human eye;

4) Ultraviolet light with the shortest wavelength;

5) An X-ray used in the Compton experiment [2];

6) γ-rays produced by electron pair annihilation;

7) γ-rays produced by proton pair annihilation;

As well known that the order of magnitude of the diameter of an atom is 10^{-10} - 10^{-9} m. The table indicates that the electric field size of ultraviolet light with the shortest wavelength is greater than the atomic diameter. The electric field size of photons with a longer wavelength than ultraviolet light with the shortest wavelength is larger than the atom diameter.

According to the comparison between the size of the photon electric field and the atom diameter, photons are divided into two categories. Photons whose electric field size is larger than the atom diameter are called soft photons, and photons whose electric field size is smaller than the atom diameter are called hard photons.

Table 1. The wavelength, electric field size, and cross-sectional area of some photons.

Photon	Wavelength/m	Electric field size/m	Cross-sectional area/m^2
1	7.4×10^{-2}	4.7×10^{-2}	4.0×10^{-8}
2	1.0×10^{-5}	6.4×10^{-4}	7.4×10^{-14}
3	5.3×10^{-7}	3.4×10^{-7}	2.1×10^{-16}
4	1.0×10^{-8}	6.4×10^{-9}	7.4×10^{-20}
5	7.1×10^{-11}	4.5×10^{-11}	3.7×10^{-24}
6	2.4×10^{-12}	1.5×10^{-12}	4.2×10^{-27}
7	1.3×10^{-15}	8.3×10^{-14}	1.2×10^{-33}

3.2. Soft Photons and Hard Photons Collide with Atoms to Produce Different Effects

Soft and hard photons have different physical effects when they collide with atoms.

Because the electric field size of a soft photon is greater than that of an atom, when a photon collides with the atom, the whole will be immersed in the photon electromagnetic field, resulting in the atomic nucleus and electrons in the atom being affected by the photon electromagnetic field simultaneously. As shown in Figure 1 is the collision model of soft photon-atom.

Because the electric field size of the photon is shorter than that of the atom when a hard photon collides with it, the photon can't be to collide with the whole atom but enter its interior. The photon can collide only with one of the nucleus or electrons in the atom, and it is impossible to collide with the electron and nucleus simultaneously. As shown in Figure 2 is the collision model of hard photon-atom.

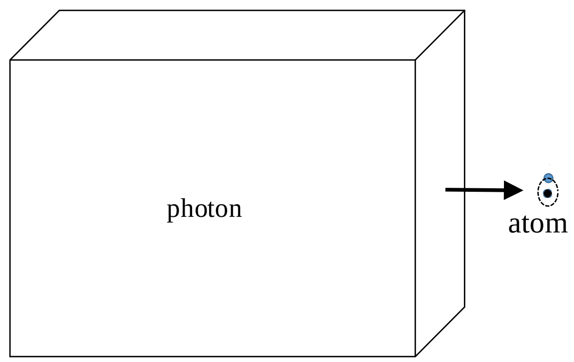

Figure 1. A soft photon collides with an atom.

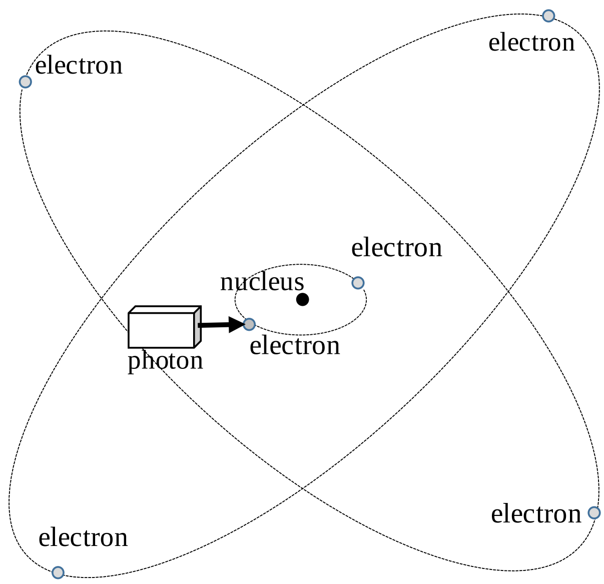

Figure 2. A hard photon enters into an atom and strikes one of electrons.

In this way, when a photon enters the atom, one of the following two situations may occur:

The first is Compton scattering, in which the propagation direction of photons will change.

The second is that if the cross-sectional area of the hard photon is small enough, the photon may penetrate atoms unimpeded without colliding with any kinds of particles.

Summary:

When a single photon collides with an atom, it is necessary to distinguish between soft photons and hard photons. Only soft photons can interact with the nucleus and extranuclear electrons simultaneously.

4. The Energy Loss in a Collision between the Photon and Hydrogen Atom

The focus of the following study is the collision of a soft photon with a hydrogen atom.

Why study the collision of a soft photon with a hydrogen atom? It is for two reasons:

First, only the soft photon can collide with the nuclei and the electron simultaneously because of its large size.

Second, in quantum mechanics textbooks, the only atom studied is hydrogen, and the treatment of helium and the higher elements is approximate.

4.1. Correction of Hamiltonian

Classical electrodynamics can deal with the collision between photons and free electrons. Quantum mechanics can deal with that between a photon with bound electrons.

When there is no external electromagnetic field, extranuclear electron of a hydrogen atom are only affected by the electric field of the nucleus, and the Hamiltonian can express as

$$\mathcal{H}_0 = \frac{\boldsymbol{P}_0^2}{2m_e} + U(r) \tag{19}$$

where $\boldsymbol{P}_0$ is the momentum of the extranuclear electron and $U(r)$ is the electric potential energy of the electron in the electric field of the atomic nucleus, which can express as

$$U(r) = -\frac{1}{4\pi\varepsilon_0}\frac{e^2}{r} \tag{20}$$

When the photon electromagnetic field suddenly acts on the hydrogen atom, the nucleus and the extranuclear electron are affected by the photon electromagnetic field simultaneously, which will change their kinetic energy and potential energy. Since the mass of the hydrogen nucleus is 1836 times that of the electron, the kinetic energy it gets is negligible, so only the electron is considered.

Suppose the functions of electric field strength and magnetic induction strength of electromagnetic wave of a photon be

$$\begin{cases} \boldsymbol{E} = E_0 \sin\omega\left(t-\frac{z}{c}\right)\boldsymbol{e}_x & (21\text{-}1) \\ \boldsymbol{B} = B_0 \sin\omega\left(t-\frac{z}{c}\right)\boldsymbol{e}_y & (21\text{-}2) \end{cases}$$

whose vector potential $\boldsymbol{A}$ conforms to

$$\begin{cases} \boldsymbol{E} = -\frac{\partial \boldsymbol{A}}{\partial t} & (22\text{-}1) \\ \boldsymbol{B} = \nabla\times\boldsymbol{A} & (22\text{-}2) \end{cases}$$

Regardless of the integral constant, integrating can obtain

$$\boldsymbol{A} = -\int \boldsymbol{E}\mathrm{d}t = -E_0\boldsymbol{e}_x\int \sin\omega\left(t-\frac{z}{c}\right)\mathrm{d}t \tag{23-a}$$

$$= \frac{E_0}{\omega}\cos\omega\left(t-\frac{z}{c}\right)\boldsymbol{e}_x \tag{23-b}$$

$$= \frac{E_0}{2\omega}\left[\mathrm{e}^{i\omega\left(t-\frac{z}{c}\right)} + \mathrm{e}^{-i\omega\left(t-\frac{z}{c}\right)}\right]\boldsymbol{e}_x \tag{23-c}$$

The sudden appearance of the electromagnetic field of the photon causes two changes of extranuclear electrons:

The first is the change of electron momentum caused by the vector potential of the photon electromagnetic field

$$\Delta\boldsymbol{P}' = -e\boldsymbol{A} \tag{24}$$

Acted by the photon electromagnetic field, the momentum of the electron becomes

$$\boldsymbol{P} = \boldsymbol{P}_0 + \Delta\boldsymbol{P}' = \boldsymbol{P}_0 - e\boldsymbol{A} \tag{25}$$

The second is that the scalar potential of the photon electric field causes the change of the electric potential energy of the electron:

$$V(r) = -e\boldsymbol{E}\cdot\boldsymbol{r} = -eE_0 x\sin\omega\left(t-\frac{z}{c}\right) \tag{26}$$

Thus, when the photon electromagnetic field acts on the hydrogen atom, the Hamiltonian is

$$\mathcal{H} = \frac{1}{2m_e}\left(\boldsymbol{P}_0 - e\boldsymbol{A}\right)^2 + U(r) + V(r) \tag{27}$$

In addition, the orbital magnetic moment and spin magnetic moment of the electron will also cause the change of potential energy in the photon magnetic field. This potential-energy term can incorporate into the term $V(r)$. The calculation result can show the splitting of atomic energy-level, that is, the Zeeman effect. Quantum mechanics textbooks have a detailed discussion [3] ①, which omits here.

Discussing the correction term $V(r)$ in detail in quantum mechanics textbooks clarifies the physical mechanism by which photons are absorbed by atoms as a whole or atoms are excited by photons to emit photons. The change in momentum $\Delta \boldsymbol{P}' = -e\boldsymbol{A}$, which is overlooked usually in textbooks, hides a profound secret.

4.2. Basic Theory of Hamiltonian Operator Operation

According to the general textbook of quantum mechanics [4], the Hamiltonian operator corresponding to the Hamiltonian of Equation (27) is

$$\hat{\mathcal{H}} = \frac{1}{2m_e}\left(\hat{\boldsymbol{P}}_0 - e\boldsymbol{A}\right)^2 + \hat{U}(r) + \hat{V}(r) \tag{28-a}$$

$$= \frac{1}{2m_e}\hat{\boldsymbol{P}}_0^2 + \hat{U}(r) + \hat{V}(r) - \frac{e}{2m_e}\left(\hat{\boldsymbol{P}}_0 \cdot \boldsymbol{A} - \boldsymbol{A} \cdot \hat{\boldsymbol{P}}_0\right) + \frac{e^2}{2m_e}\boldsymbol{A}^2 \tag{28-b}$$

where the momentum operator is

$$\hat{\boldsymbol{P}}_0 = -i\hbar\nabla \tag{29}$$

Generally speaking, $\hat{\boldsymbol{P}}_0$ does not commute with $\boldsymbol{A}$, so there is a relationship

$$\hat{\boldsymbol{P}}_0 \cdot \boldsymbol{A} - \boldsymbol{A} \cdot \hat{\boldsymbol{P}}_0 = -i\hbar\nabla \cdot \boldsymbol{A} \tag{30}$$

However, for photons, since the electromagnetic wave is a transverse wave, applying Equation (23-b) can obtain $\nabla \cdot \boldsymbol{A} = 0$, then $\hat{\boldsymbol{P}}_0$ commutes with $\boldsymbol{A}$, so Equation (30) becomes $\hat{\boldsymbol{P}}_0 \cdot \boldsymbol{A} - \boldsymbol{A} \cdot \hat{\boldsymbol{P}}_0 = 0$ that the Hamiltonian operator (28) can express as

$$\hat{\mathcal{H}} = \frac{1}{2m_e}\hat{\boldsymbol{P}}_0^2 + U(r) + V(r) - \frac{e}{m_e}\boldsymbol{A} \cdot \hat{\boldsymbol{P}}_0 + \frac{e^2}{2m_e}\boldsymbol{A}^2 \tag{31}$$

Group this representation into four parts:

The first part is

$$\hat{\mathcal{H}}_0 = \frac{1}{2m_e}\hat{\boldsymbol{P}}_0^2 + \hat{U}(r) \tag{32}$$

It is the Hamiltonian operator of the Hydrogen atom when it is not affected by the photon electromagnetic field, and it is the Eigen-operator of the hydrogen atomic system.

The second part is

$$\hat{\mathcal{H}}_1' = \hat{V}(r) = -eE_0\hat{x}\sin\omega\left(t - \frac{z}{c}\right) \tag{33}$$

It is the potential energy of an atom as an electric dipole, and this term takes as a perturbation term. This paper refers to herein as the first correction term.

The third part is

$$\hat{\mathcal{H}}_2' = -\frac{e}{m_e}\boldsymbol{A} \cdot \hat{\boldsymbol{P}}_0 \tag{34}$$

This term is proportional to the dot product of the momentum vector of the extranuclear electron caused by the action of the photon electromagnetic field and the Eigen-momentum vector, which is called the second correction term in this paper.

Since the photon propagates along the Z-axis, the photon electric field vibrates along the X-axis, as described in Equation (21-1); The vector potential of the photon vibrates along the X-axis, as described in Equation (23), so that

$$\boldsymbol{A}\cdot\hat{\boldsymbol{P}}_0 = A\hat{P}_x = A\left(-i\hbar\frac{\partial}{\partial x}\right) \tag{35}$$

For a photon whose wavelength far exceeds the atomic radius, the time difference $\omega z/c$ can ignore, so that

$$\boldsymbol{A} = \frac{E_0}{2\omega}\left(\mathrm{e}^{i\omega t}+\mathrm{e}^{-i\omega t}\right)\boldsymbol{e}_x \tag{36}$$

Combining (35) and (36) obtain

$$\boldsymbol{A}\cdot\hat{\boldsymbol{P}}_0 = \frac{E_0}{2\omega}\left(\mathrm{e}^{i\omega t}+\mathrm{e}^{-i\omega t}\right)\left(-i\hbar\frac{\partial}{\partial x}\right) \tag{37}$$

Substituting (37) into (34) obtain

$$\hat{\mathcal{H}}_2' = -\frac{e}{m_e}\boldsymbol{A}\cdot\hat{\boldsymbol{P}}_0 \tag{38-a}$$

$$= -\frac{eE_0}{2m_e\omega}\left(\mathrm{e}^{i\omega t}+\mathrm{e}^{-i\omega t}\right)\left(-i\hbar\frac{\partial}{\partial x}\right) \tag{38-b}$$

The fourth part is

$$\hat{\mathcal{H}}_3' = \frac{e^2}{2m_e}\boldsymbol{A}^2 = \frac{e^2E_0^2}{8m_e\omega^2}\left(\mathrm{e}^{i\omega t}+\mathrm{e}^{-i\omega t}\right)^2 \tag{39}$$

This term is purely a change in kinetic energy caused by photon action. It refers to as the third correction term.

So the representation of the Hamiltonian operator is

$$\begin{aligned}\hat{\mathcal{H}} = {} & \frac{1}{2m_e}\hat{\boldsymbol{P}}_0^2 + U(r) + V(r) - \frac{eE_0}{2m_e\omega}\left(\mathrm{e}^{i\omega t}+\mathrm{e}^{-i\omega t}\right)\left(-i\hbar\frac{\partial}{\partial x}\right) \\ & + \frac{e^2E_0^2}{8m_e\omega^2}\left(\mathrm{e}^{i\omega t}+\mathrm{e}^{-i\omega t}\right)^2\end{aligned} \tag{40}$$

This representation is relatively complete, including both kinetic energy correction term and potential energy correction term. Usually, to highlight the focus of the problem, textbooks only consider the potential-energy correction term rather than the kinetic energy correction term.

4.3. Derivation Using Perturbation Theory

In quantum mechanics, successfully solving the Schrödinger equation for hydrogen atoms obtain a set of eigenvalues and eigenfunctions of the atomic state. Considering a hydrogen atom is in an eigenstate and is affected by an external single photon electromagnetic field. According to the usual treatment method, use the $\hat{\mathcal{H}}$ of Equation (40) acting on the assumed wave function, set up the Schrödinger equation, and solve it to obtain the eigenfunction and eigenvalue. But it is too complicated to deal with the problem in this way. It is not easy to solve the new Schrödinger equation. Therefore, quantum mechanics usually regards the electromagnetic field of incident photons as a perturbation in the steady-state. Therefore, using perturbation theory to deal with the collision of a photon with a hydrogen atom is appropriate. To deal with the perturbation problem is to use the approximation method [3] ② [5] ①. This paper only makes the first-order approximation, ignoring the second-order and higher-order corrections.

Under the steady-state wave function of the hydrogen atom Φ_n, there is a relationship

$$\hat{\mathcal{H}}_0\Phi_n = i\hbar\frac{\partial\Phi_n}{\partial t} = E_n\Phi_n \tag{41}$$

The eigenfunction of $\hat{\mathcal{H}}$ is Ψ, expanding in eigenfunction Φ_n of $\hat{\mathcal{H}}_0$ is

$$\Psi = \sum_n a_n(t)\Phi_n \tag{42}$$

Its Schrödinger equation is

$$i\hbar\frac{\partial\Psi}{\partial t} = \hat{\mathcal{H}}\Psi \tag{43}$$

Substituting (42) into (43) to get

$$i\hbar\sum_n \Phi_n\frac{\mathrm{d}a_n(t)}{\mathrm{d}t} + i\hbar\sum_n a_n(t)\frac{\partial\Phi_n}{\partial t} = \sum_n a_n(t)\hat{\mathcal{H}}_0\Phi_n + \sum_n a_n(t)\hat{\mathcal{H}}'\Phi_n \tag{44}$$

Applying Equations (41) and (44) can obtain the following equation

$$i\hbar\sum_n \Phi_n\frac{\mathrm{d}a_n(t)}{\mathrm{d}t} = \sum_n a_n(t)\hat{\mathcal{H}}'\Phi_n \tag{45}$$

Multiply the conjugate wave function Φ_n^* of Φ_n on both sides and integrate over the whole space to get

$$i\hbar\sum_n\frac{\mathrm{d}a_n(t)}{\mathrm{d}t}\int\Phi_m^*\Phi_n\mathrm{d}\tau = \sum_n a_n(t)\int\Phi_m^*\hat{\mathcal{H}}'\Phi_n\mathrm{d}\tau \tag{46}$$

where

$$\int\Phi_m^*\Phi_n\mathrm{d}\tau = \delta_{mn} \tag{47}$$

The eigenfunction of $\hat{\mathcal{H}}_0$ is ϕ_n, thus

$$\hat{\mathcal{H}}_0\phi_n = E_n\phi_n \tag{48}$$

In this way, expanding the steady-state wave function Φ_n of $\hat{\mathcal{H}}_0$ in its eigenfunction ϕ_n can obtain

$$\Phi_n = \phi_n\mathrm{e}^{-\frac{i}{\hbar}E_n t} \tag{49}$$

Substituting it into the integral on the right side of (46) and setting

$$\mathcal{H}'_{mn} = \int \phi_m^* \hat{\mathcal{H}}' \phi_n \mathrm{d}\tau \tag{50}$$

Equation (46) becomes

$$i\hbar \sum_n \frac{\mathrm{d}a_m(t)}{\mathrm{d}t} = \sum_n a_n(t) \mathcal{H}'_{mn} \mathrm{e}^{i\omega_{mn}t} \tag{51}$$

where

$$\omega_{mn} = \frac{1}{\hbar}(E_m - E_n) \tag{52}$$

is the Bohr frequency.

Before the perturbation starts, the system is in the k th eigenstate Φ_k of $\hat{\mathcal{H}}_0$, which can obtain the following from Equation (42)

$$a_n(0) = \delta_{nk} \tag{53}$$

Now consider only the first order approximation, that is, substitute Equation (53) for the $a_n(t)$ in the summation sign Σ in Equation (42), thus obtained by Equation (51)

$$i\hbar \frac{\mathrm{d}a_m(t)}{\mathrm{d}t} = \sum_n \delta_{nk} \mathcal{H}'_{mn} \mathrm{e}^{i\omega_{mn}t} = \mathcal{H}'_{mk} \mathrm{e}^{i\omega_{mk}t} \tag{54}$$

Hence, the first-order approximation is

$$a_m(t) = \frac{1}{i\hbar} \int_0^t \mathcal{H}'_{mk} \mathrm{e}^{i\omega_{mk}t'} \mathrm{d}t' \tag{55}$$

In this way, the change probability can calculate based on the following:

$$p = a_m^*(t) a_m(t) = |a_m(t)|^2 \tag{56}$$

4.4. The Operation of the Three Correction Terms of the Hamiltonian Operator

1) The Operation of the First Correction Term

All quantum mechanics textbooks are very detailed in the first correction term of Hamiltonian operator [3] ③ [5] ②.

Applying the correction value of Hamiltonian operator (33) to Equation (50) can obtain

$$\mathcal{H}'_{1mk} = \int \phi_m^* \hat{\mathcal{H}}_1 \phi_k \mathrm{d}\tau \tag{57-a}$$

$$= -\frac{1}{2i} eE_0 \int \phi_m^* \hat{x} \phi_k \left(\mathrm{e}^{i\omega t} - \mathrm{e}^{-i\omega t}\right) \mathrm{d}\tau \tag{57-b}$$

$$= -\frac{1}{2i} eE_0 x_{mk} \left(\mathrm{e}^{i\omega t} - \mathrm{e}^{-i\omega t}\right) \tag{57-c}$$

where

$$x_{mk} = \int \phi_m^* \hat{x} \phi_k \mathrm{d}\tau \tag{58}$$

Substitute (57-c) into (55) to get

$$a_{1m}(t) = \frac{1}{i\hbar} \int_0^t \mathcal{H}'_{1mk} \mathrm{e}^{i\omega_{mk}t'} \mathrm{d}t' \tag{59-a}$$

$$= \frac{eE_0}{2\hbar}\int_0^t x_{mk}\left(e^{i\omega t'} - e^{-i\omega t'}\right)e^{i\omega_{mk}t'}dt' \tag{59-b}$$

$$= \frac{eE_0}{2\hbar}x_{mk}\int_0^t\left(e^{i\omega t'} - e^{-i\omega t'}\right)e^{i\omega_{mk}t'}dt' \tag{59-c}$$

$$= \frac{eE_0}{2\hbar}x_{mk}\int_0^t\left[e^{i(\omega_{mk}+\omega)t'} - e^{i(\omega_{mk}-\omega)t}\right]dt' \tag{59-d}$$

$$= \frac{eE_0}{2\hbar}x_{mk}\left[\frac{e^{i(\omega_{mk}+\omega)t}-1}{i(\omega_{mk}+\omega)} - \frac{e^{i(\omega_{mk}-\omega)t}-1}{i(\omega_{mk}-\omega)}\right] \tag{59-e}$$

The probability of change is

$$P_1(t) = a_{1mk}^*(t)a_{1mk} = \left|a_{1m}(t)\right|^2 \tag{60-a}$$

$$= \frac{e^2E_0^2\left|x_{mk}\right|^2}{\hbar^2}\Gamma_1 \tag{60-b}$$

where

$$\Gamma_1 = \left[\frac{\sin^2\frac{1}{2}(\omega_{mk}-\omega)t}{(\omega_{mk}-\omega)^2} + \frac{\sin^2\frac{1}{2}(\omega_{mk}+\omega)t}{(\omega_{mk}+\omega)^2} - \frac{\cos^2\omega t - \cos\omega_{mk}t\cos\omega t}{\omega_{mk}^2-\omega^2}\right] \tag{61}$$

$\left|x_{mk}\right|$ in the above formulas can't get a clear expression. This paper won't go deep into what value to take.

2) The Operation of the Second Correction Term

For the operation of the second correction term of the Hamiltonian operator $\hat{\mathcal{H}}_2'$, follow the steps from Equation (57) to Equation (61):

Applying Equation (38-b) to Equation (51)

$$\mathcal{H}_{2mk}' = \int\phi_m^*\hat{\mathcal{H}}_2'\phi_k d\tau \tag{62-a}$$

$$= -\frac{eE_0}{2m_e\omega}\int\phi_m^*\left(-i\hbar\frac{\partial}{\partial x}\right)\phi_k\left(e^{i\omega t} + e^{-i\omega t}\right)d\tau \tag{62-b}$$

$$= -\frac{eE_0}{2m_e\omega}\left(e^{i\omega t} + e^{-i\omega t}\right)\int\phi_m^*\left(-i\hbar\frac{\partial}{\partial x}\right)\phi_k d\tau \tag{62-c}$$

$$= -\frac{eE_0}{2m_e\omega}\left(e^{i\omega t} + e^{-i\omega t}\right)P_{xmk} \tag{62-d}$$

where

$$P_{xmk} = \int\phi_m^*\left(-i\hbar\frac{\partial}{\partial x}\right)\phi_k d\tau \tag{63}$$

Substitute (62-d) into (55) to get

$$a_{2m}(t) = \frac{1}{i\hbar}\int_0^t\mathcal{H}_{2mk}'e^{i\omega_{mk}t'}dt' \tag{64-a}$$

$$= -\frac{1}{i\hbar}\frac{eE_0P_{xmk}}{2m_e\omega}\int_0^t\left(e^{i\omega t'} + e^{-i\omega t'}\right)e^{i\omega_{mk}t'}dt' \tag{64-b}$$

$$= -\frac{1}{i\hbar}\frac{eE_0P_{xmk}}{2m_e\omega}\int_0^t\left[e^{i(\omega_{mk}+\omega)t'} + e^{i(\omega_{mk}-\omega)t}\right]dt' \tag{64-c}$$

$$= -\frac{1}{i\hbar}\frac{eE_0 P_{xmk}}{2m_e\omega}\left[\frac{e^{i(\omega_{mk}+\omega)t}-1}{i(\omega_{mk}+\omega)}+\frac{e^{i(\omega_{mk}-\omega)t}-1}{i(\omega_{mk}-\omega)}\right] \quad (64\text{-d})$$

$$= \frac{eE_0 P_{xmk}}{2m_e\hbar\omega}\left[\frac{e^{i(\omega_{mk}+\omega)t}-1}{(\omega_{mk}+\omega)}+\frac{e^{i(\omega_{mk}-\omega)t}-1}{(\omega_{mk}-\omega)}\right] \quad (64\text{-e})$$

The probability of change is

$$P_2(t) = a^*_{2mk}(t)a_{2mk} = |a_{2m}(t)|^2 \quad (65\text{-a})$$

$$= \frac{e^2E_0^2|P_{xmk}|^2}{m_e^2\hbar^2\omega^2}\Gamma_2 \quad (65\text{-b})$$

$$\Gamma_2 = \left[\frac{\sin^2\frac{1}{2}(\omega_{mk}-\omega)t}{(\omega_{mk}-\omega)^2}+\frac{\sin^2\frac{1}{2}(\omega_{mk}+\omega)t}{(\omega_{mk}+\omega)^2}+\frac{\cos^2\omega t-\cos\omega_{mk}t\cos\omega t}{\omega_{mk}^2-\omega^2}\right] \quad (66)$$

$|P_{xmk}|$ in the above formulas can't get a clear expression. This paper won't go deep into what value to take.

The operation results $P_1(t)$ and $P_2(t)$ of $\hat{\mathcal{H}}_1'$ and $\hat{\mathcal{H}}_2'$ are very similar: First, $|x_{mk}|^2$ corresponds to $|P_{xmk}|^2$, further discussion of these two factors will explain the selection rule of atomic energy-level transition. Second, Γ_1 corresponds to Γ_2 in the formulas.

The meaning of these formulas is clear that when $\omega = \pm\omega_{mk}$, the system resonates, so there are two possibilities: In the first case, $\omega = \omega_{mk}$, the atom takes the energy of the photon as $\hbar\omega$ whole absorbed, the photons disappear, and the atomic energy level changes from low energy level E_k transition to high energy level E_m;In the second case, $\omega = -\omega_{mk}$, excited by photons, its energy level changes from high energy level E_k transition to low energy level E_m, emitting a photon with energy $\hbar\omega_{mk}$.

However, if $m = k$, from Equation (52) can obtain $\omega_{mk} = 0$, so that Equation (60) becomes

$$P_1(t) = \frac{e^2E_0^2}{\hbar^2\omega^2}|x_{mm}|^2(1-\cos\omega t)^2 \quad (67)$$

Since the photon length is $L = \lambda$, substituting the vibration period T of the photon into the above formula can get

$$P_1(T) = \frac{e^2E_0^2}{\hbar^2\omega^2}|x_{mm}|^2(1-\cos\omega T)^2 = 0 \quad (68)$$

Similarly, if $m = k$, Equation (65) becomes

$$P_2(t) = \frac{e^2E_0^2}{m_e^2\hbar^2\omega^2}|P_{xmk}|^2\sin^2\omega t \quad (69)$$

Substituting the vibration period T of the photon into the above formula can get

$$P_2(T) = \frac{e^2E_0^2}{m_e^2\hbar^2\omega^2}|P_{xmk}|^2\sin^2\omega T = 0 \quad (70)$$

Equations (68) and (70)show that that the results of the first correction term $\hat{\mathcal{H}}_1'$ and the second correction term $\hat{\mathcal{H}}_2'$ operating on the wave function of the hydrogen atom are that the atom absorbs or emits photons, and its energy level undergoes a transition. At the same energy level, the photon energy cannot be absorbed or emitted.

Therefore, it is more appropriate to combine $P_1(t)$ and $P_2(t)$ for discussion.

$$P_{1+2}(t) = P_1(t) + P_2(t) = \frac{e^2 E_0^2}{\hbar^2}\left[\left|x_{mk}\right|^2 \Gamma_1 + \frac{\left|P_{xmk}\right|^2}{m_e^2 \omega^2}\Gamma_2\right] \tag{71-a}$$

Employing Equation (12) can get

$$P_{1+2}(t) = \frac{\omega^2}{c^2}\left[\omega^2 \left|x_{mk}\right|^2 \Gamma_1 + \frac{\left|P_{xmk}\right|^2}{m_e^2}\Gamma_2\right] \tag{71-b}$$

The characteristic of these two effects is that the energy of photon absorbed by the atom either absorbs the whole photon or does not absorb the photon energy at all.

3) The Operation of the Third Correction Term

Now consider the third correction term $\hat{\mathcal{H}}_3'$ of the Hamiltonian operator. According to Equation (39) and (50), this part of the Hamiltonian operator does not contain parameters about spatial coordinates. Therefore, for function integration over space, the integrand function is constant, so can obtain

$$\mathcal{H}_{3mk}' = \int \phi_m^* \hat{\mathcal{H}}_3' \phi_k \mathrm{d}\tau \tag{72-a}$$

$$= \frac{e^2 E_0^2}{8 m_e \omega^2}\left(\mathrm{e}^{i\omega t} + \mathrm{e}^{-i\omega t}\right)^2 \delta_{mk} \tag{72-b}$$

Substituting it into Equation (55) can get

$$a_{3m}(t) = \frac{1}{i\hbar}\int_0^t \mathcal{H}_{mk}' \mathrm{e}^{i\omega_{mk}t'} \mathrm{d}t' \tag{73-a}$$

$$= \frac{1}{i\hbar}\frac{e^2 E_0^2}{8 m_e \omega^2}\int_0^t \left(\mathrm{e}^{i\omega t'} + \mathrm{e}^{-i\omega t'}\right)^2 \delta_{mk} \mathrm{e}^{i\omega_{mk}t'} \mathrm{d}t' \tag{73-b}$$

$$= \frac{1}{i\hbar}\frac{e^2 E_0^2}{8 m_e \omega^2}\int_0^t \left(\mathrm{e}^{i\omega t'} + \mathrm{e}^{-i\omega t'}\right)^2 \mathrm{d}t' \tag{73-c}$$

$$= \frac{1}{i\hbar}\frac{e^2 E_0^2}{4 m_e \omega^2}\left(t + \frac{\sin 2\omega t}{2\omega}\right) \tag{73-d}$$

This formula shows that the absorption of photon energy by an atom is independent of the change of the atom state; that is, it can absorb the fractional energy of photon only under the condition of the same energy level. The probability of absorbing photon energy is

$$P_3(t) = \left|a_{3m}(t)\right|^2 = \left[\frac{e^2 E_0^2}{4\hbar m_e \omega^2}\left(t + \frac{\sin 2\omega t}{2\omega}\right)\right]^2 \tag{74}$$

The energy absorbed by an atom from a photon is

$$\Delta E_3(t) = \hbar\omega P_3(t) = \frac{(eE_0)^4}{16\hbar m_e^2\omega^3}\left(t + \frac{\sin 2\omega t}{2\omega}\right)^2 \tag{75}$$

Since the interaction time between photon and atom is equal to the period T of photon vibration [1], using the physical quantity Equation (12) of a single photon and the relationship $\omega T = 2\pi$, from Equation (75), the energy absorbed by the atom from the photon is

$$\Delta E_3 = \frac{\pi^2}{4}\frac{(\hbar\omega)^3}{(m_e c^2)^2} \tag{76-a}$$

Using the classical electron cross-sectional area Equation (15) and photon cross-sectional area Equation (16), the Equation (76-a) can change into

$$\Delta E_3 = \frac{3\pi}{8\alpha}\frac{\sigma_T}{\sigma_P}\hbar\omega \tag{76-b}$$

where α is the fine structure constant, as Equation (13).

Obviously, from Equation (76) that after a single photon collides with a hydrogen atom, the photon energy absorbed by the hydrogen atom is $\pi/8\alpha = 53.8$ times of the energy absorbed by the electron when Thomson scattering occurs between the photon and the free electron.

The characteristic of this effect is that the atom absorbs the fractional energy of a photon and will not cause the energy level transition of the atom.

4.5. Comparison of Results

Comparing the operation results of the correction terms of the Hamiltonian $\hat{\mathcal{H}}_1'$, $\hat{\mathcal{H}}_2'$ and $\hat{\mathcal{H}}_3'$ is helpful for a deep understanding of their physical meaning.

1) The Difference in Physical Mechanism

Although both $P_{1+2}(t)$ and $P_3(t)$ have the meaning of probability, they have different physical meanings.

At present, quantum mechanics is interested in the absorption and emission of photons and the energy level transition of atoms. Therefore, there is often only the Hamiltonian operator correction term $\hat{\mathcal{H}}_1'$ and $\hat{\mathcal{H}}_2'$ but not $\hat{\mathcal{H}}_3'$.

Then, how to understand that the physical meaning of $P_{1+2}(t)$ is the probability of an atom absorbing or emitting a photon, or the probability of an atom's transition.

For example, if $P_{1+2}(t) = 0.01$, the atom has a 1% chance of absorbing the entire photon. That is to say, if 100 photons hit 100 atoms respectively, on average, one of the atoms absorbs one of the photons. The atom either absorbs all the photon energy or does not absorb the photon energy at all. It doesn't mean that each atom absorbs 1% energy of each photon. If resonance occurs, the probability that the atom absorbs a photon will have a resonance peak.

Therefore, the physical meaning of $P_{1+2}(t)$ is the rate of loss or increase in the number of photons when photons collide with atoms. So, the effect of $\hat{\mathcal{H}}_1'$ and $\hat{\mathcal{H}}_2'$ correspond to the attenuation effect of the number of photons.

Equation (74) is generally ignored in quantum mechanics. An important reason is that compared with the resonance phenomenon represented in Equations (60) and (65), this term is insignificant; Another reason is that it is impossible to derive Equation (76) from Equation (74) under the condition that the size and shape of a single photon are unknown.

Then, what is the effect of the term $\hat{\mathcal{H}}_3'$?

The physical meaning of $P_3(t)$ is that an atom fractionally absorbs the energy of a photon, and it does not have an energy-level transition. Since the interaction time between them is equal to the vibration period of the photon, hence $t = T$ in Equation (74), from which can obtain

$$P_3(T) = \frac{\pi^2}{4}\left(\frac{\hbar\omega}{mc^2}\right)^2 \tag{77}$$

For example, if a photon with an energy of 5.1 eV collides with an atom, because $m_e c^2 = 0.51\,\text{MeV} = 5.1\times 10^5\,\text{eV}$, the energy lost by the photon is only $2.46\times 10^{-10}\times\hbar\omega$. The rest of the photon energy is not absorbed, and the photon continues to travel forward after reducing fractional of energy.

Generally speaking, the energy loss rate of a photon colliding with an entire atom is insignificant due to $\hbar\omega/m_e c^2 \ll 1$.

Therefore, the physical meaning of $P_3(t)$ is the loss rate of photon energy when a photon collides with an atom.

If a distant celestial body emits a large group of independent photons, it will encounter atoms on the way to the Earth. The number of these photons will decrease according to the probability of $P_{1+2}(t)$, and the remaining photons will continue to propagate. The energy of each photon decreases in proportion to $P_3(t)$.

It means that the effect of $\hat{\mathcal{H}}_3'$ corresponds to the energy attenuation effect of a single photon. If the phenomenon that the photon energy decreases on the way of propagation is called redshift, then this paper calls it the quantum redshift effect.

It is a newly discovered redshift effect different from the previously Doppler effect redshift, gravitational redshift, Compton effect redshift, etc.

The correction term of the Hamiltonian operator $\hat{\mathcal{H}}_3'$ shows that the essence of this effect is that the atom absorbs a fractional of energy of the incident photon and converts it into the kinetic energy of the extranuclear electron. What happens after the electron absorbs this part of the energy? The atomic system does not undergo a transition, but the atom converts this part of energy into low-frequency radio radiation.

The classical electrodynamic method cannot accurately express the two different absorption concepts. Only by applying quantum mechanics can the theory of quantum redshift effect be derived.

2) Meaning in Photometry

A large number of photons in a beam of light, as long as they encounter a large number of atoms on the way of propagation, the number of photons will inevitably decrease, resulting in absorption lines on the photometric spectrum. The absorption lines in photometry as the Lyα forest is the result of the Hamiltonian $\hat{\mathcal{H}}_1'$ and $\hat{\mathcal{H}}_2'$. This effect does not occur during the collision of photons with free electrons. Therefore, the appearance of the absorption line of the photometric spectrum as the Lyα forest proves that photons encounter atoms on the way of propagation.

In the photometry of distant luminous objects, absorption lines and redshifts are always accompany each other; that is, any spectrum with redshift must have absorption lines; conversely, any spectra with absorption lines must appear redshift.

Summary:

1) The correction terms of the Hamiltonian operator, $\hat{\mathcal{H}}_1'$, $\hat{\mathcal{H}}_2'$, in the electromagnetic interaction between photons and atoms represents the probability of the number of photons absorbed or emitted by atoms, that is, the rate of increase or decrease in the number of photons, and also represents the probability of the energy level transition of the atom. The effect of decreasing or increasing the number of photons appears as absorption lines and emission lines on the photometric spectrum.

2) The correction term of the Hamiltonian operator, $\hat{\mathcal{H}}_3'$,in the electromagnetic interaction between photons and atoms represents the absorption rate of single-photon energy or the loss rate of single-photon energy by the atoms. The redshift of the spectral line is evidence of the quantum redshift effect.

5. Collision between Photon and Helium Atom and Its Analogy

5.1. Energy Loss in the Collision of Photon and Helium Atom

With the successful treatment of the collision between photons and hydrogen atoms, solving the problem of that between photons and other element atoms will be easy. As long as adding a momentum change term caused by the photon vector potential, as in Equation (24), and adding a scalar potential-energy of each extranuclear electron caused by the photon electric field.

When there is no photon electromagnetic field disturbance, the Hamiltonian of the helium atom is

$$\mathcal{H}_{H_{e0}} = \frac{\boldsymbol{P}_{10}^2}{2m_e} + \frac{\boldsymbol{P}_{20}^2}{2m_e} + U_1(r_1) + U_2(r_2) + U_{12}(r_{12}) \tag{78}$$

Due to the emergence of photon electromagnetic field, adding the correction momentum term generated by a vector potential to the momentum of each extranuclear electron, such as Equation (24), and at the same time, adding electric potential energy term generated by a scalar potential to each electron, such as Equation (26), the Hamiltonian of helium atom becomes:

$$\mathcal{H}_{He} = \frac{(\boldsymbol{P}_{10} - e\boldsymbol{A})^2}{2m_e} + \frac{(\boldsymbol{P}_{20} - e\boldsymbol{A})^2}{2m_e} + U(r_1) + U_2(r_2) + U_{12}(r_{12}) + V_1(r) + V_2(r) \tag{79}$$

In the same way as the hydrogen atom problem, the Hamiltonian operator can be divided into four parts:

$$\begin{aligned}\hat{\mathcal{H}}_{He} &= \frac{1}{2m_e}\left(\hat{\boldsymbol{P}}_{10}^2+\hat{\boldsymbol{P}}_{20}^2\right)+U\left(r_1\right)+U_2\left(r_2\right)+U_{12}\left(r_{12}\right)\\ &+V_1\left(r\right)+V_2\left(r\right)\\ &-\frac{eE_0}{2m_e\omega}\left(\mathrm{e}^{i\omega t}+\mathrm{e}^{-i\omega t}\right)\left(-i\hbar\frac{\partial}{\partial x_1}\right)-\frac{eE_0}{2m_e\omega}\left(\mathrm{e}^{i\omega t}+\mathrm{e}^{-i\omega t}\right)\left(-i\hbar\frac{\partial}{\partial x_2}\right)\\ &+\frac{e^2E_0^2}{4m_e\omega^2}\left(\mathrm{e}^{i\omega t}+\mathrm{e}^{-i\omega t}\right)^2\end{aligned} \tag{80}$$

The meaning of each part of the Hamiltonian operator represented by this formula is:

The first part (the first row) is the Hamiltonian $\hat{\mathcal{H}}_{He0}$ corresponding to Equation (78) when the helium atom is not disturbed by the photon electromagnetic field. The result of the operation on the steady-state wave function of the helium atom is the eigenvalue of the helium atom.

The second part (the second row), $V_1\left(r\right)+V_2\left(r\right)$, is the scalar potential energy of two extranuclear electrons of helium atom acted by photon electromagnetic field, which operator is $\hat{\mathcal{H}}'_{He1}$, and represents the first correction term of the Hamiltonian operator. The result of its operation can explain the number probability of atomic absorption and emission of photons. If the atom is in a state where the photon energy reaches the energy level difference, the probability of absorption or emission increases sharply, resulting in a resonance peak.

The third part (the third row) represents the second correction term $\hat{\mathcal{H}}'_{He2}$ of the Hamiltonian operator. When it acts on the eigenfunction of the helium atom, two similar to Equation (38-b) appear in the Hamiltonian operator; It can explain the number probability of atomic absorption and emission of photons.

The fourth part (the fourth row) represents the third correction term $\hat{\mathcal{H}}'_{He3}$ of the Hamiltonian operator of the helium atom. When it operates on the eigenfunction of the helium atom, the value of the operation result is twice that of the Hamiltonian operator of the hydrogen atom.

The method to deal with helium atoms interacting with photons is the same as the method to deal with hydrogen atoms interacting with photons. At first, regarding the eigenvalue and eigenfunction of the Hamiltonian operator $\hat{\mathcal{H}}_{He0}$ as known quantities, then treating the other three factors $\hat{\mathcal{H}}'_{He1}$, $\hat{\mathcal{H}}'_{He2}$, and $\hat{\mathcal{H}}'_{He3}$ as correction terms, rather than using the Hamiltonian operator to directly calculate on the preset wave function to set up the Schrödinger equation and then solve it.

Disregard the first correction term $\hat{\mathcal{H}}'_{He1}$ to highlight the other point because this term describes the probability of energy level transition due to atomic absorption or emission of photons.

Like the second correction term of the hydrogen atom, the second correction term of the Hamiltonian operator of helium atom, $\hat{\mathcal{H}}'_{He2}$, will produce two values like Equation (65).

Like hydrogen atoms, the physical effect of $\hat{\mathcal{H}}'_{He1}$ and $\hat{\mathcal{H}}'_{He2}$ operation results is that the photon energy absorbed by the atom either absorbs the whole photon or does not absorb the photon energy at all.

Now, pay special attention to the last term of the Hamiltonian operator, the correction term is as follows

$$\hat{\mathcal{H}}'_{He3} = \frac{e^2 E_0^2}{4m_e\omega^2}\left(\mathrm{e}^{i\omega t} + \mathrm{e}^{-i\omega t}\right)^2 \tag{81}$$

Corresponding to the calculation result of the hydrogen atom, Equation (76), the energy lost by a single photon in collision with a helium atom is

$$\Delta E_{He} = 2\times\frac{\pi^2}{4}\frac{(\hbar\omega)^3}{\left(m_e c^2\right)^2} \tag{82-a}$$

or

$$\Delta E_{He} = 2\times\frac{3\pi}{8\alpha}\frac{\sigma_T}{\sigma_P}\hbar\omega \tag{82-b}$$

It shows that the energy lost by a photon in a collision with a helium atom is twice that expressed by the Equations (76-a) or (76-b).

5.2. Inference

For an atom of element number N, there are N extranuclear electrons. When a photon acts on it, N kinetic energy terms, $N\times\left(\boldsymbol{P}_0 - e\boldsymbol{A}\right)^2/2m_e$, appear in the Hamiltonian, and N correction terms, as described in Equation (39), appear in the Hamiltonian operator of N electrons. The operation result of each correction one corresponds to the photon energy loss as described in Equation (76).

Reasoning: a photon propagating in the thin intergalactic media, if it is not absorbed by the atom when it collides with the atom with element number N, the energy lost by unabsorbed photons is

$$\Delta E = N\frac{\pi^2}{4}\frac{(\hbar\omega)^3}{\left(m_e c^2\right)^2} = N\frac{3\pi}{8\alpha}\frac{\sigma_T}{\sigma_P}\hbar\omega \tag{83}$$

Therefore, the energy lost by a photon is proportional to the number of electrons bound in the atom that it collides with on its propagation path.

Summary:

As the photon collides with the atom, the energy loss of the photon is proportional to the number of extranuclear electrons of the atom encountered. Thus, only the total number of electrons bound in atoms is needed to calculate the energy lost by the photon.

6. Attenuation Law of Photon Frequency

6.1. Propagation of Photons in Thin Atomic Gas

If there are bound electrons on the path of photon propagation, and their number density is n_e, the cross-sectional area of a photon is σ_P, then the photon travels distance cdt in time interval $\mathrm{d}t$, and the swept volume is $\mathrm{d}V = \sigma_p c\mathrm{d}t$, the number of electrons encountered is $\mathrm{d}N_e = n_e \mathrm{d}V = n_e \sigma_p c\mathrm{d}t$, the photon loses energy every time they collide with electrons, as described in Equation (76), so the energy lost by photons in time interval $\mathrm{d}t$ is

$$\mathrm{d}\hbar\omega = -n_e \sigma_P c\mathrm{d}t \cdot \frac{3\pi}{8\alpha} \frac{\sigma_T}{\sigma_P} \hbar\omega \tag{84-a}$$

$$= -\frac{3\pi}{8\alpha} c\sigma_T n_e \hbar\omega \mathrm{d}t \tag{84-b}$$

where $n_e \sigma_P c$ can be called the collision frequency of a photon and bound electrons.

Equation (84) can express as four equivalent equations

$$\begin{cases} \dfrac{\mathrm{d}(\hbar\omega)}{\mathrm{d}t} + \dfrac{3\pi}{8\alpha} c\sigma_T n_e (\hbar\omega) = 0 & (85\text{-}1) \\ \dfrac{\mathrm{d}}{\mathrm{d}t}\left(\dfrac{\hbar\omega}{c}\right) + \dfrac{3\pi}{8\alpha} c\sigma_T n_e \left(\dfrac{\hbar\omega}{c}\right) = 0 & (85\text{-}2) \\ \dfrac{\mathrm{d}\omega}{\mathrm{d}t} + \dfrac{3\pi}{8\alpha} c\sigma_T n_e \omega = 0 & (85\text{-}3) \\ \dfrac{\mathrm{d}\nu}{\mathrm{d}t} + \dfrac{3\pi}{8\alpha} c\sigma_T n_e \nu = 0 & (85\text{-}4) \end{cases}$$

When $t = 0$, the initial frequency is ν_0, and set

$$H_0 = \frac{3\pi}{8\alpha} c\sigma_T n_e \tag{86}$$

If n_e is homogeneous, integrating the Equation (85) can obtain

$$\nu = \nu_0 \mathrm{e}^{-H_0 t} = \nu_0 \mathrm{e}^{-\frac{H_0}{c} r} \tag{87-1}$$

where the relationship between distance and time, $r = ct$, is used.

If n_e is inhomogeneous, integrating the Equation (85) can obtain

$$\nu = \nu_0 \mathrm{e}^{-\int_0^r \frac{H_0}{c} \mathrm{d}r} = \nu_0 \mathrm{e}^{-\frac{3\pi}{8\alpha} \sigma_T \int_0^r n_e(r) \mathrm{d}r} \tag{87-2}$$

Representing the above formula as the wavelength changes with time or distance can obtain

$$\lambda = \lambda_0 \mathrm{e}^{H_0 t} \tag{87-3}$$

or

$$\lambda = \lambda_0 \mathrm{e}^{\int_0^r \frac{H_0}{c} \mathrm{d}r} = \lambda_0 \mathrm{e}^{\frac{3\pi}{8\alpha} \sigma_T \int_0^r n_e(r) \mathrm{d}r} \tag{87-4}$$

Equation (87) shows that if a photon encounters atoms when propagating in space, its frequency decreases with distance in exponential attenuation law; In other words, its wavelength increases with distance in exponential growth law.

In the above formula, H_0 is the attenuation rate of the photon frequency. The speed of light c, the fine structure constant α and the electron Thomson scattering cross-sectional area σ_T are all known physical constants; only the bound electron density n_e is an unknown constant. To be sure, n_e is inhomogeneous along the path of photon propagation.

6.2. Damped Motion of A photon

Photon propagates in intergalactic space with neutral atoms, and its momentum decreases gradually due to the damping effect of the medium.

From Equation (85-2), it is apparent that photons make damping motion in intergalactic space. It shows that the constant H_0 is the damping coefficient of photon motion. This damping coefficient is also the attenuation rate of photon frequency, energy, and momentum; or the growth rate of wavelength.

Summary:

The collision between photons and atoms on the propagation path causes the photon frequency to decrease with distance in exponential attenuation law or the wavelength increase with distance in exponential growth law. The motion of photons is a damped one. The attenuation rate of photon frequency, *i.e.*, the damping coefficient of the photon, is directly proportional to the number density of extranuclear electrons encountered on the path of photon propagation.

7. Negation of Hubble's Law

7.1. Comparison with Hubble Redshift Formula

In 1924, Hubble studied a large number of data of extragalactic galaxies and concluded that the redshift is

$$Z = \frac{\lambda - \lambda_0}{\lambda_0} = \frac{H_0}{c} r \tag{88}$$

This relationship is called Hubble's law of redshift. Here H_0 is the Hubble constant, c is the speed of light, and r is the distance from the observed galaxy to the Earth.

Using Equation (87-3), the redshift formula is

$$Z = \frac{\lambda - \lambda_0}{\lambda_0} = \mathrm{e}^{\frac{H_0}{C} r} - 1 \tag{89}$$

Under the first-order approximation, $\mathrm{e}^{\frac{H_0}{C} r} = 1 + \frac{H_0}{c} r$, the formula above is given by

$$Z = \frac{\lambda - \lambda_0}{\lambda_0} = \frac{H_0}{c} r \tag{90}$$

It is apparent, Hubble's redshift law is only another expression under the first-order approximation of the Equation (87-3).

If interpreting formula (87-3) as classical Doppler effect, then

$$1 + \frac{V}{c} = \mathrm{e}^{\frac{H_0}{C} r} \tag{91}$$

or

$$V = H_0 r \tag{92}$$

This formula is known as Hubble's law.

Due to the redshift effect in the photon-atom collision, the energy of photons decreases with the propagation distance, *i.e.*, the redshift depends on the propagation distance of photons. Therefore, mainstream scholars often attribute this phenomenon to the universe expansion, the so-called cosmological redshift [5] ③. Even they almost express the redshift Z directly as the regression speed of luminaries and intergalactic media. It is a serious misinterpretation. How can the phenomenon caused by the quantum redshift effect of photons take as evidence that the universe is expanding?

In the Big Bang theory, the reciprocal of the photon's damping coefficient, $1/H_0$, is regarded as the universe's age. It is unbelievable.

7.2. Comparison between Damping Coefficient and Hubble Constant

H_0 in Equations (90) (92) is called the Hubble constant in Big Bang cosmology. After nearly a century of measurement, the recognized value of this constant is close to

$$H_0 = 70\ \text{km/s} \cdot \text{Mpc} = 2.27 \times 10^{-18}/\text{s} \tag{93}$$

As can be seen from Equation (86), H_0 is not a constant. No one has ever obtained an exact value in the measurement of nearly a century. Because it is related to the bound electron density on the path of photon propagation, but the atom density in intergalactic space is not uniform, H_0 is not a constant. However, with the increase of the measurement distance, the measured atom density in intergalactic space tends to average, so n_e is also getting closer to the average electron density in cosmology space.

If considering the redshift as caused by the collision between photons and electrons in atoms, the electron density in intergalactic space in the whole universe is given by

$$n_e = \frac{8\alpha}{3\pi c \sigma_T} H_0 = 0.705/\text{m}^3 \tag{94}$$

The results show that to meet the numerical requirements of the Hubble constant, the average density of bound electrons in intergalactic space is 0.7electrons per cubic meter. Hydrogen is the most abundant element in nature, accounting for about 71% by mass; followed by helium, accounting for about 27%; The total atomic mass of the other ones is about 2%.

According to the number of atoms, hydrogen atoms account for 91.2%, helium atoms account for 8.6%, and the total number of one of the other elements is less than 0.2%. Because hydrogen atoms have the minimum mass and are easy to escape from stars and galaxies, the proportion of hydrogen atoms in intergalactic space may be higher than 91.2%. So it can estimate that the mass density of intergalactic matter is about 1.2×10^{-27} kg/m^3.

The actual observations [6] are that the typical density of intergalactic matter within the large clusters is 2×10^{-24} kg/m^3 and that outside is 4.6×10^{-31} kg/m^3.

The density of electrons bound to atoms in the intergalactic matter can meet the numerical requirement for the photon energy attenuate rate. But because the mass density in intergalactic space differs by seven orders of magnitude, the attenuate rate of photon energy varies with the path it travels. Therefore, the Hubble constant is not a natural constant and cannot be accurately measured.

Summary:

The attenuation law of photon frequency is evidence of the photon quantum redshift effect. It is unreasonable to regard it as evidence of the expansion of the universe.

8. Discussion

8.1. Classic Problems Worth Discussing

1)Will the Image of the Light Source Become Blurred?

Does the redshift caused by photons passing through the intergalactic medium make the light source look fuzzy?

Since the discovery of redshift, some scholars always think that if there is a medium on the way of light propagation, the image of the light source will become blurred.

Of course, there is always a small amount of plasma in the intergalactic medium. So part of photons are scattered by the plasma, but these photons cannot enter the eyes of observers on the Earth. Therefore, the image of the light source will not be blurred.

Because the medium is mainly composed of electrically neutral atoms, however, there is always a part of photons that do not change their propagation direction after the collision.

Because there are positive and negative charges in neutral atoms; for example, in the hydrogen atom, the nucleus has a positive charge $+e$, and the extranuclear electron has a negative one $-e$. In the soft photon electromagnetic field, the proton and the extranuclear electron are acted by an electric field force with equal magnitude and opposite direction simultaneously. So they obtain recoil momentum with the same size and opposite direction simultaneously.

Conversely, the photon is simultaneously acted by the two forces of the nucleus and the extranuclear electron, which are equal in magnitude and opposite in direction. The photon momentum in the direction perpendicular to the propagation direction remains unchanged, and the photon still propagates in the original one.

However, there is plasma near some celestial bodies. When the photons emitted by these objects pass through the plasma, the photons are scattered by the plasma around these objects, so they cannot travel in a straight line. Therefore, their images are very blurry. Some quasars are such confused celestial bodies.

2) Will the Intergalactic Medium Temperature Rise? Will Space Become Bright?

The existence of the intergalactic medium is a fundamental condition for causing redshift. Perhaps opponents will refute: will photons collide with atoms in the medium and transfer fractional energy to them, make the medium temperature rise continuously, raise the temperature of cosmic space, and even become bright?

It should explain from two aspects:

First, the intergalactic medium is so thin that it emits light weakly, if at all.

Second, from the principle of atomic absorption of photon energy, the unabsorbed photons only lose a fractional, as described in Equation (76). It will not cause the medium temperature to rise continuously. Because atoms absorb this part of the energy, they radiate it as radio waves, which is why high redshift objects are often radio sources. In the whole space, the light energy emitted by the luminescent body is transformed into radio waves by the medium, so the absorbed energy equals the emitted radio wave energy. Therefore, the temperature of the medium remains unchanged. The photons reduce to that of microwave background radiation, which is invisible light. Finally, the photons disappear gradually.

8.2. Several Ideas to Explain Redshift Are Worth Discussing

1) Is the New Tired Light Theory Correct?

The new tired light theory should be the latest theory before the quantum redshift effect.

The scholar Lyndon Ashmore proposed a New Tired Light theory [7] [8]. He believed that the universe is static, and redshifts are produced by an interaction between photons and the electrons in the intergalactic medium.

He derived the Hubble constant as $H_0 = 2n_e h r_e / m_e$ is very close to Equation (86) derived by this author through quantum mechanics. (Here n_e is the electron density in intergalactic space, h is the Planck constant, r_e is the classical electron radius, and m_e is the electron mass).

He also believes that electron gas condenses to a crystal state when both the Fermi energy and electron temperature are small compared to the energy of mutual repulsion, so the electron gases are arranged into Wigner crystals regularly [9].

Although the main point of the new tired light theory has some correct ingredients, there are at least three difficulties in this view.

The first difficulty was that the author had no idea of the size of the photon. Since any one-dimensional size of a photon in the optical band is much smaller than the Debye length of a plasma, the probability of a photon colliding simultaneously with an electron and proton is extremely low. As a result, as revealed by Compton scattering and Thomson scattering, the propagation direction of photons must change.

The second difficulty is that the intergalactic medium must be highly ionized or composed of an electronic lattice. If so, how to explain the absorption of atoms in intergalactic space?

The third difficulty is that the electrons of intergalactic matter are composed of electrons arranged in Wigner crystal, which is purely imaginary and too unrealistic.

2) Have There Been Any Other Correct Theories in History?

In the history of physics, there have been Doppler effect theory, tired light theory, photon aging theory, intrinsic redshift theory, gravitational redshift theory, general relativity universe expansion theory, new tired light theory. However, in these views, except that the new tired light theory has some correct ingredients, the other cannot stand theoretical scrutiny.

Electrodynamics has no correct method to explain the origin of redshift. Only quantum mechanics is the right way to explain the origin of redshift. However, if the physical quantities of a single photon structure are unknown in advance, can a concise and clear formula such as Equation (76) be derived only from the theory of quantum mechanics? Quantum mechanics is successful in dealing with the law of atomic energy-level transition and understanding the spectral structure. However, it is unable to deal with the collision between a single photon and an atom.

This paper can accurately deduce the energy loss formula of a single photon in the photon-atom collision, "The size and shape of a single photon" is the theoretical basis. Only by understanding the size, shape, and structure of a single photon can the author deal with the collision between a single photon and a single atom with quantum mechanics and discover the quantum redshift effect.

Summary:

1) The physical mechanism of the redshift caused by the photon-atom collision will neither blur the image of the light source nor cause the universe temperature to rise or even the space to become bright.

2) The theory of the shape and size of a single photon is the basis and premise for solving redshift. The physical mechanism of the redshift has not been correctly explained for a long time in history because of errors in physics theories. The quantum redshift effect is a newly discovered natural law.

9. Conclusion

The explanation of the physical mechanism of the origin of the Hubble Redshift by Big Bang cosmologists cannot withstand theoretical scrutiny. Applying the correction of the Hamiltonian operator in quantum mechanics and the derivation of time-dependent perturbation theory conclude that Hubble redshift or cosmological redshift is the result of photon energy loss caused by photon collision with atoms on the path of propagation. On the way of propagation, part of the photons is absorbed by the atoms in a resonance manner, so absorption lines appear on the photometric spectrum. For those unabsorbed photons, the average energy loss caused by each extranuclear electron is $\Delta\mathcal{E} = \pi^2 (\hbar\omega)^3 \big/ 4\left(m_e c^2\right)^2 = \left(3\pi\sigma_T / 8\alpha\sigma_P\right)\hbar\omega$. In this way, photons frequency decreases with propagation distance in the attenuation law $\nu = \nu_0 \exp\left\{-(3\pi/8\alpha)\sigma_T \int_0^r n_e(r)\,\mathrm{d}r\right\}$, or the wavelength of photons increases with propagation distance in the growth law $\lambda = \lambda_0 \exp\left\{(3\pi/8\alpha)\sigma_T \int_0^r n_e(r)\mathrm{d}r\right\}$. This phenomenon is the quantum redshift effect. The so-called Hubble constant is essentially the attenuation rate of photon energy, momentum, and frequency; or the growth rate of wavelength. The Hubble constant can express as $H_0 = 3\pi c\sigma_T n_e/8\alpha$, which is not a true constant. Its value is directly proportional to the bound electron density in intergalactic space on the path of photon propagation. Hubble constant has nothing to do with the age of the universe. Photon redshift cannot support the theory of the universe's expansion and that of the big bang.

Acknowledgements

Thanks my family for supporting my scientific research!

Conflicts of Interest

The author declares no conflicts of interest regarding the publication of this paper.

References

[1] Xu, Z.L. (2021) *Open Access Library Journal*, **8**, e7179.

[2] Compton, A.H. (1913) *The Physical Review*, *Second Series*, **21**, 483-502.

[3] Zhou, S.X. (1979) Quantum Mechanics Course. Higher Education Press, Beijing.

[4] Zeng, J.Y. (1984) Modern Physics Series, Quantum Mechanics, Chapter 7. The Motion of Particles in Electromagnetic Field. Science Press of China, Beijing.

[5] Harris, E.G. (1975) Introduction to Modern Theoretical Physics. John Wiley &Sons, Inc., New York.

[6] He, X.T. (2007) Observational Cosmology, Postgraduate Textbook of New Century Colleges and Universities. Beijing Normal University Press, Beijing.

[7] Ashmore, L. (2016) *Journal of High Energy Physics*, *Gravitation and Cosmology*, **2**, 512-530. https://doi.org/10.4236/jhepgc.2016.24045

[8] Ashmore, L. (2006) *Galilean Electrodynamics*, **17**.

[9] Ashmore, L. (2019) *Journal of High Energy Physics*, *Gravitation and Cosmology*, **5**, 181-192. https://doi.org/10.4236/jhepgc.2019.51010

Journal of Modern Physics, 2021, 12, 2031-2040
https://www.scirp.org/journal/jmp
ISSN Online: 2153-120X
ISSN Print: 2153-1196

Difference between the Time Intervals in the Special Relativistic Theory Calculated with the Aid of an Invariance Property between the Mechanical Expressions

Stanisław Olszewski

Institute of Physical Chemistry, Polish Academy of Sciences, Warsaw, Poland
Email: olsz@ichf.edu.pl

How to cite this paper: Olszewski, S. (2021) Difference between the Time Intervals in the Special Relativistic Theory Calculated with the Aid of an Invariance Property between the Mechanical Expressions. *Journal of Modern Physics*, **12**, 2031-2040.
https://doi.org/10.4236/jmp.2021.1214116

Received: November 24, 2021
Accepted: December 28, 2021
Published: December 31, 2021

Abstract

In the relativistic mechanics, we obtain a difference between the time scale of a one-dimensional motion having a larger velocity and the time scale of a similar motion with a lower velocity. This calculation does involve usually also the differences of parameters other than time. Basing on the invariance of a pair of the mechanical parameters, it can be shown that the difference of two scales of time can be attained independently from the differences of the other physical parameters.

Keywords

Time in the Special Relativity Theory, Relativistic Invariance of Some Special Differences of the Mechanical Parameter

1. Introduction

In principle, any calculation of a change of the scale of some mechanical parameter in the special relativistic theory is accompanied by an insight into the scale changes belonging also to other parameters than that taken into account [1]. But recently an invariance of the differences of parameters belonging to different mechanical scales has been pointed out [2]. Our aim became to demonstrate that this situation allows us to estimate the size change of a single mechanical parameter alone. The scale of time has been chosen as our basic example.

In the first step, we present the Lorentz transformation of the variables pair t, x into the pair t', x' [2]. Next the intervals $t'-t$ and $x'-x$ are calculated in terms of t and x. Finally the quanta of the electric capacitance in the hydrogen atom and their change with the quantum number are examined.

2. Lorentz Transformation and the Invariant Expressions for the Mechanical Parameters

If the Lorentz transformation is specified for the variables pair (t,x) going into the pair (t',x'), the corresponding transformation formulae are:

$$t' = t\frac{1}{\sqrt{1-\frac{v^2}{c^2}}} - \frac{x\frac{v}{c}}{\sqrt{1-\frac{v^2}{c^2}}} \tag{1}$$

and

$$x' = -\frac{t\frac{v}{c}}{\sqrt{1-\frac{v^2}{c^2}}} + \frac{x}{\sqrt{1-\frac{v^2}{c^2}}}. \tag{2}$$

The t and t' are the time coordinates, the x and x' are coordinates of position in the particle one-dimensional motion along the axis x, so the changes of two parameters are involved. The v is a speed between the system labelled by (t',x') and that labelled by (t,x). We obtain for the difference [2]

$$\begin{aligned} t'^2 - x'^2 &= \left[t^2 - 2xt\frac{v}{c} + x^2\frac{v^2}{c^2}\right]\frac{1}{1-\frac{v^2}{c^2}} - \left[t^2\frac{v^2}{c^2} - 2xt\frac{v}{c} + x^2\right]\frac{1}{1-\frac{v^2}{c^2}} \\ &= \left[t^2\left(1-\frac{v^2}{c^2}\right) - x^2\left(1-\frac{v^2}{c^2}\right)\right]\frac{1}{1-\frac{v^2}{c^2}} = t^2 - x^2. \end{aligned} \tag{3}$$

The result in (3) indicates the invariant behaviour of the difference

$$t'^2 - x'^2 = t^2 - x^2 \tag{3a}$$

upon the Lorentz transformation formulae in (1) and (2). From (3a) it comes out that

$$t'^2 - t^2 = x'^2 - x^2 = \Delta t\left(t'+t\right) = \Delta x\left(x'+x\right) \tag{4}$$

on condition we put

$$\Delta t = t' - t \tag{4a}$$

and

$$\Delta x = x' - x. \tag{4b}$$

Our aim is to point out that the above properties concerning the transformed and non-transformed parameters of t and x can lead to a simple reference between t' and t.

3. The Difference of t' and t Represented as a Function of Some Remainder Parameters

We multiply Equation (1) by t and Equation (2) by x. A simple rearrangement of terms leads to the formulae:

$$t't - \frac{t^2}{\left(1 - \frac{v^2}{c^2}\right)^{1/2}} = -\frac{vxt}{\sqrt{1 - \frac{v^2}{c^2}}} \frac{1}{c} \tag{5}$$

and

$$x'x - \frac{x^2}{\left(1 - \frac{v^2}{c^2}\right)^{1/2}} = -\frac{vtx}{\sqrt{1 - \frac{v^2}{c^2}}} \frac{1}{c}. \tag{6}$$

The difference of (5) and (6) leads to the result:

$$t't - x'x - \frac{t^2 - x^2}{\left(1 - \frac{v^2}{c^2}\right)^{1/2}} = 0, \tag{7}$$

or with the aid of (3a) to the formula:

$$t't - x'x = \frac{t^2 - x^2}{\left(1 - \frac{v^2}{c^2}\right)^{1/2}} = \frac{t'^2 - x'^2}{\left(1 - \frac{v^2}{c^2}\right)^{1/2}}. \tag{8}$$

The result in (8) is dictated by the property (3a). The calculations done farther in the paper refer to the non-primed coordinates system

Another approach to the rearrangement of terms in (8) gives:

$$t'^2 - t^2 = x'^2 - x^2. \tag{9}$$

By taking into account (4a) and (4b) we have:

$$\begin{aligned} t'^2 - t^2 &= (t' - t)(t' + t) = \Delta t (2t + \Delta t), \\ x'^2 - x^2 &= (x' - x)(x' + x) = \Delta x (2x + \Delta x), \end{aligned} \tag{9a}$$

but in virtue of (9):

$$\Delta t (2t + \Delta t) = \Delta x (2x + \Delta x). \tag{10}$$

The left-hand side of (8) can be transformed into

$$(t + \Delta t)t - (x + \Delta x)x = t^2 - x^2 + t\Delta t - x\Delta x, \tag{11}$$

so

$$t\Delta t - x\Delta x = \frac{t^2 - x^2}{\left(1 - \frac{v^2}{c^2}\right)^{1/2}} - (t^2 - x^2) = (t^2 - x^2)\left[\frac{1}{\left(1 - \frac{v^2}{c^2}\right)^{1/2}} - 1\right] \tag{11a}$$

indicating a positive value of (11a) on condition $t > x$.

An effect of (4a) and (4b) leads together with the relation (3) to the formula:

$$\begin{aligned} t'^2 - x'^2 &= (t + \Delta t)^2 - (x + \Delta x)^2 \\ &= t^2 - x^2 + 2(t\Delta t - x\Delta x) + (\Delta t)^2 - (\Delta x)^2 \\ &= t^2 - x^2 \end{aligned} \tag{12}$$

so the last step of (12) gives

$$2(t\Delta t - x\Delta x) = -\left[(\Delta t)^2 - (\Delta x)^2\right] \tag{13}$$

or

$$(\Delta x)^2 + 2x\Delta x - (\Delta t)^2 - 2t\Delta t = 0. \tag{13a}$$

4. An Equation for the Interval Δt and Its Properties

Because of (11a) we have

$$t\Delta t - (t^2 - x^2)\left[\frac{1}{\left(1-\left(\frac{v}{c}\right)^2\right)^{1/2}} - 1\right] = x\Delta x, \tag{14}$$

therefore

$$\frac{t}{x}\Delta t - \frac{1}{x}(t^2 - x^2)\left[\frac{1}{\left[1-\left(\frac{v}{c}\right)^2\right]^{1/2}} - 1\right] = \Delta x. \tag{14a}$$

A final equation for the interval Δt is obtained from the relations (11a), (13) and (14a):

$$\begin{aligned}
2(t\Delta t - x\Delta x) &= 2(t^2 - x^2)\left[\frac{1}{\left[1-\left(\frac{v}{c}\right)^2\right]^{1/2}} - 1\right] = -(\Delta t)^2 + (\Delta x)^2 \\
&= -(\Delta t)^2 + \left\{\frac{t}{x}\Delta t - \frac{1}{x}(t^2 - x^2)\left[\frac{1}{\left[1-\left(\frac{v}{c}\right)^2\right]^{1/2}} - 1\right]\right\}^2 \\
&= -(\Delta t)^2 + \left(\frac{t}{x}\right)^2(\Delta t)^2 - \frac{2}{x^2}t\Delta t(t^2 - x^2)\left[\frac{1}{\left[1-\left(\frac{v}{c}\right)^2\right]^{1/2}} - 1\right] \\
&\quad + \frac{1}{x^2}(t^2 - x^2)^2\left[\frac{1}{\left[1-\left(\frac{v}{c}\right)^2\right]^{1/2}} - 1\right]^2.
\end{aligned} \tag{15}$$

In effect the equation coupling the pairs (t', x') and (t, x) becomes

$$\left[\left(\frac{t}{x}\right)^2 - 1\right](\Delta t)^2 - \frac{2t}{x^2}\left(t^2 - x^2\right)\left[\frac{1}{\left[1-\left(\frac{v}{c}\right)^2\right]^{1/2}} - 1\right]\Delta t$$
$$+\frac{\left(t^2 - x^2\right)^2}{x^2}\left[\frac{1}{\left[1-\left(\frac{v}{c}\right)^2\right]^{1/2}} - 1\right]^2 - 2\left(t^2 - x^2\right)\left\{\frac{1}{\left[1-\left(\frac{v}{c}\right)^2\right]^{1/2}} - 1\right\} = 0. \tag{16}$$

We divide (16) by $\left[\left(\frac{t}{x}\right)^2 - 1\right]$ and get the equation:

$$(\Delta t)^2 - 2t\Delta t\left[\frac{1}{\left[1-\left(\frac{v}{c}\right)^2\right]^{1/2}} - 1\right] + \left(t^2 - x^2\right)\left[\frac{1}{\left[1-\left(\frac{v}{c}\right)^2\right]^{1/2}} - 1\right]^2$$
$$-2x^2\left[\frac{1}{\left[1-\left(\frac{v}{c}\right)^2\right]^{1/2}} - 1\right] = 0 \tag{17}$$

which gives

$$(\Delta t)^2 - 2t\Delta t[\,] + t^2[\,]^2 = x^2[\,]^2 + 2x^2[\,] \tag{17a}$$

or

$$\left\{\Delta t - t[\,]\right\}^2 = x^2[\,]^2 + 2x^2[\,]. \tag{18}$$

The contents of the square brackets in (17a) and (18) is represented in (17). Taking the square root of (18) we obtain:

$$\Delta t - t\left[\frac{1}{\left[1-\left(\frac{v}{c}\right)^2\right]^{1/2}} - 1\right] = x\left\{[\,]^2 + 2[\,]\right\}^{1/2}. \tag{19}$$

We divide both sides of (19) by t:

$$\frac{\Delta t}{t} - \left[\frac{1}{\left[1-\left(\frac{v}{c}\right)^2\right]^{1/2}} - 1\right] = \frac{x}{t}\left\{[\,]^2 + 2[\,]\right\}^{1/2}. \tag{20}$$

From this equation we have:

$$\frac{\Delta t}{t} = \frac{1}{\left[1-\left(\frac{v}{c}\right)^2\right]^{1/2}} - 1 + \frac{x}{t}\left\{[\ ]^2 + 2[\ ]\right\}^{1/2}. \tag{21}$$

We see from (21) that the ratio $\Delta t/t$ is a sum of a constant dependent solely on v/c increased by the ratio x/t multiplied by another constant term depend solely on v/c.

The next step concerns solution of the equation for Δx. We obtain from (13a)

$$(\Delta x)^2 + 2x\Delta x - \left[(\Delta t)^2 + 2t\Delta t\right] = (\Delta x)^2 + 2x\Delta x - \Delta t\left[2t + \Delta t\right] = 0. \tag{22}$$

This gives

$$\Delta x_{1,2} = \frac{-b \pm \sqrt{\Delta}}{2a} \tag{23}$$

where

$$b = 2x, \tag{24}$$

$$\Delta = b^2 - 4ad, \tag{25}$$

$$a = 1, \tag{26}$$

$$-d = \Delta t\left[2t + \Delta t\right]. \tag{27}$$

The solution of (22) gives:

$$\begin{aligned}\Delta x_{1,2} &= \frac{-2x \pm \sqrt{4x^2 + 8t\Delta t + 4(\Delta t)^2}}{2} = -x \pm \sqrt{x^2 + 2t\Delta t + (\Delta t)^2} \\ &= -x \pm x\sqrt{1 + 2\frac{t\Delta t}{x^2} + \frac{(\Delta t)^2}{x^2}}.\end{aligned} \tag{28}$$

Assuming Δx to be a small number the square root in (28) is taken next only with a positive sign. We obtain $(\Delta x + x)^2 = x^2 + 2t\Delta t + (\Delta t)^2$ or

$$(\Delta x)^2 + 2x\Delta x = 2t\Delta t + (\Delta t)^2. \tag{29}$$

On the basis of the result in (21) we obtain for the right-hand side of (29) the expression dependent solely on t and x:

$$2t\Delta t + (\Delta t)^2 = 2t^2\left[\frac{1}{\left[1-\left(\frac{v}{c}\right)^2\right]^{1/2}} - 1\right] + 2tx\left\{[\ ]^2 + 2[\ ]\right\}^{1/2} + (\Delta t)^2. \tag{30}$$

The term $(\Delta t)^2$ can be readily obtained from (21) as a function of t and x.

5. The Calculation of $\Delta x = x' - x$

We do it by taking into account the relation (9):

$$\begin{aligned}t'^2 - t^2 &= (t' - t)(t' + t) = \Delta t(2t + \Delta t) \\ &= x'^2 - x^2 = (x' - x)(x' + x) = \Delta x(2x + \Delta x).\end{aligned} \tag{31}$$

We obtain:

$$\frac{\Delta x}{x}+1=\sqrt{\frac{(\Delta x+x)^2}{x^2}}=\sqrt{\frac{x^2+2x\Delta x+(\Delta x)^2}{x^2}}=\sqrt{1+\frac{\Delta t(2t+\Delta t)}{x^2}} \tag{32}$$

where expression $\Delta t(2t+\Delta t)$ is represented by (30).

It seems interesting to compare both terms entering the product entering the last square root in (32). We have [see (19)]

$$\Delta t=t\left[\frac{1}{\left(1-\frac{v^2}{c^2}\right)^{1/2}}-1\right]+x\left\{[\,]^2+2[\,]\right\}^{1/2} \tag{33}$$

whereas

$$2t+\Delta t=t\left[\frac{1}{\left(1-\frac{v^2}{c^2}\right)^{1/2}}+1\right]+x\left\{[\,]^2+2[\,]\right\}^{1/2}. \tag{34}$$

In effect:

$$\Delta t(2t+\Delta t)=\frac{t^2}{1-\frac{v^2}{c^2}}-t^2+2t\frac{x}{\left(1-\frac{v^2}{c^2}\right)^{1/2}}\left\{[\,]^2+2[\,]\right\}^{1/2}+x^2\left\{[\,]^2+2[\,]\right\}. \tag{35}$$

Therefore

$$\frac{\Delta x}{x}+1=\left\{1+\frac{t^2}{x^2}\left[\frac{1}{1-\frac{v^2}{c^2}}-1\right]+\frac{2t}{x}\frac{1}{\left(1-\frac{v^2}{c^2}\right)^{1/2}}\left\{[\,]^2+2[\,]\right\}^{1/2}+[\,]^2+2[\,]\right\}^{1/2}. \tag{36}$$

The expressions entering the empty brackets in (17a)-(21) as well as in (30) and (33)-(36) are fully represented in Equation (17).

6. Example of Distance x Representing the Quanta of the Electric Capacitance and Their Change

An example of x and Δx can be presented by considering the electric capacitance C of the condenser. A reference to C and the charge q of the condenser is given by the formula [3]:

$$V=\frac{q}{C} \tag{37}$$

where V is the potential difference. On the other side, when the potential difference (37) is applied to the resistance R, the current intensity i produced by V and R becomes

$$i=\frac{V}{R}. \tag{38}$$

Let us assume that i is representing the electric current done along the n-th electron orbit about the nucleus of the hydrogen atom. Then

$$Ri_n = R\frac{e}{T_n} = \frac{q}{C}. \tag{39}$$

Here [4]

$$T_n = \frac{2\pi\hbar^3 n^3}{e^4 m} \tag{40}$$

is the time period of the electron motion along the n th orbit, m is the electron mass;

$$q = e \tag{41}$$

is the absolute value of the electron charge. Then it can be shown that R is the quantum parameter [5]

$$R = \frac{h}{e^2} \tag{42}$$

valid for all orbits n in the atom. It is worth to note that the R size in (42) is equal to the resistance characteristic for the integer quantum Hall effect; see e.g. [6].

By taking into account (39), (41) and (42) we obtain for C:

$$C_n = \frac{T_n}{R} = \frac{2\pi\hbar^3 n^3}{e^4 m}\frac{e^2}{h} = \frac{\hbar^2 n^3}{e^2 m}. \tag{43}$$

Evidently the lowest quantum of the capacitance C_n corresponds to the orbit $n = 1$:

$$C_1 = \frac{\hbar^2}{e^2 m} = 0.53\times10^{-8}\ \text{cm}. \tag{44}$$

The size of C_1 is equal to the radius of the shortest orbit in the hydrogen atom. Further $C_n(n > 1)$ increase proportionally to n^3 [see (43)], whereas the orbit length remains proportional to n^2.

The dimension of C_n is

$$C_n \sim \frac{\hbar^2}{e^2 m} \sim \frac{\text{erg}^2\cdot\text{sec}^2}{\text{erg}\cdot\text{cm}\cdot\text{g}} \sim \text{cm}. \tag{45}$$

In this way we find that

$$C_n \sim \text{cm} \sim x. \tag{46}$$

A relativistic change of x modifies the x entering (46) into $x + \Delta x$.

7. Euler-Lagrange Equation Applied in Examining the Particle Mass

In [2] an attempt is done to apply the Euler-Lagrange equation in examining the behaviour of the particle mass m. A special application may concern the force F acting on a moving particle when it is reduced to a single term [3]:

$$F=\frac{\mathrm{d}(m\dot{x})}{\mathrm{d}t}=m\frac{\mathrm{d}\dot{x}}{\mathrm{d}t}+\frac{\mathrm{d}m}{\mathrm{d}t}\dot{x}=\frac{\mathrm{d}m}{\mathrm{d}t}\dot{x}. \tag{47}$$

This holds on condition

$$\frac{\mathrm{d}\dot{x}}{\mathrm{d}t}=0, \quad \text{or} \quad \dot{x}=\text{const}. \tag{48}$$

The Lagrangian function let be [2]:

$$L=-\left[m+\varphi(t,x)\right]\sqrt{1-\dot{x}^2} \tag{49}$$

where φ is a time component of the vector potential denoted—for historical reasons—by $-\varphi(t,x)$. The derivative $\frac{\mathrm{d}\varphi}{\mathrm{d}t}$ can be joined with the mass derivative $\frac{\mathrm{d}m}{\mathrm{d}t}$, so the Euler-Lagrange equation becomes

$$\frac{\mathrm{d}}{\mathrm{d}t}\frac{\partial L}{\partial \dot{x}}=\left(\frac{\mathrm{d}m}{\mathrm{d}t}+\frac{\mathrm{d}\varphi}{\mathrm{d}t}\right)\frac{\dot{x}}{\sqrt{1-\dot{x}^2}}=\frac{\partial L}{\partial x}=-\frac{\partial \varphi}{\partial x}\sqrt{1-\dot{x}^2}. \tag{50}$$

Equation (50) gives:

$$F=\dot{x}\frac{\mathrm{d}m}{\mathrm{d}t}=-\frac{\mathrm{d}\varphi}{\mathrm{d}t}\dot{x}-\frac{\partial\varphi}{\partial x}\left(1-\dot{x}^2\right)=-\frac{\mathrm{d}\varphi}{\mathrm{d}t}\dot{x}-\frac{\partial\varphi}{\partial x}+\frac{\partial\varphi}{\partial x}\dot{x}^2. \tag{51}$$

Evidently for $\frac{\partial\varphi}{\partial x}>0$ beginning from $\dot{x}=0$ the formula (51) can provide us with F tending to an expression representing a positive $F>0$.

8. Summary

In the paper, the problem of a change of the interval Δt of a single mechanical variable—namely the time t—due to the existence of a non-vanishing velocity v of a moving one-dimensional system has been examined. First a simple dependence on v for the change Δt of the variable t is obtained, next a similar dependence is calculated for Δx equal to the change of the position coordinate x.

Conflicts of Interest

The author declares no conflicts of interest regarding the publication of this paper.

References

[1] Sommerfeld, A. (1949) Mechanik. 4th Edition, Akademische Verlagsgesellschaft Geest & Portig, Leipzig.

[2] Susskind, L. and Friedman, A. (2019) Special Relativity and Classical Field Theory. Prószyński Media, Warszawa. (In Polish)

[3] Jauncey, G.E.M. (1948) Modern Physics. 3rd Edition, Van Nostrand, New York.

[4] Sommerfeld, A. (1931) Atombau und Spektrallinien. Vol. 1, 5th Edition, Vieweg,

Braunschweig.

[5] Olszewski, S. (2016) *Journal of Modern Physics*, **7**, 1725.
https://doi.org/10.4236/jmp.2016.713155

[6] MacDonald, A.H. (1989) Quantum Hall Effect. A Perspective. Kluwer, Milano.
https://doi.org/10.1007/978-94-010-9709-3

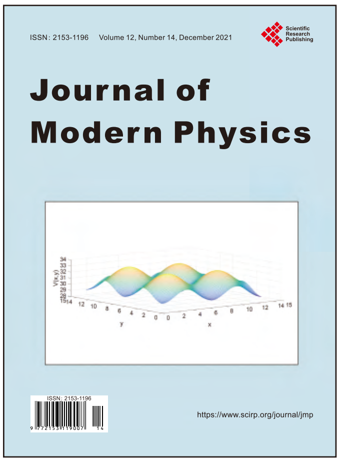

Call for Papers

Journal of Modern Physics

ISSN: 2153-1196 (Print) **ISSN: 2153-120X (Online)**
https://www.scirp.org/journal/jmp

Journal of Modern Physics **(JMP)** is an international journal dedicated to the latest advancement of modern physics. The goal of this journal is to provide a platform for scientists and academicians all over the world to promote, share, and discuss various new issues and developments in different areas of modern physics.

Editor-in-Chief

Prof. Yang-Hui He City University, UK

Subject Coverage

Journal of Modern Physics publishes original papers including but not limited to the following fields:

Biophysics and Medical Physics
Complex Systems Physics
Computational Physics
Condensed Matter Physics
Cosmology and Early Universe
Earth and Planetary Sciences
General Relativity
High Energy Astrophysics
High Energy/Accelerator Physics
Instrumentation and Measurement
Interdisciplinary Physics
Materials Sciences and Technology
Mathematical Physics
Mechanical Response of Solids and Structures
New Materials: Micro and Nano-Mechanics and Homogeneization
Non-Equilibrium Thermodynamics and Statistical Mechanics
Nuclear Science and Engineering
Optics
Physics of Nanostructures
Plasma Physics
Quantum Mechanical Developments
Quantum Theory
Relativistic Astrophysics
String Theory
Superconducting Physics
Theoretical High Energy Physics
Thermology

We are also interested in: 1) Short Reports—2-5 page papers where an author can either present an idea with theoretical background but has not yet completed the research needed for a complete paper or preliminary data; 2) Book Reviews—Comments and critiques.

Notes for Intending Authors

Submitted papers should not have been previously published nor be currently under consideration for publication elsewhere. Paper submission will be handled electronically through the website. All papers are refereed through a peer review process. For more details about the submissions, please access the website.

Website and E-Mail

https://www.scirp.org/journal/jmp **E-mail: jmp@scirp.org**

What is SCIRP?

Scientific Research Publishing (SCIRP) is one of the largest Open Access journal publishers. It is currently publishing more than 200 open access, online, peer-reviewed journals covering a wide range of academic disciplines. SCIRP serves the worldwide academic communities and contributes to the progress and application of science with its publication.

What is Open Access?

All original research papers published by SCIRP are made freely and permanently accessible online immediately upon publication. To be able to provide open access journals, SCIRP defrays operation costs from authors and subscription charges only for its printed version. Open access publishing allows an immediate, worldwide, barrier-free, open access to the full text of research papers, which is in the best interests of the scientific community.

- High visibility for maximum global exposure with open access publishing model
- Rigorous peer review of research papers
- Prompt faster publication with less cost
- Guaranteed targeted, multidisciplinary audience

Scientific Research Publishing

Website: https://www.scirp.org
Subscription: sub@scirp.org
Advertisement: service@scirp.org